8-3-2016 12:00 AM

Optimal Scheduling of Energy Storage for Energy Shifting and Ancillary Services to the Grid

Hadi Khani
The University of Western Ontario

Supervisor
Dr. Rajiv K. Varma
The University of Western Ontario Joint Supervisor
Dr. Mohammad R. Dadash Zadeh
The University of Western Ontario

Abstract

The increase in renewable energy penetration into Ontario's electricity market has altered the overall behaviour of the energy market, with negative electricity prices even starting to appear. Negative prices represent a greater supply than the market demands, mostly appearing at night and during off-peak periods. Energy storage can be deployed in Ontario for peak shaving and energy shifting from off-peak to peak periods to address the above-mentioned issues. This is also the concern of many other system operators across the world.

This thesis is mainly focused on developing optimization-based models for scheduling of energy storage units. At first, a real-time optimal scheduling algorithm is developed seeking to maximize the storage revenue by exploiting arbitrage opportunities available due to the inter-temporal variation of electricity prices. The electricity price modulation is proposed as an approach to competitively offer incentive by the utility regulator to storage to fill the gap between current and a stable rate of return.

Subsequently, the application of large-scale storage for congestion relief in transmission systems as an ancillary service to the grid is investigated. An algorithm is proposed for the following objectives: (i) to generate revenue primarily by exploiting electricity price arbitrage opportunities and (ii) to optimally prepare the storage to maximize its contribution to transmission congestion relief.

In addition, an algorithm is proposed to enable independently operated, locally controlled storage to accept dispatch instructions issued by Independent System Operators (ISOs). Storage in this case is referred to as *dispatchable storage*. While the operation of locally controlled storage is optimally scheduled at the owner's end, using the proposed algorithm, storage is fully dispatchable at the ISO's end.

Finally, a model is proposed and analyzed to aggregate storage benefits for a large-scale load. The complete model for optimal operation of storage-based electrical loads considering both the capital and operating expenditures of storage is developed.

The applications of the proposed algorithms and models are examined using real-world market data adopted from Ontario's electricity market and actual load information from a large-scale institutional electricity consumer in Ontario.

Keywords: Bidding, congestion relief, distributed storage, electricity market, energy reserves, energy shifting, energy storage, incentive, large-scale load, load forecast, optimization, optimal scheduling, peak-shaving, price forecast, real-time, time-of-use electricity rates, wholesale electricity prices.

Acknowlegements

I would like to express my sincere gratitude to my supervisors, Dr. Rajiv K. Varma and Dr. Mohammad R. Dadash Zadeh, for their excellent supervision and continuous encouragement throughout the course of this research work. Their professionalism and dedication have always been inspiring for me, and working with them has been a truly enriching experience.

I am grateful to Dr. Amir H. Hajimiragha for his insightful comments during my Ph.D. research.

I should thank the great efforts of the entire Ph.D. examination committee.

Also, the administrative help and guidelines provided by the graduate co-ordinator of the ECE department is appreciated.

I would like to thank Ms. Mary Quintana, with the Facilities Management of Western University, for providing the actual load data of Western University campus.

I gratefully acknowledge the financial support provided by Western University and NSERC to pursue this research work.

Contents

List of Figures

List of Tables

List of Appendices

Abbreviations and Symbols

CAES	Compressed-air Energy Storage.
CAPEX	Capital Expenditure.
CES	Cryogenic Energy Storage.
CMSC	Congestion Management Settlement Credit.
DAM	Day-ahead Market.
DER	Distributed Energy Resource.
FFT	Fast Fourier Transform.
GLPK	Gnu Linear Programming Kit.
HOEP	Hourly Ontario Energy Price.
IESO	Independent Electricity System Operator.
IRR	Internal Rate of Return.
ISO	Independent System Operator.
LES	Least Error Square.
MCP	Market Clearing Price.

MILP   Mixed Integer Linear Programming.

MPC   Model Predictive Control.

NPP   Nuclear Power Plant.

OPEX   Operating Expenditure.

PDP   Pre-dispatch Price.

PDF   Probability Density Function.

PHES   Pumped-hydro Energy Storage.

ROR   Rate of Return.

RTOS   Real-time Optimal Scheduling.

SOC   State of Charge.

STF   Short-term Forecasting.

STLF   Short-term Load Forecasting.

TOU   Time-of-Use.

Nomenclature

$P_{min}^{S,Chg}$	Minimum charging power of storage (MW).
$P_{max}^{S,Chg}$	Maximum charging power of storage (MW).
$P_{min}^{S,Dhg}$	Minimum discharging power of storage (MW).
$P_{max}^{S,Dhg}$	Maximum discharging power of storage (MW).
SOC_{min}^{S}	Minimum state of charge (MWh).
SOC_{max}^{S}	Maximum state of charge (MWh).
$SOC^{S,Res}$	Reserved state of charge (MWh).
$\eta^{S,Chg}$	Efficiency of the storage charging plant (%).
$\eta^{S,Dhg}$	Efficiency of the storage discharging plant (%).
$\eta^{S,Dsp}$	Energy dissipation rate of the storage reservoir (%/h).
$C^{S,Main}$	Maintenance cost of storage ($/hour of operation).
$C^{S,ChgO}$	Charging operating expenditure ($/MWh).
$C^{S,DhgO}$	Discharging operating expenditure ($/MWh).
$C^{S,Cap}$	Capital cost (total investment) per hour ($/h).
$C^{S,EInc}$	Hourly expected income due to investment ($/h).
$\beta^{LB,SOC}$	Factor to adapt the lower bound of state of charge (> 1).
$\beta^{UB,SOC}$	Factor to adapt the upper bound of state of charge (< 1).
$\rho^{Pnl,SOC}$	Penalty factor for slack variables of state of charge ($/MWh^2) $\gg 1$.
$\rho^{Pnl,Res}$	Penalty factor for reserve-control slack variable ($/MWh^2) $\gg 1$.
$\rho^{Pnl,LCr}$	Penalty factor for load-curtailing slack variable ($/MWh) $\gg 1$.

Time-dependent Parameters

E_t^{FMrk} Forecast of electricity market price (\$/MWh).

S_t^{Grd} Binary parameter representing online / offline status of the grid.

P_t^L Load power (MW).

P_t^{HL} Historical load power to fit forecast model (MW).

P_t^{FL} Forecast of load power (MW).

P_t^{WIL} Weather-independent component of load (MW).

P_t^{WDL} Weather-dependent component of load (MW).

P_t^{CR} Commanded power for congestion relief (MW).

M_t^{CR} Congestion relief mode, 0: OFF and 1: ON.

P_t^{Dsp} System operator's dispatch instructions (MW).

$\rho_t^{Pnl,CR}$ Penalty factor for slack variables of congestion relief (\$/MWh) $\gg 1$.

$\rho_t^{Pnl,DI}$ Penalty factor for slack variables of dispatch instructions (\$/MWh) $\gg 1$.

T_t^k Ambient temperature at each time step t (°C).

$T_t^{Avg,k}$ Average temperature of the two adjacent time steps t and $t - \Delta T$ (°C).

A_k, B_k Model parameters representing the weather-independent load (MW).

$C_{\{1,2,3\}k}$ Model parameters representing the weather-dependent load (MW/°C).

Vectors and Matrices

$\vec{M}$ Model parameters vector representing total load.

$\vec{\epsilon}$ Load modeling error to be minimized (MW).

$\underline{Y}$ Matrix of time series and temperature functions.

$\underline{Y}^F$ Matrix of forecast functions.

Decision Variables

$P_t^{S,Chg}$	Storage charging power (MW).
$P_t^{S,Dhg}$	Storage discharging power (MW).
$P_t^{Slk,CR}$	Slack variable of congestion relief (MW).
$P_t^{Slk,CR'}$	Auxiliary slack variable of congestion relief (MW).
$P_t^{Slk,CR''}$	Auxiliary slack variable of congestion relief (MW).
P_t^{MCR}	Modified power for congestion relief (MW).
$P_t^{Slk,DI'}$	Slack variables to adapt system operator's dispatch instructions (MW).
$P_t^{Slk,DI''}$	Slack variables to adapt system operator's dispatch instructions (MW).
$P_t^{Slk,LCr}$	Slack variable for potential load curtailment (MW).
SOC_t^{S}	State of charge (MWh).
$SOC_t^{Slk,Res}$	Slack variable to adapt state of charge for reserved energy (MWh).
$SOC_t^{Slk,LB}$	Slack variable to adapt the lower bound of state of charge (MWh).
$SOC_t^{Slk,UB}$	Slack variable to adapt the upper bound of state of charge (MWh).
$b_t^{S,Chg}$	Binary variable representing online / offline status of charging plant.
$b_t^{S,Dhg}$	Binary variable representing online / offline status of discharging plant.

Chapter 1

Introduction

1.1   Statement of Problem

In Ontario's power system, all coal power plants have been recently phased out. The major power generation in Ontario, Canada is provided by Nuclear Power Plants (NPPs) which cannot quickly ramp down or up to track demand changes; thus, they are operated for base-load generation. Additionally, the increase in renewable energy penetration into Ontario's market has altered the behaviour of the energy market, with negative electricity prices even starting to appear. Negative energy prices represent a greater supply than the market demands [1]. The trend of integrating more non-dispatchable renewable sources into the electric grid and phasing out more dispatchable fossil-fueled power plants in the near future reduces the operational flexibility, increases the chance of transmission congestion, and endangers the stability of electric systems. This is also a common concern of many other system operators across the world.

Grid-scale storage units can be deployed to address the above-mentioned issues by energy shifting from off-peak to peak periods and profit through arbitrage. However, a grid-scale storage unit relies on certain geographic conditions and an accessible transmission line that has sufficient capacity. Another approach is to deploy small/medium-scale storage at the consumer end. Several market operators around the world have already started setting regulatory policies to facilitate energy storage deployment in the market [2]. Besides, in today's competitive markets, utility regulators and policy makers are encouraging private investors to build, own, and operate their own storage units, referred to as *locally controlled storage.* In such a case, appropriate methods and models are needed to aggregate various benefits of locally controlled storage for the private owner. Optimization-based models can be developed to achieve this goal. This thesis is mainly focused on developing optimization-based models for scheduling of energy storage.

1.2   Energy Storage

Energy storage is used to store energy at the present moment, so that the energy can be used for some more useful operations at the later time. For example, a battery converts electric energy to chemical energy and then converts it back to the electric energy when needed. The electric energy can be stored when there is excess generation while it is released when there is a need of electricity. The two types of energy storage units considered in this thesis are as follows:

- Compressed-air Energy Storage (CAES) is a storage option for large-scale energy shifting. A compressed-air plant stores electricity in the form of compressed air, then recovers it when needed to generate power. Off-peak or inexpensive electricity is used for pre-compressing the air, which is then stored typically in an underground cavern. When the storage plant works to regenerate power, the compressed air is released and heated; then, it is mixed with fuel and expanded to make a turbine turn to generate electricity. The electricity is injected to the power grid during peak periods or when it is needed.

- Cryogenic Energy Storage (CES) is a newly emerging storage technology which is suitable for massive energy shifting. A cryogenic storage unit comprises three major components: Liquefaction plant, Liquefied and Cold air reservoirs, and Power recovery plant. In this technology, cryogen (liquid air) is produced using electric energy (during off-peak) in the liquefaction plant. The resultant cryogen is stored at low pressure in the liquefied air reservoir which is vacuum insulated. During power recovery, auxiliary heat is added to the cryogen converting it into the super-heated vapor at a high pressure. The high-pressure gas then expands in a series of expansion turbines driving synchronous generator(s) to generate electric energy. The generated electric energy is injected to the power grid during peak periods or when it is needed.

1.3   Optimal Scheduling of Storage

In order to find the optimal charging/discharging power set-points of the energy storage, an optimization-based algorithm is needed. Either deterministic or stochastic techniques could be employed to formulate the optimization problem. The deterministic model uses the point forecast of market prices for storage scheduling. However, it suffers from price forecast inaccuracy. The stochastic programming approach is employed to deal with price

forecast inaccuracy to some extent. The stochastic model does not require the point forecast of market prices, rather statistical behaviour of the energy price is used. Stochastic models are computationally challenging due to the large number of scenarios that have to be considered. The model also requires knowledge of the probability distribution of uncertain variables, which may not be available. In this thesis, deterministic optimization approaches have been used.

1.4 Literature Review and Research Potential

Literature review has been organized for the main topics of the thesis and presented in Sections 1.4.1–1.4.4. The research potential in each topic is also presented.

1.4.1 Scheduling of Storage for Exploiting Arbitrage

1.4.1.1 Literature Review

The base-load power generation in Ontario is currently provided by NPPs which cannot turn down their generation quickly when the demand is low, mostly during nighttime. Additionally, the costs of energy generation from such a capital-intensive power plant (i.e., NPP) can be sizable if facilities are operated at less than full capacity [3]. Moreover, in many locations, wind generation is maximum at night, a time period when the demand is minimum [4]. This raises the idea of deployment of large-scale storage in Ontario to shift the surplus energy from nighttime to peak hours during the day. This is also a common concern of many other utilities across the world [2].

While the amount of surplus power available during off-peak periods and the amount of load demand during peak periods are not still significant for generating an attractive energy price arbitrage benefit to make storage investments economical today, it is expected that more arbitrage opportunities will become available in the market in the near future. This is because as the wind power penetration into the grid increases, and more push is applied to minimize the use of hydrocarbons for electric energy generation, there would be more surplus power available during off-peak periods and more demand during peak periods. In addition, as the technology grows, more efficient storage with lower capital costs are expected to emerge in the near future. Although price arbitrage benefits in current electricity markets do not offer an attractive Rate of Return (ROR) to make storage investments economical, storage diffusion for large-scale energy shifting can be still justified due to several technical and environmental benefits of storage.

On the other hand, in today's competitive electricity markets, utility regulators and

policy makers are encouraging private investors to build, own, and operate large-scale storage as merchant operators [5]. In such a case, the main objective of the storage from the private owner's perspective would be to generate profit by exploiting arbitrage opportunities. This is achieved mainly by optimally storing inexpensive electric energy during off-peak periods and releasing it back to the grid when the electricity is expensive during peak periods [5].

The optimal scheduling algorithms proposed in some prior studies have been developed for storage where the storage operation is governed to benefit operation of renewable generation sources as part of a grid/microgrid or to achieve some technical objectives for the grid, e.g., in [6]– [18]. A branch of research aims to optimally operate a storage unit in the electricity market to generate revenue while it is combined with a wind or solar farm, e.g., in [4], [19]– [32]. In these studies, storage is considered as part of the wind farm, and therefore, the wind farm owner must invest in storage. In such a case, storage cannot be operated as a single entity in the market. Another stream of research seeks to develop deterministic or stochastic optimization tools for storage operated as a single entity in the market. The main objective of these optimization tools is to generate different financial benefits for storage in a competitive market, e.g., in [5], [33]– [35]. Another branch of research aims to investigate the economic viability and profitability of two types of storage technologies (i.e., pumped-hydroelectric and compressed-air storage) operated in an electricity market to generate revenue, e.g., in [36]– [46].

A newly emerging storage technology suitable for massive energy shifting referred to as *CES* is about to be commercialized. It offers a smaller footprint with a higher density of stored energy. The concept of storing energy in the form of liquefied air (i.e., CES) was first investigated in 1977 [47]. Later on, numerous theoretical and experimental studies were conducted on the subject by both industries, such as [48]– [51] and academic institutes, such as [3], [52]– [57]. Finally, all of these efforts led to a completely operational grid-tied pilot plant in UK in 2011 [58]. There are few studies in the literature about CES applications as peak-shaving solutions, such as follows: In [54], off-peak electricity is used to produce liquid nitrogen and oxygen in air separation and liquefaction units, respectively. During peak periods, natural gas is burned by the oxygen from the air separation unit to generate electricity. In [55], the energy use of the air separation unit of a 530 MW coal-fired power plant has been shifted from peak to off-peak periods to obtain some financial benefits. A model is proposed in [3] by integrating a NPP with a large-scale CES unit to achieve time shifting of the electric power output. The combination of the nuclear power generation and the CES technology provides an efficient way to use significant thermal energy of the NPP during the power extraction process.

In the prior optimization algorithms, either deterministic or stochastic techniques are employed to formulate the optimization problem. The deterministic model uses the point forecasts of market prices in the optimization problem to find the storage schedule. However, it suffers from price forecast inaccuracy [5]. The stochastic programming approach is employed to deal with price forecast inaccuracy to some extent. However, stochastic models are computationally challenging due to the large number of scenarios that have to be considered [27]. The model also requires knowledge of the probability distribution of uncertain variables, which may not be available [27].

Among those studies which aim to investigate the economic profitability of storage in real-world markets, some studies have estimated the storage revenue of single or multiple applications, using simplified scheduling assumptions and actual historical market prices, e.g., in [36]– [40]. In [36], three strategies are proposed which aim to optimally schedule the storage in the day-ahead electricity market based on historical actual prices. The first strategy, called back-casting approach, duplicates the actual prices of the day-behind market for storage scheduling in the Day-ahead Market (DAM). The others take the average of last actual and future prices in a user-specified period and find the storage schedule correspondingly; such strategies require the presence of accurate price forecasts, which may not be available. The back-casting approach has been used in some studies as a practical strategy since it would not assume the optimal operation of the storage with the perfect/accurate price forecast.

In [37]– [40], the revenue captured using back-casting approach in different markets has been compared with the ideal revenue generated with the assumption of the availability of the perfect price forecast; authors have concluded that a considerable amount of revenue can be captured using the back-casting method because off-peak and peak periods of prices have fairly consistent daily and seasonal patterns. The lower bound of revenue could be captured by storage using back-cast method. If the storage operation is scheduled using the perfect price forecast, the higher bound of revenue can be generated. Any other price forecast with an accuracy in between the perfect and back-cast methods can generate a revenue level between the lower and higher bounds of revenue. Short-term scheduling of storage or other market participants could be carried out using a price forecast. Although various techniques have been reported in the literature to improve price forecast accuracy, short-term scheduling in a liberalized electricity market is still a very challenging task due to the uncertainty associated with future electricity prices [59].

The economic viability of large-scale storage deployment exploiting energy price arbitrage opportunities has not been adequately addressed in previous contributions. Moreover, prior studies have not proposed effective mechanisms for storage incentivization by

grid operators. In addition, the value and benefit of a storage unit optimized to utilize wholesale and contract-based electricity prices have not been compared in the literature.

1.4.1.2   Research Potential

Due to the high capital cost, relatively low round-trip efficiency, and small electricity price arbitrage, large-scale storage may not be economical in current electricity markets. Storage deployment will be becoming more economical in the near future due to the growing storage technologies and higher arbitrage benefits in future electricity markets. To fill the gap between current and a stable expected ROR in today's electricity markets, storage could be incentivized by utility regulators and system operators due to considerable environmental and technical benefits of storage diffusion [60]. Large-scale storage deployment for energy shifting can also result in peak shaving. In such a case, peak-shaving gas generators, which usually cause air pollution, can be shut/turned down, thereby generating less CO_2 emission. Moreover, large-scale energy-shifting storage can allow a higher penetration of wind and solar energy to electric grids. This is because the sporadic availability of renewable sources can be handled by introducing storage to (partially) decouple energy generation from demand [61].

Comprehensive economic studies are required to investigate the economic viability of large-scale storage deployment exploiting energy price arbitrage opportunities. Further work is needed to study the economic aspects associated with large-scale storage units such as CAES and CES systems. Possible mechanisms to appropriately incentivize storage units by grid operators shall be examined. Comparative studies would be required to compare the value and benefit of a storage unit optimized to utilize wholesale and contract-based electricity prices.

1.4.2   Scheduling of Storage for Congestion Relief

1.4.2.1   Literature Review

Congestion in transmission systems is a situation where the demand for transmission capacity exceeds the grid capabilities; this condition might result in a violation of network security limits, such as thermal, voltage stability, or angular stability [62]. Considerable penetration of renewable sources, including solar and wind power, could adversely affect the power flow in the system and may cause congestion in parts of transmission or distribution systems. Thus, it is expected that congestion relief will become more important in the near future with a higher expected penetration of renewable generation [63].

In today's power systems, coordination of the system operations and preserving the system reliability are the responsibilities of an Independent System Operator (ISO). In such a case, managing transmission congestion in a power system poses a challenge to an ISO [64]. Increasing the transmission capacity by reinforcing the system with additional network elements, such as adding overhead lines or by thermal/voltage upgrades of existing lines, could be considered as one approach to reduce congestion. Changing the philosophy of operation from preventive to corrective mode is another way to increase the transmission capacity [62]. Nowadays, generation re-dispatch, startup of a fast generation unit, and load management are some effective ways for long-term congestion relief [62].

Energy storage units have great potential to enhance the flexibility of electric grids and are key elements envisioned to enable smart grid realization. Accordingly, policy makers and regulators have become increasingly interested in promoting different energy storage technologies for various objectives [60]. Moreover, in today's competitive electricity markets, there have been policies set by regulators to reinforce private investments in large-scale storage. The main objective of storage owners as private investors would be to generate revenue by utilizing energy price arbitrage opportunities. This goal is achieved by optimally purchasing and storing inexpensive electricity during off-peak periods and selling it back to the market when electricity is expensive during peak periods. A large-scale storage is also able to contribute to congestion relief by injecting/absorbing a certain amount of power to/from the grid.

As stated in Section 1.4.1.1, in most previous studies related to large-scale storage deployment, the objective has been to utilize a storage unit to generate revenue by exploiting arbitrage opportunities. The prior studies, however, do not consider the possibility for a large-scale storage to provide ancillary services, such as congestion relief, to the grid as part of the optimization problem.

1.4.2.2 Research Potential

Transmission congestion has become more important since the penetration of renewable sources into the grid is increasing. Therefore, power system operators are encouraging market participants to contribute to congestion relief as an alternative or complementary solution for long-term congestion relief [65]. Thus, there is a potential for large-scale storage to generate profit, in addition to the arbitrage profit, through contribution to congestion relief. However, storage needs to be prepared in advance in order to effectively contribute to congestion relief in real-time. Due to its contribution to congestion relief, the storage owner is financially compensated by the ISO. Therefore, storage can generate extra profit through contribution to transmission congestion relief, in addition to the

energy price arbitrage benefit. It is emphasized that the goal of storage application in this mechanism is completely different from that of prior studies, which is to utilize a utility-procured small-capacity battery storage for short-term relief of transmission congestion, such as [62], [66]– [71]. In these studies, a battery storage unit aims to relieve congestion for certain corridors during a contingency event for several minutes until the ISO can initiate a long-term solution such as generation re-dispatch or load management.

New optimization algorithms are required to optimally prepare the storage for both the aforementioned purposes, i.e., energy shifting and contribution to congestion relief.

1.4.3 Scheduling of Storage as a Dispatchable Asset

1.4.3.1 Literature Review

As a single entity, a grid-scale storage unit can be operated in the energy and reserve markets. The storage benefits the grid through handling the issues appearing due to the sporadic availability of renewable sources. At the same time, storage profits by utilizing energy price arbitrage opportunities, also known as load shifting or peak shaving, e.g., in [5], [33]– [46], [72], [73]. The storage in this category can also be employed to provide ancillary services to the grid so that more financial benefits are generated for the private owner of storage. In such a case, the following question needs to be answered: Should storage freely purchase and sell energy at wholesale market prices without accepting ISO's dispatch instructions (a non-dispatchable asset); or should it submit its schedule to the DAM and accept ISO's dispatch instructions (a dispatchable asset)?

In Ontario's electricity market, an offer refers to the amount of energy a supplier plans to sell with a price suggested by that supplier. A bid, on the other hand, is defined as the amount of energy a consumer plans to purchase with a price suggested by that consumer [74]. For the sake of simplicity, only one terminology (i.e., the bid) can be used for both the offer (submitted by generators) and the bid (submitted by loads). Different categories of assets currently operated in Ontario's market are defined as follows:

i) *Dispatchable assets:* Dispatchable assets submit their bids to the ISO several hours ahead of real-time. Depending on schedules and prices offered by all market participants and grid's technical constraints, their bids may or may not be accepted for each time interval. The ISO modifies their bids to meet both the demand and technical constraints of the grid. The final dispatch instructions are then sent to market participants by the ISO. Market participants have to follow these instructions, or they will be financially penalized by the ISO. Dispatchable assets have the greatest certainty since they both bid in the DAM and accept dispatch instructions [74].

ii) *Non-dispatchable assets:* Non-dispatchable assets do not accept any dispatch instruction. However, they accept Market Clearing Prices (MCPs) when they generate or consume energy [74]. They are categorized as follows:

- *Self-scheduling generators:* Self-scheduling generators submit their schedules to the ISO indicating the amount and time of energy production. Then, they follow their schedules. The ISO does not send any dispatch instruction to these assets. These are less certain than dispatchable assets since they do not accept dispatch instructions, but more certain than intermittent assets [74].

- *Intermittent generators:* Intermittent generators are operated intermittently in the market. These are the most uncertain assets since they are not even able to determine their generation in advance of real-time [74].

- *Non-dispatchable loads*: Non-dispatchable loads absorb energy from the grid as needed and pay for it based on wholesale market prices at the time they consume energy [74].

Basically, independently operated, locally controlled storage can be categorized in each of the aforementioned categories, i.e., intermittent, self-scheduling, or dispatchable.

In some prior studies, investigating the optimal operation of independently operated storage, the storage does not bid in the market and does not accept ISO's dispatch instructions, e.g., in [36]– [46]. The storage in this case is referred to as *non-dispatchable storage.* The operation of non-dispatchable storage can create uncertainties in the market since the ISO does not have any control over the storage operation [74].

Other studies in this area have proposed bidding strategies to enable an independently operated storage unit to bid in the DAM, e.g., in [5], [33], [35], [75].

In previous algorithms, storage is either locally controlled at the owner's end and cannot optimally accept ISO's instructions; or it is centrally controlled by the grid operator to achieve some technical objectives for the grid. The possibility for an independently operated, locally controlled storage unit to follow dispatch instructions issued by the ISO has not been adequately addressed in prior studies. It is emphasized that this goal is completely different from that of some prior studies, which is to schedule the storage as a centralized asset to achieve some technical objectives for the grid, e.g., in [76] – [78].

Dispatchability considerations of independently operated, locally controlled storage has not been addressed in previous contributions in this area.

1.4.3.2   Research Potential

From the ISO's point of view, privately owned storage could be categorized as dispatchable or non-dispatchable assets. Since dispatchable assets play an essential role in preserving the stability of the grid, utility-scale storage units are preferred to be operated as dispatchable assets in the market. For an independently operated storage unit (i.e., not jointly operated with another source), the outflow energy from storage to the grid is dependent only upon the inflow energy to storage from the grid. In this case, if the storage charging bid is not accepted by the ISO in certain hours, the storage may not be able to follow its discharging bid in all hours. On the other hand, if the storage discharging bid is not accepted by the ISO in certain hours, storage may not be able to follow its charging bid in all hours. Final dispatch instructions for storage in the market are determined by the ISO based on accepted bids of storage and the grid's technical constraints; these instructions are usually different from the storage original bids [74]. Using the conventional scheduling algorithm, storage is not able to follow all of the dispatch instructions, and thus, it is not considered as a fully dispatchable asset in the market.

Appropriate algorithms are required to clear the aforementioned issue in order for the storage to be operated in the market as a dispatchable asset. Studies are required to compare the operation of dispatchable and non-dispatchable storage units.

1.4.4   Scheduling of Load-storage Systems

1.4.4.1   Literature Review

Grid-scale storage can be deployed to address the issues that have appeared as a result of the intermittent operation of renewable sources; at the same time, storage can profit through arbitrage by shifting surplus energy from off-peak to peak periods. However, a grid-scale storage unit relies on certain geographic conditions and an accessible transmission line that has sufficient capacity. Another approach is to deploy small/medium-scale storage at the consumer end.

Some studies in the literature show development of different optimization-based models for the operation of grid-scale storage, e.g., in [79]. Some technical reports in the literature evaluate the economic viability of grid-scale storage deployment in real-world electricity markets, e.g., in [80], [81]. Based on these studies, the intensive capital cost of grid-scale storage is one of the most important obstacles for storage deployment. Geographic limitations and unavailability of transmission lines with sufficient capacity at storage sites may add even more challenges for grid-scale storage deployment to succeed.

Distributed storage deployment is another way for energy shifting. In such a case,

the aforementioned issues are less challenging since specific locations for storage and availability of transmission lines with a large free capacity at storage sites are not needed. Several studies in the literature consider the application of small/medium-scale storage at the distribution level to achieve various objectives, e.g., energy shifting and load leveling.

One stream of research seeks to employ medium-scale storage in microgrids in which renewable generation sources are also included, e.g., in [10], [82]– [86]. The microgrid, in this case, can both absorb power from the grid and inject power into the grid. Another stream of research aims to optimally operate small-scale storage units for household energy management in the presence of renewable energy sources at a residential location, e.g., in [87]– [92]. However, from the consumers' perspective, investments for local generation may not always be economically attractive due to the availability of surplus energy during off-peak periods where inexpensive or even negative prices occur in several markets, such as Ontario's electricity market. Inexpensive energy in the grid could then be purchased and stored by consumers during off-peak periods and used later during peak periods when energy is expensive.

Some studies in the literature seek to optimally operate small-scale storage for optimal load shifting of residential sites, e.g., in [93], [94]. They assume residential sites are priced according to wholesale market prices. However, this assumption does not hold in practice since residences are priced based on Time-of-Use (TOU) rates. In [95]– [98], the aim is to optimally operate small-scale storage units for residential use based on TOU rates. TOU rates are fixed electricity prices with different levels depending on the time of the day. There are no negative or spike values in TOU rates; thus, there are always less arbitrage opportunities in TOU rates compared to wholesale prices. There are also several practical limitations to deploying storage for residential places due to the huge numbers of storage units needed and the complicated coordination of these storage units.

A load forecast is needed for optimal scheduling of residential storage. Since there is no regular and predictable trend in the energy consumption of an average residence (e.g., a house), a deterministic forecast of the load is not usually possible. Hence, the load forecast in this case is considered as a random variable in a stochastic optimization problem. However, for a large-scale consumer (e.g., a big company, university, or data center), load forecasting with a reasonable forecast accuracy would be a viable task due to the fairly consistent daily and seasonal trends of energy consumption.

The optimal operation of storage for load shifting or load leveling of large-scale electricity consumers has been previously investigated in the literature, e.g., in [99]; where authors have developed self-scheduling optimization models for hourly scheduling of a distributed storage unit in the DAM. In the self-scheduling model, the load-storage system

submits a schedule to the DAM, indicating the amount and time of energy consumption. Then, the load-storage system has to follow that schedule in the operating day. The forecasts of load and market prices are assumed as given inputs to the model in [99]; thus, the impact of forecast inaccuracies on the storage operation is not investigated.

In the self-scheduling model, the storage schedule cannot be updated in real-time, and thus, the self-scheduling model performs less than optimally. For this reason, the self-scheduling model suffers significantly from forecast error since storage is scheduled based on an inaccurate market price forecast, and there is no opportunity to correct optimal decisions in real-time. Therefore, in practice, the self-scheduling model limits the opportunities to attract investments in building new storage units at the consumer's end. According to the regulations set in most electricity markets, large-scale loads are not required to be self-scheduled in the market; thus, they can update their operational schedules in real-time [74]. Additionally, in previous contributions in this area, storage is assumed to be already available; therefore, the Capital Expenditure (CAPEX) and Operating Expenditure (OPEX) of storage are not included in their economic analyses.

The economic viability of a load-storage system governed by a real-time optimization-based model considering the storage CAPEX and OPEX has not been addressed in previous contributions.

1.4.4.2   Research Potential

Storage units can be procured by large-scale electricity consumers and jointly operated with their loads. Consumers benefit through shifting their loads from peak to off-peak periods and availability of power in case of grid power outages. The grid benefits through peak-shaving and less chance of congestion in both the transmission and distribution lines. From the grid's perspective, this type of storage utilization could be referred to as *distributed storage deployment*. Regardless of distributed storage benefits for the grid, private consumers only invest in storage if its profit outperforms its capital cost.

New mechanisms are needed to aggregate various benefits of storage for large-scale electricity consumers and compare the costs of consumers with and without storage. This has not been adequately addressed in the previous contributions in this area.

1.5   Objectives and Scope of the Thesis

The main objectives and scope of the thesis for the main topics are listed below.

1.5.1   Scheduling of Storage for Exploiting Arbitrage

i) To develop a Real-time Optimal Scheduling (RTOS) algorithm by formulating a Mixed Integer Linear Programming (MILP) optimization problem which aims to generate revenue by utilizing arbitrage opportunities available due to the volatility of electricity prices.

ii) To develop the electricity price modulation as part of the optimization problem to competitively offer incentive by utility regulators to private investors in storage.

iii) To study the economic viability of the operation of large-scale energy storage technologies in electricity markets.

1.5.2   Scheduling of Storage for Congestion Relief

i) To develop a new optimal scheduling algorithm based on an adaptive penalizing mechanism which optimally prepares the storage to follow external congestion relief commands.

ii) To study the required amount of financial compensation for the storage owner due to its contribution to congestion relief.

1.5.3   Scheduling of Storage as a Dispatchable Asset

i) To develop a new optimal scheduling algorithm which aims to enable an independently operated, locally controlled storage unit to accept external dispatch instructions issued by the ISO.

ii) To propose a new index to measure the storage dispatchability in a competitive electricity market.

iii) To investigate the efficacy and feasibility of the proposed algorithm using real-world data adopted from Ontario's electricity market.

1.5.4   Scheduling of Load-storage Systems

i) To develop a new real-time multi-step optimization-based model to optimally schedule the joint operation of a large-scale load and a storage unit.

ii) To incorporate a real-time load forecasting model, suitable for large-scale loads, into the optimal scheduling algorithm using soft constraints, slack variables, and penalizing mechanisms.

iii) To examine the operation of the proposed model and to compare the model operation with the self-scheduling model using a real-world case study.

1.6 Thesis Outline

This thesis has been organized in six chapters and three appendices as follows:

Chapter 1 of the thesis includes an introduction to the research topic along with its importance to the area of Power and Energy Systems. A comprehensive literature review over the relevant area is presented. The research potential is also presented in this chapter. Further, objectives and scope of the thesis are discussed.

Chapter 2 of the thesis mainly aims to investigate the economic viability of grid-scale storage deployment for massive energy shifting. The behaviour of Ontario's electricity market in the past decade is analyzed, and the need for energy storage deployment is justified to address some recent challenges in the market. Large-scale storage units are modeled and employed for evaluations. An RTOS algorithm is developed by formulating an MILP optimization problem which aims to generate revenue by exploiting arbitrage opportunities available in electricity markets. The optimization algorithm is utilized to employ a large-scale peak-shaving storage using (i) wholesale and (ii) TOU electricity prices. The arbitrage profits resulting from the storage operation in both studies are presented and compared. The price modulation is proposed and examined as a new and effective approach to provide uniform and at the same time competitive incentive to privately owned storage by utility regulators. The efficacy of the proposed method to competitively incentivize storage operation is validated.

Chapter 3 of the thesis mainly seeks to investigate the idea of employing privately owned large-scale storage for long-term transmission congestion relief. A new algorithm based on an adaptive penalizing mechanism and soft constraints is proposed. The forecast of external ISO's commands for congestion relief is incorporated into the optimization problem to best prepare the storage for such commands. The feasibility and efficacy of the proposed algorithm, which aims to optimally employ large-scale storage for congestion relief, are revealed through various simulation studies.

Chapter 4 of the thesis mainly aims to investigate strategies for storage operation as a dispatchable asset in the market. A new optimal scheduling algorithm is proposed to

enable independently operated, locally controlled storage to accept dispatch instructions issued by ISOs. Storage in this case is referred to as *dispatchable storage*. The efficacy and feasibility of the proposed algorithm are validated using real-world data. Revenue values of dispatchable and non-dispatchable storage are computed and compared.

Chapter 5 of the thesis mainly seeks to investigate the application of medium-scale storage units for energy shifting at the distribution level. Storage units are proposed to be procured by large-scale electricity consumers and jointly operated with their loads. A new model for optimal scheduling of storage-based electrical loads considering both the CAPEX and OPEX of storage is proposed and formulated. A real-time load forecaster is incorporated into the optimal scheduling algorithm using soft constraints, slack variables, and penalizing mechanisms. The application of the proposed model to a real-world large-scale institutional load in Ontario, Canada, is explained and compared with previous models in the literature.

The thesis is concluded in Chapter 6. The main outcomes of the thesis are presented. The contributions of the thesis are listed, and the significance of the thesis is presented. In addition, the future areas of research are discussed.

Appendix A presents the proof of theorem for load forecasting. Analysis of the load forecaster is presented in B. Practical aspects for implementation of the load forecaster are discussed in Appendix C.

Chapter 2

Scheduling of Storage for Exploiting Arbitrage

2.1 Introduction

In this chapter, the behaviour of Ontario's electricity market in the past decade is analyzed, and the need for energy storage deployment is justified to address some recent challenges in the market. Comprehensive economic studies are conducted to investigate the economic viability of large-scale storage deployment exploiting energy price arbitrage opportunities. Comparative studies are conducted to investigate the value and benefit of a storage unit optimized to utilize wholesale and contract-based electricity prices. The electricity price modulation is proposed as part of the RTOS algorithm to virtually increase energy price arbitrage to competitively offer incentive to storage owners. The purpose of the proposed incentivisation method is to fill the gap between current and a stable expected ROR. By implementing the proposed approach, the more the storage is operated to support the power grid by means of energy shifting/peak shaving, the more incentives it can receive from the utility regulator; this is because the amount of incentive is dependent on the charging in off-peak periods and discharging in peak periods which are appropriate for both the utility regulator/system operator and storage investor.

2.2 Investigation of Ontario's Electricity Market

Over the past decade, there has been a significant change on how electricity is generated in Ontario and across the world. The increase in renewable energy penetration into the market has altered the overall behaviour of the energy market, with negative electricity

Table 2.1: Annual Average of Ontario's Market Data

Year	HOEP ($/MWh)	Market Demand (MW)	Ontario's Demand (MW)	Wind Power (MW)	Imported Power (MW)	Exported Power (MW)
2003	54.05	18034	17320	—	1192	715
2004	49.95	18535	17456	—	1112	1080
2005	68.49	19081	17919	—	1250	1162
2006	46.38	18544	17244	59	707	1300
2007	47.81	18778	17375	119	822	1403
2008	48.83	19453	16926	162	1288	2527
2009	29.52	17614	15886	265	553	1724
2010	36.25	17963	16232	313	728	1731
2011	30.15	17616	16150	423	447	1467
2012	22.80	17749	16085	508	538	1665
2013	24.98	18099	16066	576	557	2090
2014	32.39	18068	15959	763	562	2177

prices even starting to appear [1]. Negative energy prices represent a greater supply than the market demands. Most negative price hours appear at night, when the demand is at its minimum level. At the supply end, issues have appeared as a result of intermittent operation of sources such as wind, which generate maximum power at night when it is not needed, and the inflexible generation of NPPs [1].

In this section, using the actual market data obtained from [65], studies are conducted over Ontario's market behaviour in the past decade to extract useful information about sources that have altered the market behaviour. As a result, an argument is made for deployment of large-scale storage to address the issues that have appeared due to intermittent nature of renewable sources recently penetrated more in the market.

2.2.1 Annual Changes of Market Data

Actual data, including hourly Ontario energy prices (HOEPs), market and Ontario's demands, wind power, imports, and exports are obtained from the Ontario Independent Electricity System Operator's (IESO's) Web site at [65] for 2003 to 2014. The yearly average values of these data are reported in Table 2.1. For the sake of comparison, those data that have changed significantly since 2003 are shown in Fig. 2.1. The wind power data were publicly available since March 1, 2006 [65]; thus, wind data are not indicated
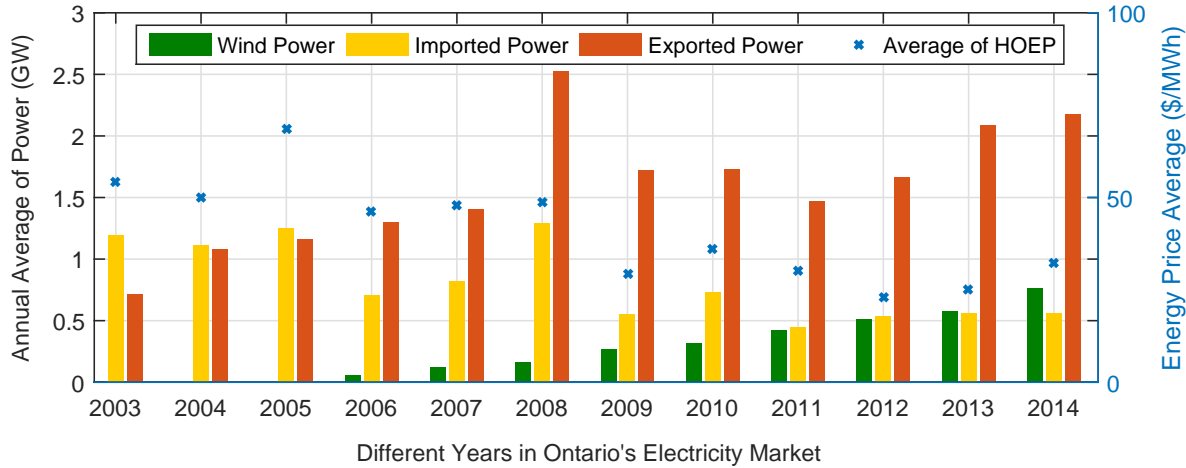
Figure 2.1: Annual changes of data in Ontario's electricity market.

in Table 2.1 and Fig. 2.1 from January 1, 2003 till March 1, 2006. Given the trend of changes in these data, the following observations are presented:

- The annual average of HOEPs has decreased in recent years. As will be discussed later in this chapter, this is partly because of negative prices appearing more often in the market since 2008 due to higher supply than the demand in certain hours.

- The annual average values of market and Ontario's demand have not changed considerably over the years.

- As represented in Fig. 2.1, wind generation has an increasing trend since 2006. In addition, the annual average value of imports and exports has an overall decrease and increase, respectively.

2.2.2   Negative Prices in the Market

Fig. 2.2 shows the annual summation of negative electricity prices in Ontario's market from 2003 to 2014. As shown in Fig. 2.2, negative prices have appeared more frequently after 2008 in the market.

In order to investigate the impact of energy suppliers on the appearance of negative prices, the annual energy supplies by different sources in Ontario's market, obtained from [65], are reported in Table 2.2 in TWh and % of the total energy. As indicated in Table 2.2, while nuclear generation has the maximum contribution, it has not changed considerably over the years. The second biggest contributer in the market is hydro generation which has not changed significantly either. However, contribution of coal generation has substantially decreased over the years with less than 1% in 2014.
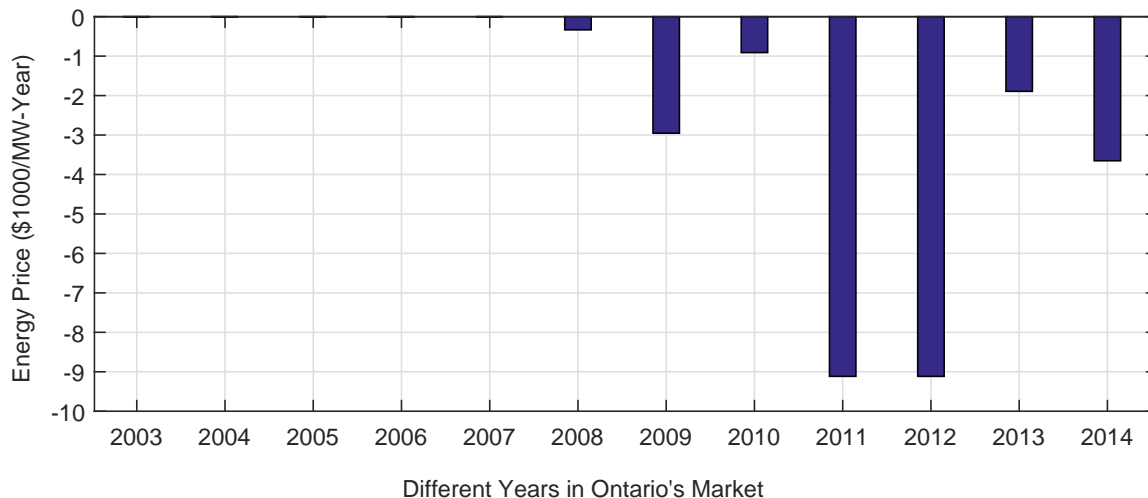
Figure 2.2: Annual summation of negative prices in Ontario's electricity market.

Table 2.2: Energy Supply in Ontario by Different Sources (in TWh and % of Total Energy) [65]

Year	Nuclear	Hydro	Coal	Gas/Oil	Wind	Other
2008	84.4	38.3	23.2	11.0	1.4	1.0
	53%	24.1%	14.5%	6.9%	0.9%	0.6%
2009	82.5	38.1	9.8	15.4	2.3	1.2
	55.2%	25.5%	6.6%	10.3%	1.6%	0.8%
2010	82.9	30.7	12.6	20.5	2.8	1.3
	55%	20.4%	8.3%	13.6%	1.9%	0.8%
2011	85.3	33.3	4.1	22.0	3.9	1.2
	56.9%	22.2%	2.7%	14.7%	2.6%	0.8%
2012	85.6	33.8	4.3	22.2	4.6	1.3
	56.4%	22.3%	2.8%	14.6%	3%	0.8%
2013	91.1	36.1	3.2	18.2	5.2	0.2
	59%	23%	2%	12%	3%	<1%
2014	94.9	37.1	0.1	14.8	6.8	0.3
	62%	24%	<1%	10%	4%	<1%

Gas/oil generation has been variable with 10% in 2014. Wind generation has considerably increased with 4% in 2014. Other sources (e.g., biofuel and solar) do not have a significant contribution, and thus, a notable impact on the market behaviour. No accurate correlation is observed between the energy supply and appearance of negative prices since other factors could be involved in creation of negative prices; however, phasing out dispatchable sources (i.e., coal-fired plants), inflexible generation of nuclear plants, must-run hydroelectric units, and generation of non-dispatchable sources (i.e., wind) can be important causes for appearance of negative prices in the market.

Table 2.3: Analysis of Negative Prices in Ontario's Electricity Market

Year	Number of Hours	HOEP Average ($/MWh)	% of Nighttime Hours
2008	38	-8.8	100
2009	351	-8.42	78
2010	41	-22.22	83
2011	166	-54.92	86
2012	167	-54.59	91
2013	366	-5.17	87
2014	861	-4.24	80

The main reason for phasing out all coal units and integration of more renewable generation into the grid has been to reduce CO_2 emissions. However, most of the renewable generation cannot be effectively utilized when needed, and thus, might be either taken off the grid or partly exported to neighbouring markets with very low or negative prices.

Negative energy prices in Ontario's electricity market have been analyzed and the results have been reported in Table 2.3. As presented in this table, the number of negative price hours has an increasing trend in general, i.e., up to 861 hours in 2014 although the average of negative prices has decreased in recent years. In addition, most negative prices have incurred during nighttime when the demand is minimum, indicating a higher energy supply than the demand as a reason for incurring negative prices. The surplus energy has to be exported to neighbouring markets in order to make a balance between the supply and the demand. Exporting energy to neighbouring markets at negative prices can cause large financial losses for Ontario's market. This is because not only does Ontario's market take no payment for the energy it exports, but also it has to pay to eliminate the excess energy in the grid. As more push is applied to minimize the use of hydrocarbons for electricity generation, the penetration of non-dispatchable and intermittent energy sources (i.e., renewable sources) into the grid is expected to increase even more in the future. Thus, more negative prices are expected to arise in the market, and therefore, more financial losses can incur in the near future.

Grid-scale energy storage can be deployed to shift the surplus energy from off-peak to peak periods and straightforwardly benefit via arbitrage. Storage generates arbitrage revenue by purchasing inexpensive energy during off-peak periods and selling it back to the market during peak-periods when energy is expensive. In such a case, the overall demand increases during off-peak periods and decreases during peak periods which in the end could resolve the negative price issues. The intensive CAPEX and relatively
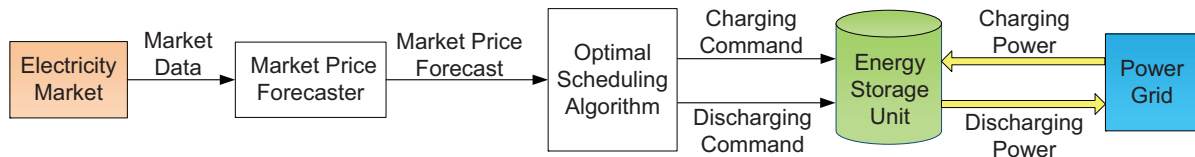
Figure 2.3: General framework of storage scheduling for utilizing arbitrage and energy shifting.

lower ROR of a storage unit are the most important obstacles for storage deployment in an electricity market. However, storage deployment will be becoming more economical in the near future due to the growth in storage technologies and availability of multiple sources of revenue for storage operation.

2.3 Real-time Optimal Scheduling of Storage

The framework for exploiting arbitrage in the electricity market is represented in Fig. 2.3. As shown in this figure, there is an optimal scheduling algorithm which computes the optimal charging and discharging powers for storage; these are commanded to the storage unit. A forecast of market prices are needed by the controller which is provided by a market price forecaster.

To develop an RTOS algorithm for a privately owned storage unit, an MILP optimization problem is formulated as explained in this section. The optimization horizon of 24 h with 1-h time steps is considered to determine optimal charging and discharging power set-points. The time step of 1 h is selected since market prices are updated every hour in the case-market of this thesis, i.e., Ontario's electricity market. Since optimal decisions are made for the present and future time steps (i.e., optimization horizon), the optimal scheduling problem would be a multi-interval optimization problem. Decisions are also updated by re-running the optimization calculations every hour to account for the time-varying nature of electricity prices in the market. In this case, the optimal scheduling problem includes $T/\Delta T = 24\,\mathrm{h}\,/1\,\mathrm{h} = 24$ time steps, each of which represents a 1-h time interval. All of the optimization variables would be 1-D arrays with 24 elements decided by the end of each hour of the scheduling horizon. The aforementioned method is referred to as *real-time scheduling* on an hourly basis in this thesis; it is also referred to as *rolling time horizon* or *model predictive control* [100], [101].

The objective function of the optimization problem aiming to maximize storage rev-

enue by exploiting arbitrage opportunities available due to the price volatility is as follows:

$$\underset{P_t^{S,Chg}, P_t^{S,Dhg}}{\text{Maximize}} \sum_{t \in \mathcal{N}_i} \left((P_t^{S,Dhg} - P_t^{S,Chg}) . E_t^{FMrk} - C^{S,DhgO} . P_t^{S,Dhg} - C^{S,ChgO} . P_t^{S,Chg} \right) . \Delta T. \tag{2.1}$$

The objective function in (2.1) includes the following terms:

$$\text{Energy price arbitrage benefit: } (P_t^{S,Dhg} - P_t^{S,Chg}) . E_t^{FMrk} . \Delta T \tag{2.2}$$

$$\text{Storage operating costs: } (C^{S,DhgO} . P_t^{S,Dhg} + C^{S,ChgO} . P_t^{S,Chg}) . \Delta T, \tag{2.3}$$

subject to the following operational constraints of the storage:

$$b_t^{S,Chg} . P_{min}^{S,Chg} \leq P_t^{S,Chg} \leq b_t^{S,Chg} . P_{max}^{S,Chg} \qquad \forall t \in \mathcal{N}_i \tag{2.4}$$

$$b_t^{S,Dhg} . P_{min}^{S,Dhg} \leq P_t^{S,Dhg} \leq b_t^{S,Dhg} . P_{max}^{S,Dhg} \qquad \forall t \in \mathcal{N}_i \tag{2.5}$$

$$SOC_{min}^{S} \leq SOC_t^{S} \leq SOC_{max}^{S} \qquad \forall t \in \mathcal{N}_i \tag{2.6}$$

$$SOC_t^{S} - SOC_{t-1}^{S} + \left(P_t^{S,Dhg} / \eta^{S,Dhg} - \eta^{S,Chg} . P_t^{S,Chg} + \eta^{S,Dsp} . SOC_t^{S} \right) . \Delta T = 0$$

$$\forall t \in \mathcal{N}_i, \tag{2.7}$$

where $\mathcal{N}_i$ is the set of time steps defined as follows:

$$\mathcal{N}_i = \{i, \ldots, i + N - 1\}, \tag{2.8}$$

where i refers to the present time step, defined in a T–hour time notation divided by the time interval ΔT. For instance, at 5:00 am and for $\Delta T = 1$, $i = 5/1 = 5$.

In (2.1)–(2.8), except E_t^{FMrk}, other parameters are non-negative (refer to the nomenclature for definitions of parameters).

The objective function, expressed in (2.1), includes the financial benefit of selling electricity to the market, the cost of purchasing electricity from the market, and the storage operating cost for charging and discharging within the optimization horizon, i.e., 24 h. In (2.1), E_t^{FMrk} is the electricity price forecast at the time step t while it is equal to the actual price at the present moment, i.e., $t = 1$. Equations (2.4)–(2.6) express charging and discharging powers and State of Charge (SOC) constraints for the storage. It is clarified that storage would not charge and discharge at the same time (i.e., at the same price level) since this is against the objective of the optimization problem.

In order to generalize the problem, minimum charging/discharging powers of storage are assumed to be non-zero if the charging/discharging plant has online status. In such a case, charging and discharging variables are not continuous from zero to the minimum

value; thus, the optimization problem becomes non-linear. As defined in the nomenclature, binary variables $b_t^{S,Chg}$ and $b_t^{S,Dhg}$ are incorporated into (2.4) and (2.5) to keep the model within the framework of a linear optimization problem. If a zero value is decided for charging or discharging power of storage, the corresponding binary variable is set to zero by the optimization problem; if a positive value is decided for charging or discharging power, the corresponding binary variable will be set to one by the optimization problem. Therefore, binary variables are indirectly included in the objective function. If charging and discharging variables can continuously change from zero to the maximum value, the binary variables will not affect the validity of the optimal decisions.

The storage energy balance is stated by (2.7), defining the relation of SOC at the two consecutive time steps t and $t - \Delta T$. Equation (2.7) accounts for power losses in charging and discharging plants as well as losses resulting from self-discharge. In (2.7), SOC_0^S (i.e., SOC_{t-1}^S at $t = 1$) represents the initial SOC and is assumed to be within the acceptable range, i.e., 10% of the maximum SOC in this thesis.

The optimization problem including variables, parameters, constraints, and the objective function are defined in a file, which is called hereafter problem mod file, using GNU MathProg modeling language in MATLAB. The values for the problem parameters are generated at each time step by a MATLAB code in another file, hereafter called data file. The data file includes storage parameters such as minimum and maximum charging/discharging powers, SOC at the present time step, etc. The real-time actual and 24-h-ahead forecast prices are also inputted to the data file as E_t^{FMrk}. If a more accurate price forecast is available up to the first few hours, it could be substituted for the first few hours of the 24-h-ahead forecast. For instance, in Ontario's electricity market, the next 3-h price forecast is published and updated every 1 h [65]. Both data and mod files are inputted to the GNU Linear Programming Kit (GLPK) package [102]. Then, the optimization problem is solved by the GLPK package to find the optimal values of charging and discharging power set-points. The charging and discharging power set-points at the present time (i.e., $P_1^{S,Chg}$ and $P_1^{S,Dhg}$) provide the required commands to the storage. In the next time step, the SOC is calculated based on the latest power set-point commands. Then, the RTOS algorithm is executed to derive new power set-point commands. This process continues until the end of the simulation period.

2.4 Sizing and Modeling of a Storage Unit

Due to its lower CAPEX and its capability to be positively influenced by the availability of waste heat, a CAES unit is sized and used for evaluations. If other types of large-scale

Table 2.4: Modeling and Operating Parameters of a Compressed-air Storage Unit

$P_{min}^{S,Chg} = 80\% \times P_{max}^{S,Chg}$	$\eta^{S,Chg} = \eta^{S,Dhg} = 84\%$
$P_{min}^{S,Dhg} = 3\% \times P_{max}^{S,Dhg}$	$C^{S,Main} = 5\% \times \text{Capital Cost} /(\text{Storage Age} = 30 \times 365 \times 24)$
$SOC_{min}^{S} = 10\% \times SOC_{max}^{S}$	$C^{S,ChgO} = 60\% \times C^{S,Main}/P_{max}^{S,Chg}$
$\eta^{S,Dsp} = 0.0416\% \times SOC_{t}^{S}$	$C^{S,DhgO} = 40\% \times C^{S,Main}/P_{max}^{S,Dhg}$

Table 2.5: Storage Revenue for Perfect Price Forecast (in Million \$) and Imperfect Price Forecast (in Million \$ and % of the Ideal Revenue) for a Typical Year in Ontario's Electricity Market

Storage Reservoir Capacity	Perfect Price Forecast (Ideal Revenue)	Imperfect Price Forecast (Real Revenue)
500 MWh	\$5.4434 M	\$2.9937 M (54.99%)
1000 MWh	\$6.9728 M	\$4.5470 M (65.21%)
1500 MWh	\$7.1985 M	\$4.7489 M (65.97%)
2000 MWh	**\$7.2063 M**	**\$4.7586 M (66.03%)**
2500 MWh	\$7.1979 M	\$4.7441 M (65.91%)
3000 MWh	\$7.1862 M	\$4.7377 M (65.93%)

storage units, e.g., Pumped-hydro Energy Storage (PHES) or CES units are used, the main outcomes will not change. A CAES unit is basically composed of three main plants as follows: Charging plant, compressed-air reservoir plant, and discharging plant. Based on its application, a CAES unit can have different ratings for each of these three plants. These ratings for the overall plant can be specified based on a feasibility study to meet the power available during off-peak time periods versus the power needed during peak time periods in the market [103]. In this thesis, a CAES unit is sized and modeled in MATLAB based on the parameters reported in Table 2.4. The capital cost of the plant is assumed to be \$1 Million/MW of discharging power [103].

In order to find the appropriate capacity for the storage reservoir, different sizes have been chosen, and accordingly, the storage revenue has been computed for a typical year in Ontario's electricity market (i.e., 2007) considering both the CAPEX and OPEX of storage. The results have been reported in Table 2.5. In this table, the ideal revenue (obtained using the perfect price forecast) and real revenue (obtained using back-casting as an imperfect forecasting approach) under six different capacities (based on the literature, e.g., [28]) has been reported. The maximum charging and discharging powers and the round-trip efficiency of storage have been considered 100 MW and 70%, respectively.

Table 2.6: Ratings of a Compressed-air Storage Unit

Storage Capital Cost	$P_{max}^{S,Chg}$	$P_{max}^{S,Dhg}$	SOC_{max}^{S}
\$100 Million	100 MW	100 MW	2000 MWh

According to the results indicated in Table 2.5, the higher the capacity is (from 500 to 2000 MWh), the higher the revenue capture would be. However, there would be no more potential for increasing revenue capture by increasing the capacity larger than 2000 MWh. In fact, the revenue could be slightly less at capacities larger than 2000 MWh due to a higher energy dissipation rate for larger capacities. Both the ideal and real revenue values are maximum at 2000 MWh capacity, i.e., \$7.21 M and \$4.76 M, respectively. For this reason, the optimal capacity is selected as 2000 MWh for the rest of the study. Considering that the cost of incremental capacity (\$/MWh) is quite low for a CAES unit, different capacities in the above-mentioned range would not considerably impact the storage capital cost even though increasing the storage capacity may be limited in practice due to geographical constrains. Nevertheless, a 2000-MWh reservoir capacity for a CAES unit falls in the ranges proposed in prior studies, e.g., in [28], [104].

The compression and generation power ratings, reservoir capacity, and the capital cost of the CAES unit are calculated and reported in Table 2.6.

The operating parameters, used for modeling and simulation of the CAES in this study, are reported in Table 2.4. The values of these parameters are typical and can be different for different types of CAES technologies. In large-scale storage including the CAES technology, to maintain the rated efficiency, it is required to operate the compression plant close to its rated value. Therefore, $P_{min}^{S,Chg}$ is set to 80% of $P_{max}^{S,Chg}$. However, the generating turbine and its supplying pump can be efficiently operated at very low power set-points. Energy storage dissipation is assumed to be 1% per day resulting in $1/24\% = 0.0416\%$ per hour. The charging efficiency (i.e., $\eta^{S,Chg}$) and discharging efficiency (i.e., $\eta^{S,Dhg}$) have been assumed to be 0.84%, causing a round-trip efficiency of 70% [28], a typical value for a highly efficient unit. With a lower efficiency, the storage would not be scheduled to exploit lower arbitrage benefits since it might not be able to overcome the energy losses during the process. Hence, it generates less revenue. Additionally, a higher portion of the energy would be lost during the process. Thus, the absolute value of revenue capture (in terms of \$) decreases with a lower efficiency.

Nevertheless, a reasonable variation of the parameters reported in Table 2.4 will not affect the ultimate outcome of the present study. Using these parameters, the CAES is modeled, and the optimization problem is solved to obtain optimization variables.

Table 2.7: Analysis of Ontario's Wholesale Electricity Market

Year	Ideal Revenue (Million $)	Average Annual Purchase Price ($/MWh)	Average Annual Sale Price ($/MWh)	Arbitrage Benefit ($/MWh)
2006	6.03	24.98	63.26	38.28
2007	7.21	29.99	75.20	45.21
2008	8.86	27.40	82.29	54.89
2009	5.26	10.76	41.63	30.87
2011	4.62	16.72	42.96	26.24
Average	6.39	21.97	61.07	39.10

2.5 Storage to Utilize Wholesale Market Prices

In this section, Ontario's wholesale market prices have been used for evaluations. The Ontario IESO publishes two sets of Pre-dispatch Prices (PDPs) as follows: 24-h-ahead and 3-h-ahead PDPs both with 1-h time resolutions (i.e., $\Delta T = 1$) [65]. The first set is the next day PDPs (starting from 1 am) published at 3:30 pm Eastern Time every day while the second set is the next 3-h PDPs published every hour. The challenge of using IESO-generated PDPs is that the complete next 24-h forecast is not available for every time step between 1 am to 3 pm. For instance, at 10 am, only the next 15 h, i.e., from 10 am to midnight is available. To mitigate this issue, PDPs at the same hours of the last day can be duplicated for the missing hours.

The real-time simulation is executed using Ontario's market prices in different years for the three cases as presented in Sections 2.5.1–2.5.3.

2.5.1 Optimal Scheduling Using a Perfect Price Forecast

The price forecasts are substituted with the actual prices. In this case, the resulting revenue would be equal to the ideal revenue. The ideal revenue values (Million $) achieved using the perfect price forecast, average purchase and sale prices ($/MWh), and the average arbitrage benefit ($/MWh), i.e., the difference between sale and purchase prices, are reported in Table 2.7. The differences in ideal revenue for different years, stemmed from different arbitrage potentials in Ontario's electricity market for different years. The higher the arbitrage benefit is, the higher the storage revenue will be.

Table 2.8: % of Ideal Revenue Capture Using Ontario's Wholesale Market Prices

Year	Conventional Method	Back-Casting Method
2006	53.99	68.28
2007	51.11	66.03
2008	39.61	69.28
2009	51.36	73.22
2011	43.25	71.69
Average	47.37	69.35

2.5.2   Optimal Scheduling Using Pre-dispatch Prices

This approach is called conventional algorithm in this study. In this case, the PDPs issued by Ontario's IESO are used (imperfect forecast). Table 2.8 reports the revenue capture for each year and the five-year average in percent of the ideal revenue. It is observed that a significant portion of revenue is lost due to forecast error in each year.

2.5.3   Optimal Scheduling Using Back-casting Method

In this approach, the storage scheduling for the next 24 h is performed using the actual prices in the last 24 h. Table 2.8 reports the annual revenue capture in percent of the ideal revenue by this approach. It is observed that back-casting method has been more effective than the conventional method in capturing higher revenue, yet a considerable amount of revenue has been lost due to inconsistency of inter-day market prices.

2.5.4   Real-time versus Non-real-time Scheduling of Storage

In a real-time algorithm, a 24-h-length window is rolled over the prices; this is also known as the Model Predictive Control (MPC). The storage scheduling could be then updated using prices in 24 h ahead at each time step. For instance, when the present time is in the middle of the day, the storage scheduling is performed not only based on the prices available for the rest of the day, but also according to the prices of the next half day. In such a case, a more precise schedule could be made for storage, and especially peak and off-peak prices in the next half of the day could be kept into consideration. However, in a non-real-time algorithm, the scheduling is performed for the next 24 h while the storage schedule is not updated until the end of the day; this is also known as the self-scheduling approach. In such a case, in each day, the prices of the next day are not taken

Table 2.9: Storage Revenue (in Million $ and % of Ideal Revenue) for a Typical Year

Scheduling Algorithm	Perfect Price Forecast (Ideal Revenue)	Imperfect Price Forecast (Real Revenue)
Non-real-time	$6.6290 M	$2.7202 M (41.03%)
Real-time	$7.2063 M	$4.7586 M (66.03%)

into consideration, and thus, the storage schedule is not corrected to take advantage of new arbitrage opportunities in the next day. In addition, under a real-time algorithm, a more accurate schedule could be created when the updated price forecast is used due to availability of a more accurate forecast in the next few hours. Moreover, since the price value in the present time is known under a real-time algorithm, it can substitute for the first hour of the next 24-h price forecast; this way, a more accurate schedule can be made, thereby higher arbitrage revenue could be generated.

For numerical evaluation, the optimization problem has been executed using Ontario's wholesale market prices in 2007, and the resultant storage revenue has been reported in Table 2.9. According to the results in Table 2.9, using the perfect price forecast, the storage revenue is $7.21 M and $6.63 M for real-time and non-real-time algorithms, respectively; these values go down to $4.76 M and $2.72 M, respectively, when an imperfect price forecast is employed using the back-casting method. Thus, the storage operation is significantly more profitable when it is scheduled using a real-time algorithm as compared to a non-real-time scheduling approach. These results also indicate that using the imperfect price forecast, only 66% and 41% of the ideal revenue could be captured under real-time and non-real-time optimal scheduling algorithms. Hence, storage revenue considerably decreases due to price forecast error under both algorithms.

2.5.5   Profitability of Investment in Storage

In order to analyze the profitability of the investment, the expected ROR needs to be determined, which could be different for each project depending on its risk profile. In the following, the ability of storage operated under different algorithms to capture an annual net revenue equal to 8.34% of the storage capital cost per year is investigated. The annual net revenue of 8.34% is composed of 5% expected return plus the exhausted capital cost over the storage life (i.e., $100\%/30 = 3.34\%$). For a $100 M capital investment, this corresponds to $8.34 M per year. The higher the capital cost is, the higher amount of net revenue would be required to achieve any given ROR, and thus, the chance of being

Table 2.10: Profitability Levels of Investment (in %) and Break-even Time (in Year)

	Perfect Forecast	Conventional Method	Back-Casting Method
Profitability Level	77%	36%	53%
Break-even Time	15.65 Yr	33 Yr	22.57 Yr

profitable for the plant would be less. To fill the gap between current and a stable ROR, incentivisation policies may be applied by the utility regulator to financially support the storage owner. Storage incentivisation is investigated in Section 2.7 of this thesis.

Given that the profitability level of 100% is required for the plant to generate $8.34 M per year, the profitability levels for different methods based on the five-year average revenue in Ontario's electricity market are calculated and compared in Table 2.10. In this table, the break-even time is also reported which is the amount of time needed for generated revenue to equal the initial capital cost. As indicated in Table 2.10, although the plant is not profitable under different algorithms, the back-casting method outperforms the conventional method due to the higher profitability level and lower break-even time. This reveals that the use of PDPs issued by the IESO is not appropriate for storage scheduling due to the significant forecast uncertainty. As a result, storage scheduling using back-casting method is preferred over the publicly available PDPs.

From another perspective, the internal rate of return (IRR) can be used to examine and compare the profitability of investment. The IRR values would be 5%, −1%, and 2% for perfect forecast, conventional method, and back-casting method, respectively. Since these values are less than the expected value of 8.34%, the plant is not profitable under different algorithms. However, the back-casting method outperforms the conventional method due to the higher IRR.

2.6 Storage to Utilize Time-of-Use Prices

In this section, the RTOS algorithm aims to utilize the same CAES technology to utilize contract-based electricity prices. The TOU electricity prices, as an example of contract-based electricity prices, are used to optimally schedule the storage where the storage seeks to generate revenue by exploiting arbitrage opportunities available in TOU rates. The economic benefits of storage utilizing TOU rates are presented and compared with storage benefits utilizing wholesale market prices. The simulation results reveal that while both TOU and wholesale electricity rates do not make any storage investments economically

Table 2.11: Five-year Average of Storage Revenue (in Million $ and % of Ideal Revenue)

Expected Revenue	For Wholesale Market Prices			For TOU Rates
	Perfect Forecast	Conventional	Back-casting	
$8.34 M	$6.39 M	$3.03 M	$4.43 M	$1.92 M

viable, the profitability of the investment in storage operated in the wholesale market is considerably higher as compared to the TOU rates.

Ontario's TOU electricity prices are used to optimally schedule the storage. TOU pricing is a rate structure that reflects the costs associated with electricity production throughout the day. Prices rise and fall over the course of the day and tend to drop overnight and on weekends, depending on the demand and the availability of supply. Currently in Ontario, TOU rates and periods are defined as follows [65], [105]:

- Off-peak is when demand is low and less expensive sources of electricity are used ($75/MWh from 7pm to 7am in summer and winter as well as the entire weekends and holidays).

- Mid-peak is when the cost of energy and demand are moderate ($112/MWh from 7am to 11am and from 5pm to 7pm in summer as well as from 11am to 5pm in winter).

- Peak is when demand is highest and more expensive forms of electricity generation are required ($135/MWh from 11am to 5pm in summer as well as from 7am to 11am and from 5pm to 7pm in winter).

Based on the above-mentioned TOU rates in specific time periods, the optimal scheduling has been executed for one year, and the storage revenue has been calculated. As discussed in Section 2.5.5, the expected annual revenue should equal 8.34% of the capital cost in order for the plant to become profitable. For the purpose of comparison, the five-year average revenue of storage using Ontario's wholesale market prices for three different methods as well as the storage annual revenue using summer and winter TOU prices in Ontario have been calculated and reported in Table 2.11. As reported in Table 2.11, the profitability of the investment in storage, operated in the wholesale electricity market using different optimization methods, is significantly higher as compared to the TOU electricity prices.

As an illustration, actual HOEPs and PDPs publicly available in Ontario's wholesale electricity market (in April, 2011) has been shown in Fig. 2.4. One can observe in
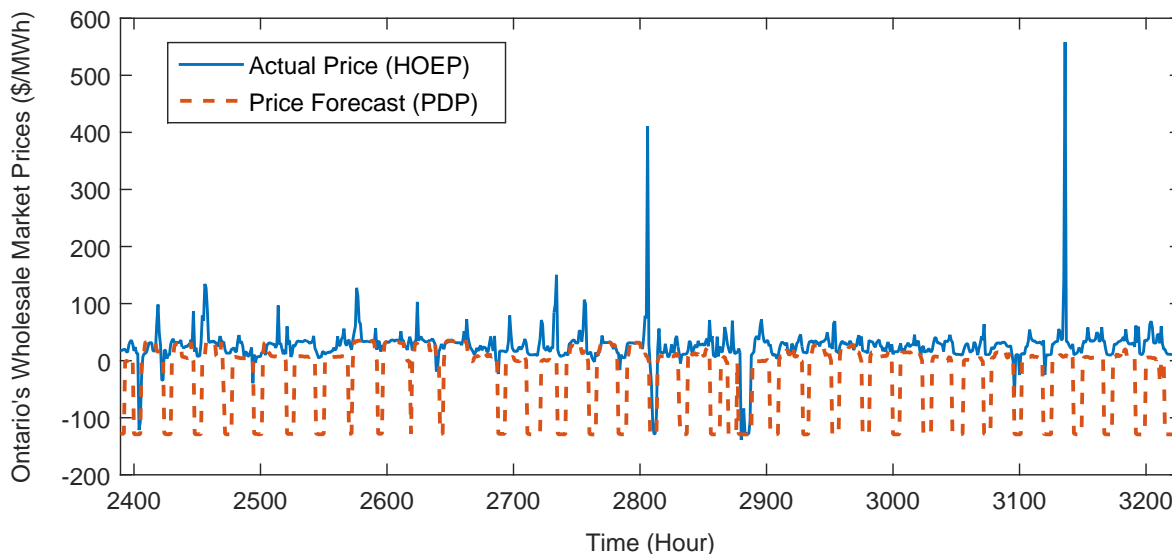
Figure 2.4: Hourly Ontario energy and pre-dispatch prices in Ontario's market (in April 2011).

Table 2.12: Storage Daily Data Utilizing Time-of-Use and Ontario's Wholesale Prices in 2011

	Wholesale Prices	Time-of-Use Rates
Average Cost for Daily Energy Purchase	$8.7 k	$74 k
Average Cost for Daily Energy Sale	$17.2 k	$78 k
Average Revenue for Daily Energy Trade	$8.5 k	$4 k

this figure that there are considerably higher peak prices (up to $560/MWh) as well as significantly lower and even negative off-peak prices (down to –$140/MWh) in wholesale prices which can be utilized by the storage. Specifically, in the wholesale electricity market, when the energy price is very low or even negative, storage charging would be a great advantage since in this way, the average cost for the energy purchase significantly decreases. For the TOU prices, however, this opportunity does not exist since there is a constant value for off-peak prices. For instance, the average cost for the daily energy purchase and the average benefit generated by the daily energy sale are calculated for TOU rates as well as for Ontario's wholesale market prices in 2011 as a sample year and reported in Table 2.12. It can be observed from Table 2.12 that although the energy being sold by the storage is more expensive for TOU rates compared to wholesale prices, it is being purchased quite inexpensively for wholesale prices as compared to TOU rates. As reported in Table 2.12, the average revenue value generated for daily energy trading
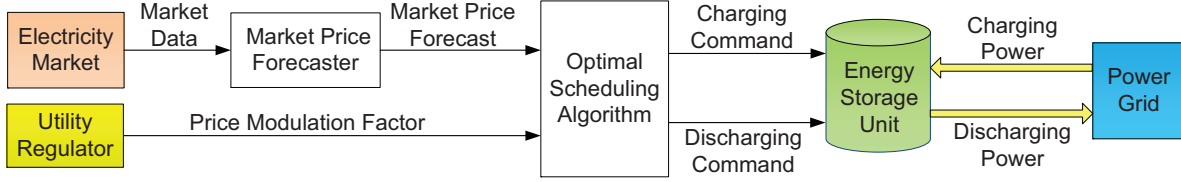
Figure 2.5: General framework of the proposed model for incentivisation of storage.

in wholesale market is \$8.5 k, which is more than two times higher than the revenue generated using TOU rates.

Consequently, although TOU prices have been recently increased, and thus, the storage scheduling models based on contracted electricity prices have been more promising, the models based on wholesale market prices are still more appropriate due to a higher profitability level of the storage investment. Nevertheless, for both TOU and wholesale electricity prices, the price arbitrage is not enough to convince investors to invest in peak-shaving storage since the current revenue is significantly below the expected one, i.e., 8.34% of the capital cost per year equal to \$8.34 M in this study. As reported in Table 2.11, while \$8.34 M would be required to reach to 100% profitability level, the ideal profitability level obtained using perfect price forecast, which is not practically possible, would be 77%. In this case, the profitability level obtained by utilizing wholesale prices (using back-casting method) and TOU prices are 53% and 23%, respectively. The revenue shortfall in the back-casting method compared to the ideal revenue is due to inconsistency of inter-day wholesale prices. Additionally, the significant revenue shortfall in the convention algorithm is due to sizable forecast error of public-domain PDPs.

To fill the gap between current and a stable expected ROR, utility regulators could provide incentives to storage owners. The incentive provision to storage technologies can be justified due to several potential environmental and technical benefits of storage diffusion. In the following section, an approach for storage incentivisation is proposed and analyzed.

2.7 Storage Incentivisation

In this section, the electricity price modulation is proposed as a new approach to competitively offer incentive by the utility regulator to storage owners to fill the gap between current and a stable expected ROR. Using the generic price profile and then real-world price data from Ontario's wholesale electricity market, the method is validated. The efficacy and feasibility of the proposed approach to incentivize storage owners are validated through simulation studies.

In this section, the RTOS algorithm modulates the electricity prices using the modulation factor offered by the utility regulator to incentivize the storage owner. The framework of the proposed model in this chapter of the thesis is depicted briefly in Fig. 2.5. This model is described in detail throughout this chapter of the thesis.

2.7.1 Proposed Method for Storage Incentivisation

As presented in Section 2.5.5, storage has not proven to be attractive for private investors. As pointed out in Section 2.1, due to the high capital cost, relatively low round-trip efficiency, and smaller electricity price arbitrage, large-scale storage may not be economical in current electricity markets; however, storage deployment will be becoming more economical in the near future due to the growing storage technologies and higher arbitrage benefits in future electricity markets.

Large-scale storage diffusion for energy shifting can also result in peak shaving. In this way, peak-shaving generators, which usually cause air pollution, can be shut/turned down, thereby generating less CO_2 emission. Moreover, large-scale energy-shifting storage can allow a higher penetration of wind and solar energy into electric grids since sporadic availability of renewable sources can be addressed by introducing storage to (partially) decouple energy generation from demand, thereby increasing system security [61]. Due to their considerable environmental and technical benefits, privately owned storage could be financially supported by utility regulators [60].

One approach to encourage potential investors to invest in storage is that utility regulators incentivize storage owners in contract setting for storage capital cost. This could be realized through constant monthly/annual payments to storage owners. In this approach, however, storage owners are not directly encouraged to operate effectively in the market to obtain their incentives; therefore, this approach is not appropriate in competitive electricity markets.

In this chapter of the thesis, price modulation is proposed as part of the RTOS algorithm to virtually increase energy price arbitrage to competitively offer incentive to storage owners to fill the gap between current and a stable expected ROR. The use of modulation factor also demonstrates how much the energy price arbitrage shall increase until the storage plant becomes economical. By implementing the proposed approach, the more the storage is operated to support the grid by energy shifting/peak shaving, the more incentives it can receive from the utility regulator since the amount of incentive is dependent on charging in off-peak periods and discharging in peak periods which are appropriate for both the utility regulator/system operator and storage investor.

One of the advantages of this method is that the level of the price modulation can be adjusted by utility regulators to incentivize all eligible market players, including storage, according to their technical and environmental benefits. By including the proposed approach to incentivize the storage as part of the optimization problem, the objective function would be expressed as follows:

$$\underset{P_t^{S,Chg},\, P_t^{S,Dhg}}{\text{Maximize}} \sum_{t\in\mathcal{N}_i}\left((P_t^{S,Dhg}-P_t^{S,Chg}).(I)E_t^{FMrk}-C^{S,DhgO}.P_t^{S,Dhg}-C^{S,ChgO}.P_t^{S,Chg}\right).\Delta T. \quad (2.9)$$

As expressed in (2.9), the electricity price (i.e., E_t^{FMrk}) is multiplied by a constant "I", called modulation factor where $I>1$. Since $I>1$, the price arbitrage, the difference between high and low levels of the price, increases. This causes to increase revenue for storage owners by purchasing and selling electricity. The extra profit is provided for storage owners indirectly by the utility regulator. The value of modulation factor "I" included in (2.9) should be so that the total revenue at least covers the expected revenue due to investment. In such a case, the extra revenue at least reaches to zero; the zero extra revenue is the border between economic and uneconomic operations of the storage. The storage extra revenue is defined in (2.10), as follows:

$$\text{Extra Revenue: } \sum_{t\in\mathcal{N}_i}\left((P_t^{S,Dhg}-P_t^{S,Chg}).(I)\,E_t^{FMrk}-C^{S,DhgO}.P_t^{S,Dhg}\right.$$
$$\left.-C^{S,ChgO}.P_t^{S,Chg}\right).\Delta T - N\times(C^{S,EInc}+C^{S,Cap}), \quad (2.10)$$

where the total revenue and expected revenue over the optimization horizon are expressed by (2.11) and (2.12), respectively, as follows:

$$\text{Total Revenue: } \sum_{t\in\mathcal{N}_i}\left((P_t^{S,Dhg}-P_t^{S,Chg}).(I)\,E_t^{FMrk}\right.$$
$$\left.-C^{S,DhgO}.P_t^{S,Dhg}-C^{S,ChgO}.P_t^{S,Chg}\right).\Delta T \qquad (2.11)$$

$$\text{Expected Revenue: } N\times(C^{S,EInc}+C^{S,Cap}), \qquad (2.12)$$

where $C^{S,Cap}$ is the hourly capital cost, defined by wasting the capital cost over the life of the plant, and $C^{S,EInc}$ is the hourly expected income due to investment As expressed in (2.10), the summation of these constant parameters has been subtracted from the total revenue to express the storage revenue excluding the capital cost and expected income over the optimization horizon, named extra revenue in this study.
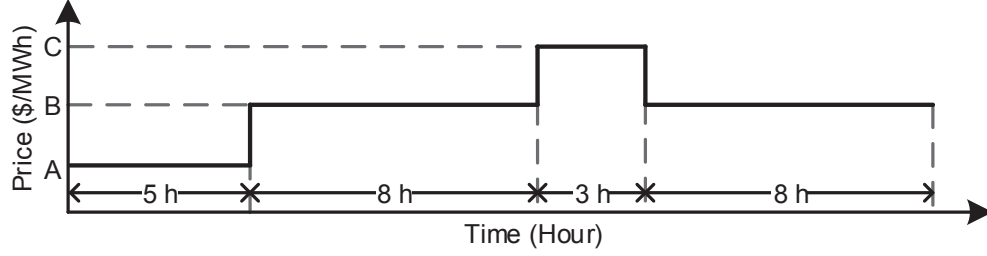
Figure 2.6: Generic electricity price profile.

Table 2.13: Different Levels of the Generic Price Profile Shown in Fig. 2.6

| Price Profiles | Price Levels ($/MWh) | | | | | |
| | For Weekdays | | | For Weekends | | |
	A	B	C	A	B	C
Profile 1	60	90	120			
Profile 2	60	120	180	50	60	70
Profile 3	60	150	240			

Theoretically, I_{min} can be calculated as stated in the following where the extra revenue (see (2.10)) equals zero:

$$I_{min} = \frac{\sum_{t \in \mathcal{N}_i}(C^{S,DhgO} \cdot P_t^{S,Dhg} + C^{S,ChgO} \cdot P_t^{S,Chg})}{\sum_{t \in \mathcal{N}_i}(P_t^{S,Dhg} - P_t^{S,Chg}) \cdot E_t^{FMrk}}$$
$$+ \frac{N \times (C^{S,EInc} + C^{S,Cap})}{\sum_{t \in \mathcal{N}_i}(P_t^{S,Dhg} - P_t^{S,Chg}) \cdot E_t^{FMrk}}. \tag{2.13}$$

I_{min} in (2.13) is the minimum required modulation factor to meet the expected revenue in each optimization horizon. However, in practice, I_{min} cannot be calculated simply by using (2.13) since electricity prices do not follow a constant pattern in each optimization horizon. In this case, the objective is not to make the storage work economically in every single optimization horizon; instead, it is expected that the monthly or annual extra revenue of storage at least reaches to zero. This is investigated in Section 2.7.2.1.

2.7.2   Numerical Evaluation

2.7.2.1   Using the Generic Price Profile

The RTOS algorithm formulated in Section 2.3 (considering the price modulation mechanism as stated by (2.9)) has been executed in a simulation environment. Three different

price profiles each with different modulation factors are used for evaluations. The generic price profile is shown in Fig. 2.6 while price levels (A, B, and C) are defined in Table 2.13 for three cases (typical price levels in Ontario's market [65]). Different values of round-trip efficiency for storage between 30% and 70% are considered. The extra revenue of the CAES sized in Section 2.4, is calculated and compared for different cases.

The RTOS algorithm is simulated for a one-year time period considering three different modulation factors and different round-trip efficiencies of storage. Annual extra revenue is calculated for the three predefined price profiles and shown in Fig. 2.7 in terms of million dollars. As represented in Fig. 2.7, as storage efficiency increases, the revenue increases almost linearly since by increasing the efficiency, the energy loss in storage system decreases. As novel technology materializes, the storage efficiency increases, and thus, storage utilization will become more economical.

Moreover, as represented in Fig. 2.7 (the left-hand and middle columns), the curves at the left side of breakpoints are approximately flat. In this area, storage is not operated since it cannot overcome the OPEX. As expressed in the following, at the left side of the breakpoint efficiency, the arbitrage benefit is less than the OPEX:

$$\sum_{t \in \mathcal{N}_i} (P_t^{S,Dhg} - P_t^{S,Chg}) \cdot E_t^{FMrk} \cdot \Delta T < \sum_{t \in \mathcal{N}_i} (C^{S,DhgO} \cdot P_t^{S,Dhg} + C^{S,ChgO} \cdot P_t^{S,Chg}) \cdot \Delta T. \quad (2.14)$$

As represented in Fig. 2.7, there are different breakpoints for Profile 1 (left-hand column) and Profile 2 (middle column), and there is no such a point for Profile 3 (right-hand column) considering storage efficiencies from 30% to 70%. As reported in Table 2.13, each profile has a different High to Low Price Ratio (HLPR) (i.e., C/A ratio) in weekdays. The larger the HLPR is, the smaller the efficiency breakpoint will be. Since the efficiency at the breakpoint depends on the value of HLPR, and HLPR does not change by price modulation, the breakpoint efficiency does not change at different modulations.

The minimum SOC constraint (see (2.6)) forces the storage once a day for compensation of energy dissipation to maintain the SOC above or equal to the SOC_{min}^S. Since any operation at efficiencies smaller than the breakpoint causes financial loss, as shown in Fig. 2.7 (left-hand column), higher operations of storage results in lower extra revenue.

As the curves of Fig. 2.7(a, d, and, g) represent, in the case of un-modulated prices (i.e., at $I = 1$), the annual extra revenue is negative for most of the operating points; negative extra revenue in one operating point means that using the storage is no longer economical. However, by modulating the price profiles, the obtained annual extra revenue increases for the operating points with efficiencies larger than the breakpoint efficiency. If the storage operating point is smaller than the breakpoint efficiency, the price modulation
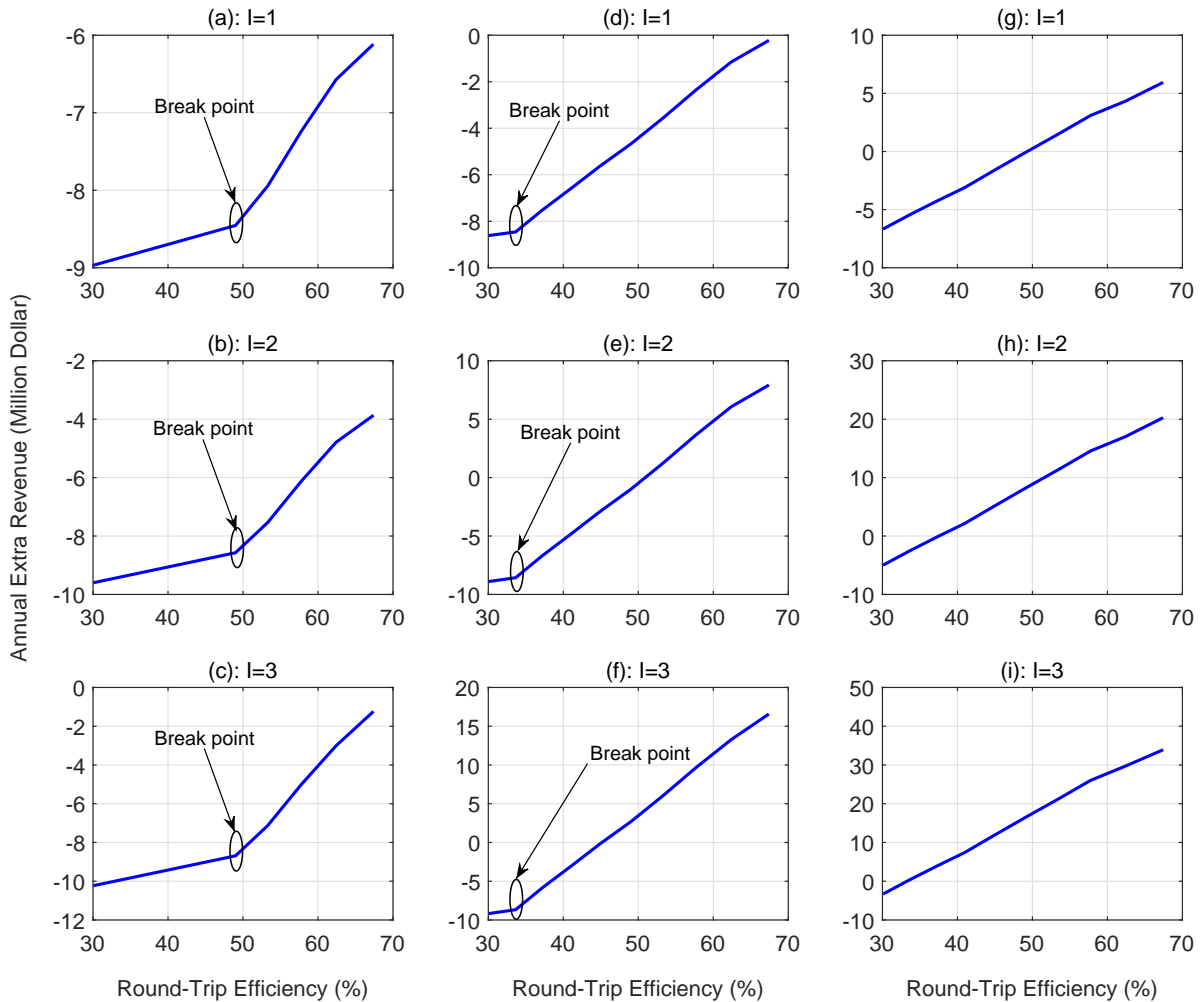
Figure 2.7: Annual extra revenue of storage operation vs. round-trip efficiency for three price profiles (see Table 2.13) each with three different price modulation factors. (a), (b), and (c): For price Profile 1; (d), (e), and (f): For price Profile 2; (g), (h), and (i): For price Profile 3.

does not have considerable effect on storage benefit since storage is not operated.

Moreover, comparing the HLPR value of price profiles, it can be observed that the larger the HLPR is, the more extra revenue is obtained (compare Fig. 2.7 (left-hand, middle, and right-hand columns). By increasing the HLPR in Profile 2 compared to Profile 1 and Profile 3 compared to Profile 2, the extra revenue increases.

2.7.2.2   Using Real-world Data

In this section, wholesale electricity prices publicly available in Ontario's market are used for evaluations. The RTOS algorithm formulated in Section 2.3 (considering the price
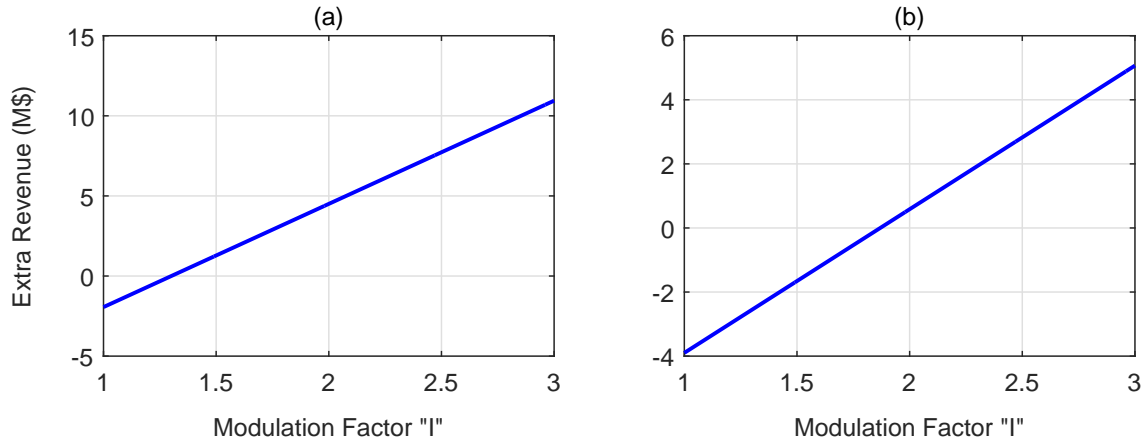
Figure 2.8: Five-year average of storage extra revenue vs. modulation factor I; (a): for the perfect price forecast and (b): for an imperfect price forecast in Ontario's electricity market.

Table 2.14: Five-year Average of the Extra Revenue in Ontario's Market (Based on Fig. 2.8)

	Perfect Forecast (Fig. 2.8 (a))		Imperfect Forecast (Fig. 2.8 (b))	
	$I = 1$	$I = 1.3$	$I = 1$	$I = 1.87$
Storage Extra Revenue	$-\$1.94\,\mathrm{M}$	$\$0.00\,\mathrm{M}$	$-\$3.9\,\mathrm{M}$	$\$0.00\,\mathrm{M}$

modulation mechanism as stated by (2.9)) has been executed in a simulation environment for Ontario's market from 2006 to 2009 and 2011. Two studies have been conducted as follows: In one study, the price forecast is assumed to be perfect; this means that the price forecast is substituted with the actual prices. The second study is conduced using an imperfect forecast of market prices using the back-casting method.

The annual extra revenue of storage operation in Ontario's market from 2006 to 2009 and 2011 has been calculated and shown in Fig. 2.8 (a) and Fig. 2.8 (b) for perfect and imperfect price forecasts, respectively, at different price modulation factors. Different modulation factors are employed to evaluate the impact of electricity price modulation on storage revenue in case of a real-world market. The five-year average of extra revenue has been reported in Table 2.14 for two important values of modulation factors: $I = 1$ (pertaining no incentive) and I_{min}, where I_{min} is considered as the modulation factor in which the annual extra revenue of storage operation reaches to zero.

As represented in Fig. 2.8 and Table 2.14, at $I = 1$, the annual extra revenue is negative revealing that the storage is not able to return the expected revenue plus OPEX. Moreover, the annual extra revenue increases linearly by increasing the price modulation factor revealing the efficacy and feasibility of the proposed method to incentivize storage owners. As reported in Table 2.14 for the perfect forecast, $I = 1.3$ is required in order

for the storage to become economical. For the imperfect price forecast, since the forecast error reduces the storage revenue, larger modulation factors are required (i.e., $I = 1.87$) to fill the gap between current and a stable expected ROR.

As demonstrated in this study, historical price data of an electricity market can be used to investigate the impact of price modulation on the storage operation; then, the level of the price modulation can be offered by the utility regulator.

According to the simulation studies, if storage is being scheduled using contract-based electricity prices with the same periods as the TOU prices, the desired off-peak rates need to be 76% of the current off-peak rates (i.e., $0.76 \times 75 = \$57/\text{MWh}$) in order for the plant to return the expected revenue. From another point of view, the desired peak rates need to be 130% of the current peak rates (i.e., $1.3 \times 135 = \$176/\text{MWh}$) in order for the plant to return the expected revenue.

2.8 Conclusion

A numerical analysis is conducted over Ontario's electricity market data. It is indicated that the overall behaviour of the energy market has been altered, with negative electricity prices even starting to appear. The application of large-scale energy storage units independently operated in the market is considered for substantial energy shifting. A Real-time Optimal Scheduling (RTOS) algorithm is developed by formulating a Mixed Integer Linear Programming (MILP) optimization problem which aims to generate revenue by exploiting arbitrage opportunities available in electricity markets. The price modulation is proposed and examined as an effective approach to provide uniform and at the same time competitive incentive to privately owned storage by utility regulators.

It is demonstrated that using the back-casting method, the five-year average revenue of storage for Ontario's wholesale market prices equals $4.43\,\text{M}$, whereas the annual revenue of storage for the Time-of-Use (TOU) rates equals $1.92\,\text{M}$. It is presented that the ideal profitability level obtained using the perfect price forecast is 77%. The profitability level obtained by utilizing a forecast of wholesale market prices and TOU rates are 53% and 23%, respectively. The storage revenue capture could increase and become closer to the ideal revenue if the error of the price forecast decreases.

It is indicated that for the perfect price forecast in Ontario's market, it is required to modulate electricity prices by 1.3 to meet the expected revenue for storage owners. It is demonstrated that the price forecast inaccuracy reduces the storage revenue, and thus, a higher price modulation factor (i.e., 1.87) would be required to fill the gap between current and a stable expected Rate of Return (ROR).

Chapter 3

Scheduling of Storage for Congestion Relief

3.1 Introduction

The trend of integrating more non-dispatchable renewable sources into the electric grid and phasing out dispatchable fossil-fueled power plants in the near future reduces the operational flexibility, increases the chance of transmission congestion and endangers the stability of electric system. Utilities are investigating the application of large-scale storage to address some of these imminent challenges to their power systems. In this chapter of the thesis, the application of privately owned large-scale storage for the purpose of congestion relief in transmission systems as an ancillary service is investigated. It is noted that currently some electricity markets do not recognize congestion relief as an ancillary service since avoiding congestion is a part of the scheduling; however, this may change in the future with integration of energy storage units in the market. It is demonstrated that in conventional optimal scheduling algorithms for storage, the storage cannot effectively contribute to congestion relief since the scheduling algorithm has not prepared the storage in advance. Hence, a new RTOS algorithm is proposed that aims to generate revenue primarily by exploiting electricity price arbitrage opportunities in the electricity market while optimally preparing the storage to maximize its contribution to congestion relief as an ancillary service. The efficacy and feasibility of the proposed algorithm are validated using the generic price profile and real-world price data from Ontario's wholesale electricity market. An analysis is presented regarding the appropriate amount of financial compensation for the storage owner due to its contribution to congestion relief in the studied electricity market.
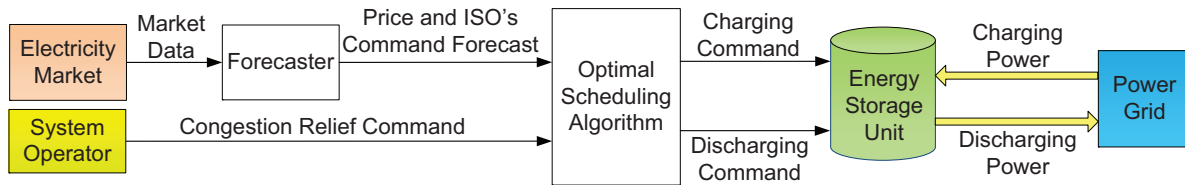
Figure 3.1: General framework of the proposed model for arbitrage and congestion relief.

3.2 Problem Description and Hypotheses

This chapter of the thesis investigates the idea of developing a new RTOS algorithm that would enable a large-scale storage to contribute to long-term congestion relief by injecting/absorbing a certain amount of power to/from the grid. The amount of power required for congestion relief is determined based on system analysis at the ISO's end, and then commanded to the storage controller by the ISO, while it is forecast and incorporated into the RTOS algorithm to optimally prepare the storage for such commands.

It is emphasized that in this study, the storage does not aim to relieve congestion problems which might occur due to system contingencies, such as transformer blow up or a line tripping; these types of events are not predictable. Instead, storage is employed to address congestion problems that can also occur due to the following reasons which could be predictable to some extent: unconstrained dispatch of generators and loads in a competitive electricity market and load or renewable generation growth which might cause overloads of transmission systems. It is also worth mentioning that congestion in the line is location specific, and therefore, storage may not be able to relieve congestion if the congestion location is far from the storage location. Nevertheless, in this study, the aim is to enable the storage to optimally accept congestion relief commands from the ISO whenever storage is technically able to relieve congestion.

For congestion relief using a privately owned storage unit that follows external commands, the following two approaches are possible: One approach is that the external commands are not incorporated into the optimization problem. In this case, (i) the optimization process is stopped when the command is issued in real-time; (ii) the storage will follow the command; (iii) and after that, the RTOS algorithm will resume. However, in this approach, the storage cannot be prepared for such commands prior to the command issuing moment, and thus, the storage contribution to congestion relief would be minimal. The alternative approach, adopted in this chapter of the thesis, is to incorporate the external congestion relief commands into the RTOS algorithm.

Fig. 3.1 represents the framework of the proposed model, which aims to optimally schedule a privately owned storage unit in the competitive electricity market while the storage can contribute to congestion relief by following the external ISO's commands. The proposed model in Fig. 3.1 will be described in detail in the thesis. In the proposed model, the following assumptions have been made:

i) The storage unit is able to freely purchase/sell electricity from/to the electricity market.

ii) Since the storage in the proposed algorithm is a privately owned asset, it is scheduled at the owner's end (locally controlled) to exploit energy price arbitrage opportunities in the DAM. The storage controller also accepts ISO's signal to contribute to transmission congestion relief. The signal can be communicated through internet, telephone, etc.

iii) Due to its contribution to congestion relief in specific time periods, the storage owner is financially compensated by the ISO. This financial benefit is assumed to be equal to or larger than the arbitrage benefit the storage would have obtained from its regular operation in those time periods.

iv) The setpoint for the power level, requested from the storage controller by the ISO, is assumed to be the ISO's need to relieve the congestion which may be fully/partially followed by the storage controller in this analysis. This approach is adopted to better compare different scheduling algorithms in terms of the percentage of their contribution to congestion relief. In reality, the ISO's official command is determined based on storage capacity; in real-time, the commands are always followed by storage.

3.3   Proposed Optimization-based Algorithm

The proposed RTOS algorithm is realized by formulating an MILP optimization problem. The optimization horizon of $24\,\mathrm{h}$ ($T = 24\,\mathrm{h}$) with a 1-h time step ($\Delta T = 1\,\mathrm{h}$) is considered. The objective function, which aims (i) to maximize storage revenue by exploiting arbitrage opportunities available due to price volatility in the DAM and (ii) to optimally prepare the storage to maximize the storage contribution to congestion relief,

is formulated as follows:

$$\underset{P_t^{S,Chg}, P_t^{S,Dhg}, P_t^{Slk,CR'}, P_t^{Slk,CR''}}{\text{Maximize}} \sum_{t \in \mathcal{N}_i} \Bigg((P_t^{S,Dhg} - P_t^{S,Chg}) \cdot E_t^{FMrk} - C^{S,DhgO} \cdot P_t^{S,Dhg}$$

$$- C^{S,ChgO} \cdot P_t^{S,Chg} - \rho_t^{Pnl,CR} \cdot (P_t^{Slk,CR'} + P_t^{Slk,CR''}) \Bigg) \cdot \Delta T. \quad (3.1)$$

This includes the following terms:

(i) Electricity price arbitrage benefit: $(P_t^{S,Dhg} - P_t^{S,Chg}) \cdot E_t^{FMrk} \cdot \Delta T$

(ii) Storage operating costs: $(C^{S,DhgO} \cdot P_t^{S,Dhg} + C^{S,ChgO} \cdot P_t^{S,Chg}) \cdot \Delta T$

(iii) Penalty terms: $\rho_t^{Pnl,CR} \cdot (P_t^{Slk,CR'} + P_t^{Slk,CR''}) \cdot \Delta T$,

subject to the following operational constraints of the storage:

$$b_t^{S,Chg} \cdot P_{min}^{S,Chg} \leq P_t^{S,Chg} \leq b_t^{S,Chg} \cdot P_{max}^{S,Chg} \qquad \forall t \in \mathcal{N}_i \quad (3.2)$$

$$b_t^{S,Dhg} \cdot P_{min}^{S,Dhg} \leq P_t^{S,Dhg} \leq b_t^{S,Dhg} \cdot P_{max}^{S,Dhg} \qquad \forall t \in \mathcal{N}_i \quad (3.3)$$

$$SOC_{min}^S \leq SOC_t^S \leq SOC_{max}^S \qquad \forall t \in \mathcal{N}_i \quad (3.4)$$

$$SOC_t^S - SOC_{t-1}^S + \left(P_t^{S,Dhg}/\eta^{S,Dhg} - \eta^{S,Chg} \cdot P_t^{S,Chg} + \eta^{S,Dsp} \cdot SOC_t^S \right) \cdot \Delta T = 0$$

$$\forall t \in \mathcal{N}_i, \qquad (3.5)$$

and subject to the following constraint set to fulfill the ISO's command for contribution to congestion relief:

$$P_t^{S,Chg} - P_t^{S,Dhg} = P_t^{MCR} \qquad \forall t \in \mathcal{N}_i \wedge M_t^{CR} = 1 \qquad (3.6)$$

$$P_t^{MCR} = P_t^{CR} + P_t^{Slk,CR} \qquad \forall t \in \mathcal{N}_i \wedge M_t^{CR} = 1 \qquad (3.7)$$

$$P_t^{Slk,CR} = P_t^{Slk,CR'} - P_t^{Slk,CR''} \qquad \forall t \in \mathcal{N}_i \wedge M_t^{CR} = 1 \qquad (3.8)$$

$$0 \leq P_t^{Slk,CR'} \leq (P_{max}^{S,Chg} + P_{max}^{S,Dhg}) \qquad \forall t \in \mathcal{N}_i \wedge M_t^{CR} = 1 \qquad (3.9)$$

$$0 \leq P_t^{Slk,CR''} \leq (P_{max}^{S,Chg} + P_{max}^{S,Dhg}) \qquad \forall t \in \mathcal{N}_i \wedge M_t^{CR} = 1, \qquad (3.10)$$

where $\mathcal{N}_i$ is the set of time steps, rolling over the T–hour time notation, defined as follows:

$$\mathcal{N}_i = \{i, \ldots, i + N - 1\}, \qquad (3.11)$$

where i refers to the present time step, defined in a T–hour time notation divided by the time interval ΔT. For instance, at 5:00 am and for $\Delta T = 1$, $i = 5/1 = 5$.

To meet storage maximum ratings, the commanded power for congestion relief shall be in the following range in case of the charging commanded power (absorbing power

from the grid):

$$P_{min}^{S,Chg} \leq P_t^{CR} \leq P_{max}^{S,Chg} \quad \forall t \in \mathcal{N}_i, \tag{3.12}$$

or in the following range in case of the discharging commanded power (injecting power to the grid):

$$-P_{max}^{S,Dhg} \leq P_t^{CR} \leq -P_{min}^{S,Dhg} \quad \forall t \in \mathcal{N}_i, \tag{3.13}$$

or equal to zero in case of the zero commanded power. ISO's command mode for congestion relief shall be as follows:

$$M_t^{CR} = \begin{cases} 0 & \text{storage contribution to congestion relief is not required} \\ 1 & \text{storage contribution to congestion relief is required.} \end{cases} \tag{3.14}$$

In (3.1)–(3.14), except E_t^{FMrk} and P_t^{CR}, other parameters are non-negative (refer to nomenclature section for definitions of parameters).

The objective function, stated in (3.1), includes the financial benefit of selling electricity to the market, the cost of purchasing electricity from the market, and the storage OPEX for charging and discharging within the optimization horizon. It also includes penalty terms which will be explained in the following sections. In (3.1), E_t^{FMrk} is the electricity price forecast at the time step t while it is equal to the actual price at the present moment, i.e., $t = 1$.

Equations (3.2)–(3.4) express charging and discharging powers and SOC constraints for the storage. The energy balance of the storage is expressed in (3.5), which defines the relation of SOC at the two consecutive time steps t and $t - \Delta T$.

In order for the RTOS algorithm to follow congestion relief commands by the proposed approach in Section 3.2, a constraint set must be added to the optimization problem to modify storage charging/discharging power set points to the commanded ones. The forecast of congestion relief commands with a 24-h optimization horizon and the 1-h time step must be incorporated into the RTOS algorithm to prepare the storage for such commands. However, due to command forecast error, the storage might not have been completely prepared to follow the commands in real-time. In such a case, hard constraints may not be suitable since they force the storage to become prepared based on an imperfectly forecast command up to 24 h before real-time. Moreover, infeasibility of the optimization problem might be inherent when hard constraints are considered. Thus, it is proposed to formulate a soft constraint set for congestion relief, expressed
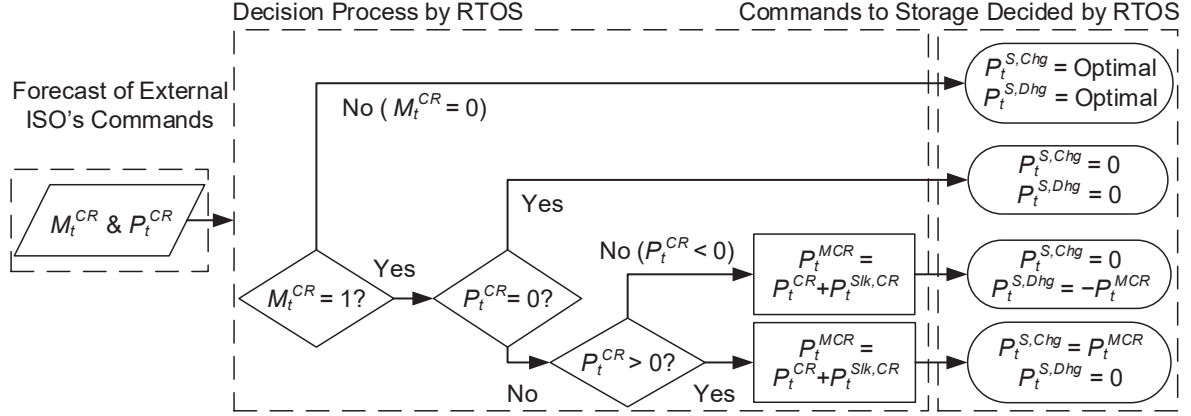
Figure 3.2: Operation of the algorithm considering system operator's command forecast.

in (3.6)–(3.10). In (3.6)–(3.10), M_t^{CR} and P_t^{CR} are two parts of the congestion relief command defined as follows:

$$M_t^{CR} = \begin{cases} \text{Forecast command mode} & \forall t \in \mathcal{N}_i \wedge t \neq 1 \\ \text{Actual command mode} & \forall t \in \mathcal{N}_i \wedge t = 1 \end{cases} \quad (3.15)$$

$$P_t^{CR} = \begin{cases} \text{Forecast command power} & \forall t \in \mathcal{N}_i \wedge t \neq 1 \\ \text{Actual command power} & \forall t \in \mathcal{N}_i \wedge t = 1. \end{cases} \quad (3.16)$$

As stated in (3.15) and (3.16), in real-time (i.e., $t = 1$), the actual command (i.e., mode and power) substitutes for the forecast.

Fig. 3.2 represents how the proposed RTOS algorithm, formulated in (3.1)–(3.10), operates to issue the required charging/discharging commands (i.e., $P_t^{S,Chg}$ and $P_t^{S,Dhg}$) to the storage by following ISO's commands. When M_t^{CR} equals one, the RTOS algorithm forces the storage to follow P_t^{MCR}, which is the modified version of P_t^{CR} by means of a slack variable (see (3.7)). As represented in Fig. 3.2, $P_t^{S,Chg}$ and $P_t^{S,Dhg}$ are not simultaneously assigned non-zero values by the RTOS algorithm since charging and discharging of the storage at the same price level is not economical.

When M_t^{CR} equals zero, the constraint set stated in (3.6)–(3.10) is relaxed, and thus, $P_t^{S,Chg}$ and $P_t^{S,Dhg}$ are assigned optimal values to generate revenue by exploiting arbitrage benefits. Real-time charging and discharging commands decided by the RTOS algorithm and the real-time actual market price are used to calculate the financial benefit from

selling electricity minus the cost for purchasing electricity and minus operating costs, which results in revenue for a certain period (daily or annually).

$P_t^{Slk,CR}$ is a slack variable optimally decided within a pre-defined range to adjust the commanded power (i.e., P_t^{CR}) so that the optimization problem can converge in case the storage cannot strictly follow the ISO's command due to its internal operational constraints. As noted in (3.8), $P_t^{Slk,CR}$ has been split into two positive auxiliary slack variables: $P_t^{Slk,CR'}$ and $P_t^{Slk,CR''}$; they can provide positive and negative values for $P_t^{Slk,CR}$, respectively. Since $P_t^{Slk,CR}$ can take both positive and negative values, it cannot be directly penalized in the objective function. Thus, it has been split into two positive variables; thereby, the variables are penalized with a penalty factor i.e. $\rho_t^{Pnl,CR}$ (see (3.1)) to preferably prevent non-zero values. If $P_t^{Slk,CR'}$ or $P_t^{Slk,CR''}$ takes any non-zero value, the storage revenue is reduced. Hence, these variables are set to zero by the optimization problem unless there is a need of non-zero values in order for the optimization problem to converge. Zero values for these slack variables are preferred since every non-zero value means the storage is not/partially following the ISO's commands (or need), and therefore, is not/partially contributing to congestion relief.

In (3.9) and (3.10), the upper bounds for slack variables are considered as $P_{max}^{S,Chg}+P_{max}^{S,Dhg}$ to enable the storage controller to fully bypass the commanded power (i.e., P_t^{CR}), if required; at the same time, it would provide the possibility of charging/discharging for the storage with full ratings, contrary to P_t^{CR}.

3.4   Numerical Analysis of the Proposed Algorithm

The same CAES unit sized in Section 2.4 is used for numerical analysis of the proposed algorithm in this chapter. The ratings of the CAES are as follows: $P_{max}^{S,Chg} = P_{max}^{S,Dhg} = 100\,\mathrm{MW}$, $SOC_{max}^S = 2000\,\mathrm{MWh}$, capital cost $= \$100\,\mathrm{Million}$. The reservoir with 2000 MWh capacity is basically larger than what is needed for regular charging and discharging in a typical day. However, as will be discussed later in Section 3.4.3.2, a storage unit with a larger reservoir could have a higher contribution to congestion relief when the storage absorbs power from the grid. Moreover, when the storage is built with a larger reservoir, it can deal with the uncertainties associated with DAM price forecast to some extent.

The charging efficiency (i.e., $\eta^{S,Chg}$) and discharging efficiency (i.e., $\eta^{S,Dhg}$) have been assumed to be 0.84%, causing a round-trip efficiency of 70%, a typical value for a highly efficient unit.
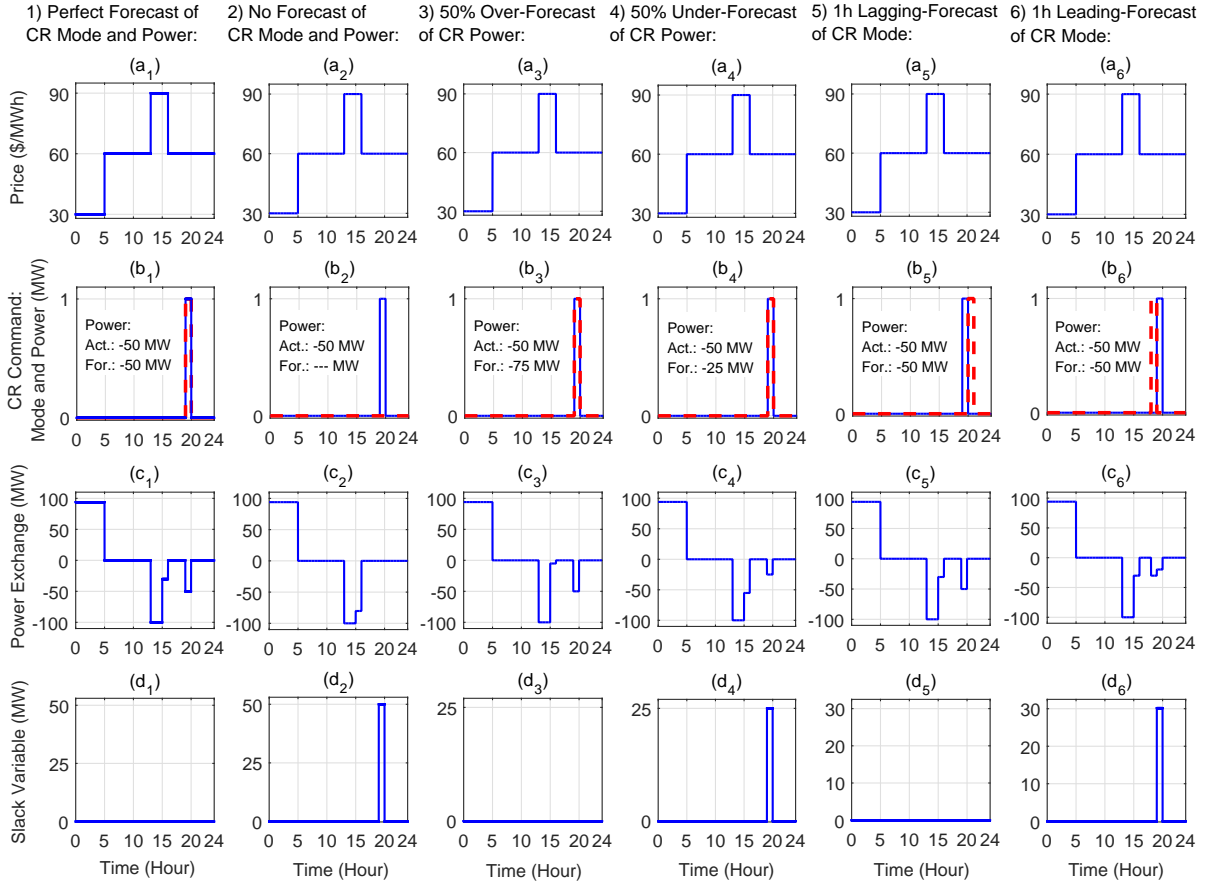
Figure 3.3: (a_1)–(a_6): Price profile, (b_1)–(b_6): Actual (bold line) & forecast (dotted line) Congestion Relief (CR) mode (M_t^{CR}) and power (P_t^{CR}), (c_1)–(c_6): Power exchange (positive: charging and negative: discharging), and (d_1)–(d_6): Slack variable ($P_t^{Slk,CR}$).

3.4.1 Numerical Analysis Using the Generic Price Profile

The generic electricity price profile (see Figs. 3.3 (a_1)–(a_6)), based on Fig. 2.6, is employed for the analysis of the proposed RTOS algorithm in this section. In order to penalize the slack variables $P_t^{Slk,CR'}$ and $P_t^{Slk,CR''}$ in the objective function of (3.1), a very large time-independent value has been considered for the penalty factor $\rho_t^{Pnl,CR}$ in this section.

The RTOS algorithm has been executed for 24 h by using the generic price profile for six types of congestion relief command forecasts, as mentioned on top of each column of Fig. 3.3. These six cases are listed as follows:

- Case 1: Perfect forecast of command

- Case 2: No forecast of command

Table 3.1: Storage Operation at Six Cases of Command Forecasting as Represented in Fig. 3.3

	Case 1	Case 2	Case 3	Case 4	Case 5	Case 6
Revenue (k$)	9.53	11.04	7.28	10.29	9.53	9.54
Contribution to Congestion Relief (MWh)	50	0	50	25	50	20

- Case 3: 50% over-forecast of command

- Case 4: 50% under-forecast of command

- Case 5: 1 h lagging-forecast of command

- Case 6: 1 h leading-forecast of command

The simulation results are presented in Fig. 3.3 and Table 3.1. In all cases, the actual commanded power is assumed to be $-50\,\mathrm{MW}$ (i.e., $50\,\mathrm{MW}$ discharging) issued by the ISO in the 19th hour of the day while it is scaled and shifted differently to generate different types of command forecast errors.

In Fig. 3.3, the price profiles are represented in (a_1)–(a_6). The actual (bold line) and forecast (dotted line) of congestion relief commands are represented in (b_1)–(b_6) in which the actual and forecast congestion relief modes (i.e., M_t^{CR}) are represented, and the actual and forecast congestion relief powers (i.e., P_t^{CR}) are stated in each figure. The power exchanges are represented in (c_1)–(c_6) where the positive and negative power exchanges indicate charging and discharging, respectively. The values of slack variable of congestion relief power, i.e., $P_t^{Slk,CR}$ are represented in (d_1)–(d_6).

The storage generates revenue by purchasing and charging inexpensive energy at low prices, and then discharging and selling it back to the market at high prices; it can also make additional profit if and when it has made any contribution to congestion relief. The storage operation under six types of congestion relief command forecasting are described in the following cases:

3.4.1.1 Perfect Forecast of Congestion Relief Command

In this case, the congestion relief command is perfectly forecast and incorporated into the RTOS algorithm. Fig. 3.3 (first column) represents the results for this case. As represented in Fig. 3.3 (c_1), the storage completely follows the ISO's command by discharging as commanded by the ISO since it has been fully prepared for it prior to real-time, causing full financial benefits for contribution to congestion relief. The storage daily revenue

and its contribution to congestion relief for this case are reported in Table 3.1 (second column). On top of this revenue, storage receives financial benefits from the ISO for its contribution to congestion relief.

3.4.1.2 No Forecast of Congestion Relief Command

In this case, the forecast of the congestion relief command is not incorporated into the optimization problem, thereby the RTOS algorithm only considers the actual command issued by the ISO at the present time step. Fig. 3.3 (second column) represents the results for this case. As represented in Fig. 3.3 (c_2), the storage is not able to follow the ISO's command since no discharging occurs when the actual command is issued, causing no financial benefits from contribution to congestion relief. As represented in Fig. 3.3 (d_2), the slack variable power (i.e., $P_t^{Slk,CR}$) is equal to the negative value of the commanded power (i.e., $-P_t^{CR}$); thus, the modified commanded power (i.e., P_t^{MCR}) results in zero (see (3.7)). The command has been fully bypassed by the RTOS algorithm since storage has not been prepared for it prior to real-time; thus, storage has no stored energy to discharge when the actual command is issued. The storage daily revenue and its contribution to congestion relief for this case are reported in Table 3.1 (third column). Storage will not receive extra financial benefit on top of this revenue since it is not contributing to congestion relief.

The higher revenue of the second case compared to that of the first case is because more energy has been sold to the market in peak hours of the price resulting in more revenue (compare Figs. 3.3 (c_1) and (c_2)).

3.4.1.3 Over-forecast of Congestion Relief Command

To investigate the impact of error in the forecast of commanded power set-point, a case has been studied in this section including over-forecasting of congestion relief command. As represented in Fig. 3.3 (third column), the actual commanded power for congestion relief is 50% over-forecast (equal to $-75\,\mathrm{MW}$). As represented in Fig. 3.3 (c_3), the storage completely follows the ISO's command by discharging as commanded, causing full financial benefits for contribution to congestion relief. The storage daily revenue and its contribution to congestion relief for this case are reported in Table 3.1 (fourth column). The revenue of this case is less than that of the case with perfect (ideal) command forecast (\$9.53 k) since the storage sells less energy in the peak hours of the price to keep enough energy for 75 MW discharging in the next hours. However, since the actual commanded power will be for 50 MW discharging, a portion of the charged

energy will be left in the storage reservoir resulting in less financial benefit. On top of the regular revenue, storage receives financial benefits from the ISO for contribution to congestion relief.

3.4.1.4   Under-forecast of Congestion Relief Command

As represented in Fig. 3.3 (fourth column), the actual commanded power for congestion relief is 50% under-forecast (equal to $-25\,\mathrm{MW}$). Due to the command under-forecasting, the storage does not have enough energy to discharge when the actual command is issued (Fig. 3.3 (c_4)). The command is partially bypassed (Fig. 3.3 (d_4)), causing partial financial benefits from contribution to congestion relief. The storage daily revenue and its contribution to congestion relief for this case are reported in Table 3.1 (fifth column). On top of this revenue, storage receives financial benefits from the ISO due to its contribution to congestion relief. However, storage will not fully benefit from contribution to congestion relief due to partially (not fully) following the ISO's command.

3.4.1.5   Lagging Forecast of Congestion Relief Command

As represented in Fig. 3.3 (fifth column), the command is forecast with one hour delay. As shown in Fig. 3.3 (c_5), the storage completely follows the ISO's command through discharging as commanded by the ISO. In such a case, storage receives full financial benefits for contribution to congestion relief. The storage daily revenue and its contribution to congestion relief for this case are reported in Table 3.1 (sixth column). On top of this revenue, storage receives financial benefits from the ISO due to its contribution to congestion relief.

3.4.1.6   Leading Forecast of Congestion Relief Command

As represented in Fig. 3.3 (sixth column), the command is forecast one hour ahead of the actual command. Due to the leading-forecast of the command, storage does not have enough energy to discharge (see Fig. 3.3 (c_6)). The command is partially bypassed in this case (see Fig. 3.3 (d_6)), causing partial financial benefit from contribution to congestion relief. The command is partially bypassed since considerable amount of energy has been released one hour before the actual command is issued, and thus, storage does not have enough energy to follow the actual command. This occurs because when the present time step reaches to one hour prior to the actual command, the RTOS algorithm incorrectly assumes that there is no congestion relief command in the hours ahead, thereby releasing energy to generate revenue (see Fig. 3.3 (c_6)). The storage daily revenue and its contribu-

tion to congestion relief for this case are reported in Table 3.1 (seventh column). On top of this revenue, storage receives financial benefits from the ISO due to its contribution to congestion relief. However, storage will not fully benefit from contribution to congestion relief due to partially (not fully) following the ISO's command.

3.4.1.7 Outcomes

The main outcomes of the analysis presented in Section 3.4.1 are summarized as follows:

- As reported in Table 3.1, when the storage is not/partially contributing to congestion relief, the storage revenue might be higher compared to the case with perfect contribution to congestion relief, since the storage can release the energy at higher prices. However, in these cases, the storage will make no/partial extra financial benefits from contributing to congestion relief.

- If the command forecast (mode: M_t^{CR} and power: P_t^{CR}) is not incorporated into the optimization problem, the storage controller might fully bypass the actual command issued in real-time since the storage has not been at all prepared for it.

- If the command forecast has sizable error but incorporated into the optimization problem, it may be modified by the slack variable to comply with storage constraints; however, it is not fully bypassed since the storage has been partially prepared for it.

3.4.2 Proposed Adaptive Penalizing Mechanism

One approach to penalize violation of congestion relief command is to consider a constant positive value for the penalty factor $\rho_t^{Pnl,CR}$ for the entire optimization horizon. In such a case, if $\rho_t^{Pnl,CR}$ is considered too small in the present study, the RTOS algorithm will inappropriately compromise the congestion relief constraint set (see (3.6)–(3.10)) in real-time; hence, the constraint set is more likely to be bypassed. On the other hand, if $\rho_t^{Pnl,CR}$ is considered too large, the RTOS algorithm will inappropriately compromise the optimal charging/discharging power set-points of the storage within the optimization horizon to prepare the storage based on an imperfectly forecast congestion relief command.

In this chapter of the thesis, it is proposed to take an adaptive approach by defining the penalty factor $\rho_t^{Pnl,CR}$ as follows:

$$\rho_t^{Pnl,CR} = \begin{cases} X & \forall t \in \mathcal{N}_i \wedge t \neq 1 \\ \alpha \,.\, X \quad (\text{where} \quad \alpha \gg 1) & \forall t \in \mathcal{N}_i \wedge t = 1. \end{cases} \tag{3.17}$$

Consequently, $\rho_1^{Pnl,CR}$ (in real-time, i.e., $t=1$) is significantly larger than $\rho_t^{Pnl,CR}$ in other time steps. The proposed approach in (3.17) for penalizing the auxiliary slack variables (i.e., $P_t^{Slk,CR'}$ and $P_t^{Slk,CR''}$) ensures that the RTOS algorithm will not compromise the congestion relief constraint set in real-time (when the actual command for congestion relief is issued); whereas the RTOS algorithm is not completely restricted for future time steps, when the imperfectly forecast command is applied.

As an illustration, using the sized CAES and Ontario's wholesale market prices, several values for the penalty factor were considered. Then, the storage revenue and its contribution to congestion relief were studied under different types of command forecast errors. Finally, two approximate ranges were determined for the penalty factor as follows:

$$\text{Low range:} \quad \$100\,/\text{MWh} < \rho_t^{Pnl,CR} \leq \$1\,\text{k/MWh} \qquad \forall t \in \mathcal{N}_i \qquad (3.18)$$

$$\text{High range:} \quad \$1\text{k}\,/\text{MWh} < \rho_t^{Pnl,CR} \leq \$10\,\text{k/MWh} \qquad \forall t \in \mathcal{N}_i. \qquad (3.19)$$

The values smaller than $\$100\,/\text{MWh}$ cause actual congestion relief commands to be significantly bypassed; this happens due to substantial compromising of the RTOS algorithm towards the congestion relief constraint set in real-time. The values larger than $\$10\,\text{k/MWh}$ cause sizable revenue loss due to significant compromising of the RTOS algorithm towards optimal charging/discharging powers of the storage. The middle of the ranges ((3.18) and (3.19)) are chosen as the small and large penalty factors, as follows:

$$\text{Small penalty:} \quad \rho_t^{Pnl,CR} = \$550\,/\text{MWh} \quad \forall t \in \mathcal{N}_i \qquad (3.20)$$

$$\text{Large penalty:} \quad \rho_t^{Pnl,CR} = \$5.5\,\text{k/MWh} \quad \forall t \in \mathcal{N}_i. \qquad (3.21)$$

To achieve the highest possible contribution to congestion relief by less command bypassing, using (3.20) and (3.21), the following adaptive penalty factor is proposed:

$$\rho_t^{Pnl,CR} = \begin{cases} \$550\,/\text{MWh (Small penalty)} & \forall t \in \mathcal{N}_i \land t \neq 1 \\ \$5.5\text{k}\,/\text{MWh (Large penalty)} & \forall t \in \mathcal{N}_i \land t = 1. \end{cases} \qquad (3.22)$$

3.4.3   Numerical Analysis Using Real-world Data

In this section, Ontario's wholesale electricity prices are used to evaluate the performance of the proposed RTOS algorithm for two different cases, including congestion relief by (i) injecting (=discharging) and (ii) absorbing (=charging) power to/from the grid. If the storage power exchange (i.e., $P_t^{S,Chg} - P_t^{S,Dhg}$) is considered in the operating range (i.e., from $-100\,\text{MW}$ to $+100\,\text{MW}$ in this study), two general cases could be considered

as follows: (i) the ISO's command to the storage is equal to or higher than the storage optimal power set-points; (ii) the ISO's command to the storage is equal to or lower than the storage optimal power set-points. In the next sections, two studies are conducted considering two above-mentioned cases. In these studies, the ISO's signal for congestion relief is assumed to be issued in certain time periods with certain values. However, these assumptions will not violate the generality of the proposed algorithm because the operation of the proposed optimization algorithm as presented in Section 3.3 of the thesis is not dependent upon the values and issuing time of the commanded power by the ISO. As expressed by (3.12) and (3.13), as long as the commanded power by the ISO does not violate the storage physical ratings, it can be considered as a valid command for the storage controller in any time period.

3.4.3.1   Congestion Relief by Injecting Power into the Grid

Let us assume that a large-scale storage is connected to the end of the transmission line where a certain amount of power, e.g., 100 MW needs to be injected into the grid by storage to relieve transmission congestion. Based on the above-mentioned assumption, the case study for Ontario's electricity market is planned as follows: the ISO's command for injecting 70–100 MW power into the grid for two hours to relieve the congestion is assumed to be issued at 5 pm and 6 pm; these commands are assumed to be issued for six months of the year and sent to the storage controller. The RTOS algorithm as formulated in Section 3.3 aims (i) to maximize the storage revenue by exploiting arbitrage benefits available due to price volatility in Ontario's DAM and (ii) to optimally prepare the storage for possible congestion relief commands.

For congestion relief command forecasting, different types of forecast errors are possible as follows: over, under, lagging, and leading forecasts. Erroneous forecasts are also possible, namely, when the congestion relief mode in real-time (i.e., M_1^{CR}) is valued as one, but its forecast has been assumed to be zero; and when it is zero while its forecast has been assumed to be one. Perfect command forecast is also possible in some cases.

Based on different types of command forecasting as well as random combinations thereof, three different command forecast signals are created for an entire year each of which includes a different combination of eleven types of forecasts. The over/under-forecast is assumed to be 40% while the lagging/leading-forecast is assumed to be 1 h. More information about transmission congestion forecasting can be obtained from the literature, such as [106], [107].

The RTOS algorithm, formulated in Section 3.3, is executed in a real-time simulation using the HOEPs in 2013 for three different command forecasts. In one study, the price
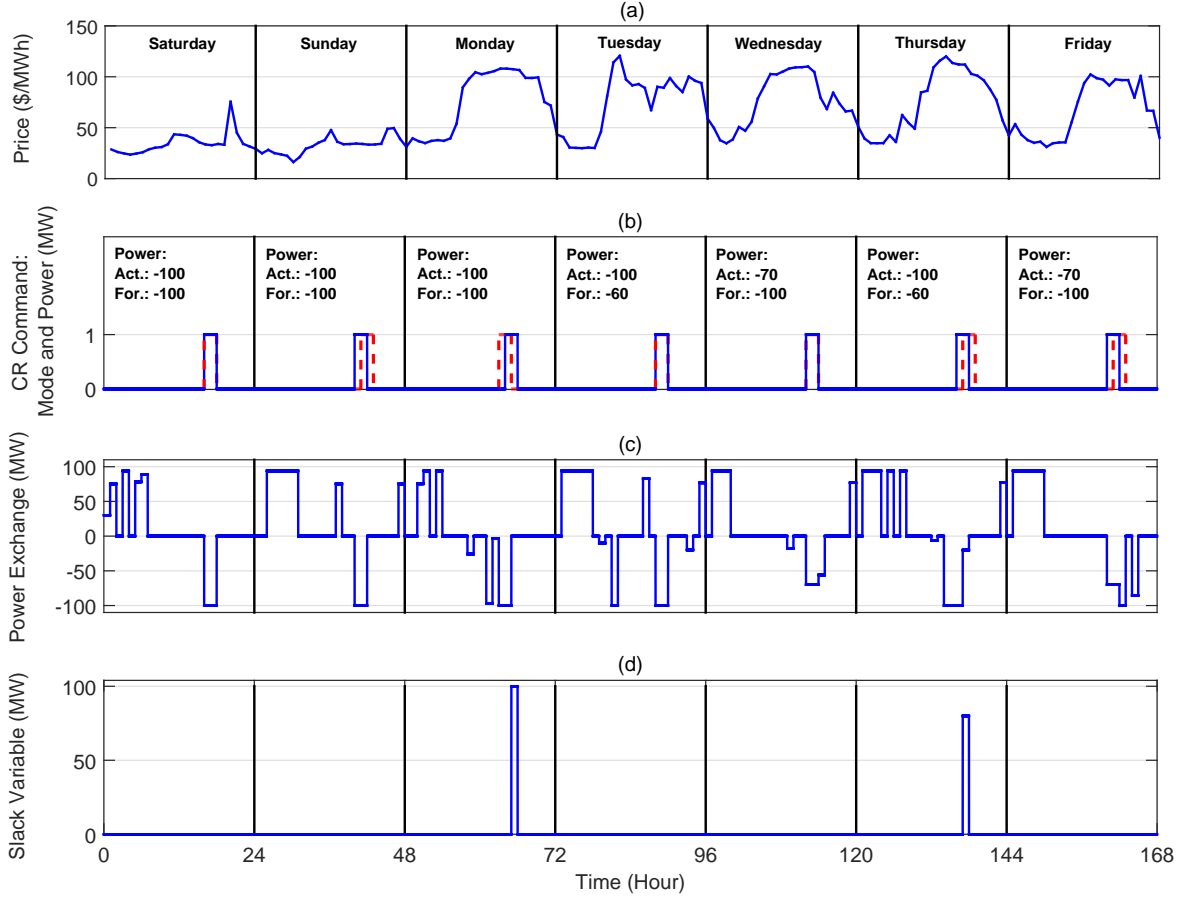
Figure 3.4: (a): Ontario's electricity market prices in one week, (b): Actual (bold line) and forecast (dotted line) Congestion Relief (CR) mode (i.e., M_t^{CR}) and power (i.e., P_t^{CR}), (c): Power exchange (i.e., $P_t^{S,Chg}-P_t^{S,Dhg}$), and (e): Slack variable (i.e., $P_t^{Slk,CR}$).

forecast is assumed to be perfect; this means the price forecast is substituted for actual prices. In the second study, an imperfect price forecast is provided using simple back-casting method in which the actual market prices of the day-behind is duplicated for storage scheduling [36]. Thus, the performance of the RTOS algorithm is investigated using cases of both perfect and imperfect market price forecasts to reveal the impact of price forecast uncertainty on the overall results.

Fig. 3.4 represents the simulation results for one complete week using the perfect price forecast and the generated command forecast signal for congestion relief. Fig. 3.4 (a) shows Ontario's wholesale market prices. Fig. 3.4 (b) shows the actual and forecast congestion relief command. In Fig. 3.4 (c), the positive and negative power exchanges indicate charging and discharging, respectively. The storage generates revenue by purchasing and storing inexpensive energy at low prices, and then discharging and
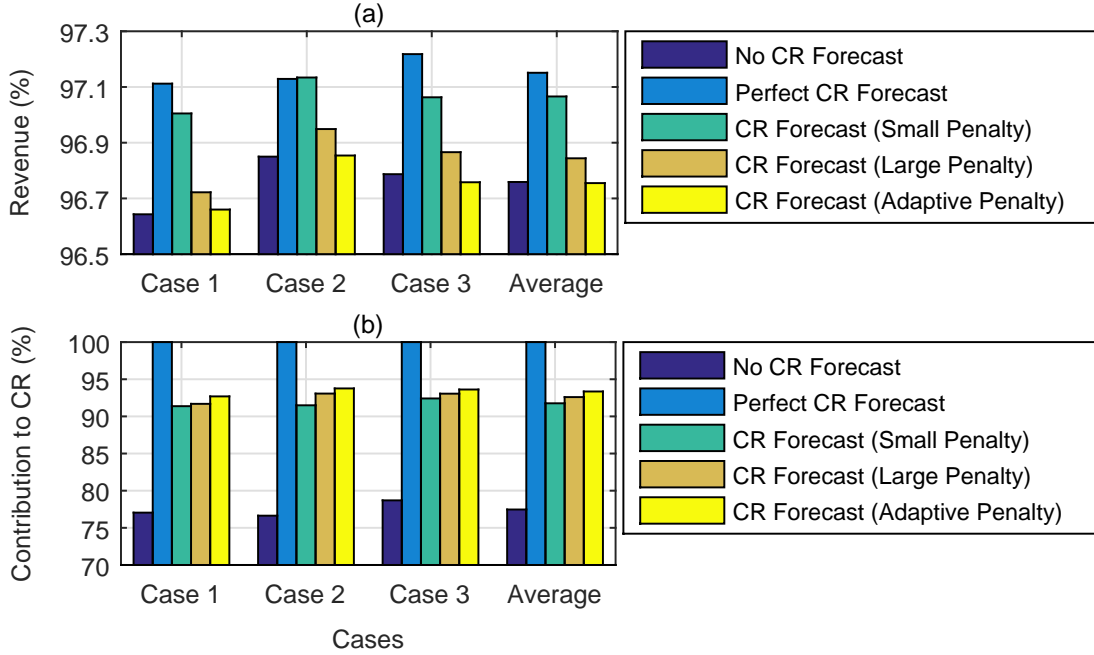
Figure 3.5: (a): Storage revenue in % of base annual revenue, (b): Storage contribution to Congestion Relief (CR) in % of actual commanded *discharging* power: for *perfect* price forecast.

selling it back to the market at high prices; it can also make additional profit if and when it has made contribution to congestion relief. The values of slack variable of congestion relief power, i.e., $P_t^{Slk,CR}$ are represented in Fig. 3.4 (d). As represented in Fig. 3.4 (c), in Saturday, Sunday, Tuesday, Wednesday, and Friday, the storage completely follows the ISO's command by discharging as ordered since it has been fully/partially prepared for it prior to real-time. On Monday, however, the storage is only able to follow the ISO's command in the first hour of command issuing time (i.e., 5 pm). Due to the 1 h leading forecast of the congestion relief command, the storage does not have enough energy to discharge in the second hour of command issuing time (i.e., 6 pm). No discharging occurs when the actual command is issued at 6 pm causing no financial benefits from contribution to congestion relief in this hour. As represented in Fig. 3.4 (d) for Monday at 6 pm, the slack variable power (i.e., $P_t^{Slk,CR}$) is equal to the negative value of the commanded power (i.e., $-P_t^{CR}$); thus, the modified commanded power (i.e., P_t^{MCR}) results in zero (see (3.7)). The command has been fully bypassed by the RTOS algorithm since storage has not been fully prepared in advance. On Thursday, due to the 1 h lagging forecast of congestion relief command, storage does not have enough energy to discharge when the actual command is issued at 6 pm (see Fig. 3.4 (c)). The command is partially bypassed in this hour (see Fig. 3.4 (d)) causing partial financial benefit from contribution to congestion relief.

Figure 3.6: (a): Storage revenue in % of base annual revenue, (b): Storage contribution to Congestion Relief (CR) in % of commanded *discharging* power: for *imperfect* price forecast.

To quantitatively evaluate the storage contribution to congestion relief, first, the storage base revenue, assuming $M_t^{CR} = 0$, is calculated for Ontario's wholesale market prices in 2013, which is \$4.5756 M and \$3.0693 M for perfect and imperfect price forecasts, respectively. When $M_t^{CR} = 0$, the constraint set expressed in (3.6)–(3.10) is relaxed; hence, the storage makes no contribution to congestion relief. Then, the storage revenue in percentage of the base revenue along with the storage contribution to congestion relief in percentage of the actual commanded power by the ISO are calculated and depicted in Figs. 3.5 and 3.6 for perfect and imperfect price forecasts, respectively. As shown in Figs. 3.5 and 3.6, each figure includes three cases (i.e., Cases 1 to 3) plus the average of all three, where each case represents the annual results obtained by a different annual congestion relief command signal. In each case, five studies are included as follows: (i) the forecast of congestion relief command is not considered; (ii) its perfect forecast is considered; (iii) its imperfect forecast is considered using the small penalty factor defined by (3.20); (iv) using the large penalty factor defined by (3.21); (v) using the adaptive penalty factor defined by (3.22). The following outcomes are obtained by analyzing Fig. 3.5 for the perfect electricity price forecast:

- When the command forecast is not incorporated into the RTOS algorithm, the storage contribution to congestion relief would be at the lowest level (i.e., 77.5% on

average) since the storage has not at all been prepared for such commands prior to real-time. A significant portion of commanded powers (i.e., 22.5% on average) is bypassed by the RTOS algorithm (see (3.7)).

- The obtained revenue in all studies (no forecast, perfect forecast, imperfect forecast with small, large, and adaptive penalties as expressed in (3.20)–(3.22)) is very close in each case of command forecasting (i.e., Cases 1 to 3).

- When the command is perfectly forecast, the storage fully (100%) contributes to congestion relief since it has been fully prepared for the command prior to real-time. However, the perfect forecast is not practically possible; thus, an imperfect command forecast along with three types of penalty factors is used as the practical study for the remainder of this thesis.

In the study of imperfect command forecasting with three types of penalty factors, the storage contribution to congestion relief is less than ideal since the storage has been partially (not fully) prepared for the command. The amount of contribution, however, is significantly higher compared to the study with no command forecast (i.e., up to 15.9% higher on average). Additionally, comparing the results of three penalty factors, one can clearly observe that the storage contribution to congestion relief has the highest value for the adaptive penalty (i.e., on average, 0.9% higher compared to large penalty and 1.6% higher compared to small penalty), revealing the efficacy of the proposed adaptive penalizing mechanism.

One can observe in Fig. 3.6 that the above-mentioned evaluations for the perfect price forecast are completely valid for the case with an imperfect price forecast, obtained using back-casting method. However, while the storage base revenue significantly decreases due to price forecast error (32.92%), this error can also slightly reduce the storage contribution to congestion relief in all studies (i.e., approximately 1% reduction on average). If other price forecasts are used rather than the one generated using back-casting method, none of the above observations are expected to change even though the storage revenue and its contribution to congestion relief would change depending on the price forecast error.

As mentioned in Section 3.2, due to its contribution to congestion relief, the storage owner must be financially compensated by the ISO. Currently in Ontario, Canada, there are financial compensation policies, such as Congestion Management Settlement Credits (CMSCs), which are payments made by the IESO to all dispatchable resources, such as generators or large consumers, who responded to instructions from the IESO to take specific actions. These directives are given to avoid possible overloads of the transmission system or to maintain the balance between supply and demand [65]. In the present study,

Table 3.2: Revenue Shortfall ($/MWh) due to Contribution to Congestion Relief by *Discharging*

	Case 1	Case 2	Case 3	Average
Perfect Price Forecast	5.5574	5.3818	5.3915	5.4416
Imperfect Price Forecast	3.9045	3.0502	2.3470	3.1032

Table 3.3: The Required *Discharging* Indices to Compensate Storage Revenue Shortfall

	Case 1	Case 2	Case 3	Average
Perfect Price Forecast	1.1630	1.1583	1.1604	1.1606
Imperfect Price Forecast	1.1170	1.0924	1.0708	1.0934

the following question needs to be answered: How much credit and with which approach is the storage owner to be paid by the ISO for its contribution to congestion relief? An extensive and descriptive answer to this question that would cover every electricity market is beyond the scope of this study. However, for Ontario's electricity market, some analyses are conducted as follows:

The imperfect congestion relief command forecasting using the proposed adaptive penalizing mechanism is proved to be the most effective approach due to higher contribution to congestion relief. In this case, the average revenue for the Cases 1 to 3 equals 96.755% (=3.245% shortfall) and 97.263% (=2.737% shortfall) of the base revenue for perfect and imperfect price forecasts, respectively. The revenue shortfall arises because the storage is deviated from optimal operation based on price arbitrage when it makes any contribution to congestion relief; this must be compensated by the ISO since the storage has made benefit for the grid by congestion relief. Moreover, the average of the storage contribution to congestion relief for the Cases 1 to 3 is 93.353% and 92.702% of the actual commanded power for perfect and imperfect price forecasts, respectively. The profit that the storage is losing per 1 MWh contribution to congestion relief is equal to revenue shortfall (in $) divided by the amount of contribution to congestion relief (in MWh). Accordingly, revenue shortfall has been calculated using Ontario's market prices in 2013 for Cases 1 to 3 as well as the average of these cases and reported in Table 3.2. As presented in Table 3.2, on average, the storage owner loses $5.44 and $3.10 per 1 MWh contribution to congestion relief for perfect and imperfect price forecasts, respectively.

Although proposing a proper policy for the compensation of the storage owner is not within the scope of this study, in order to find indices representing how energy price can
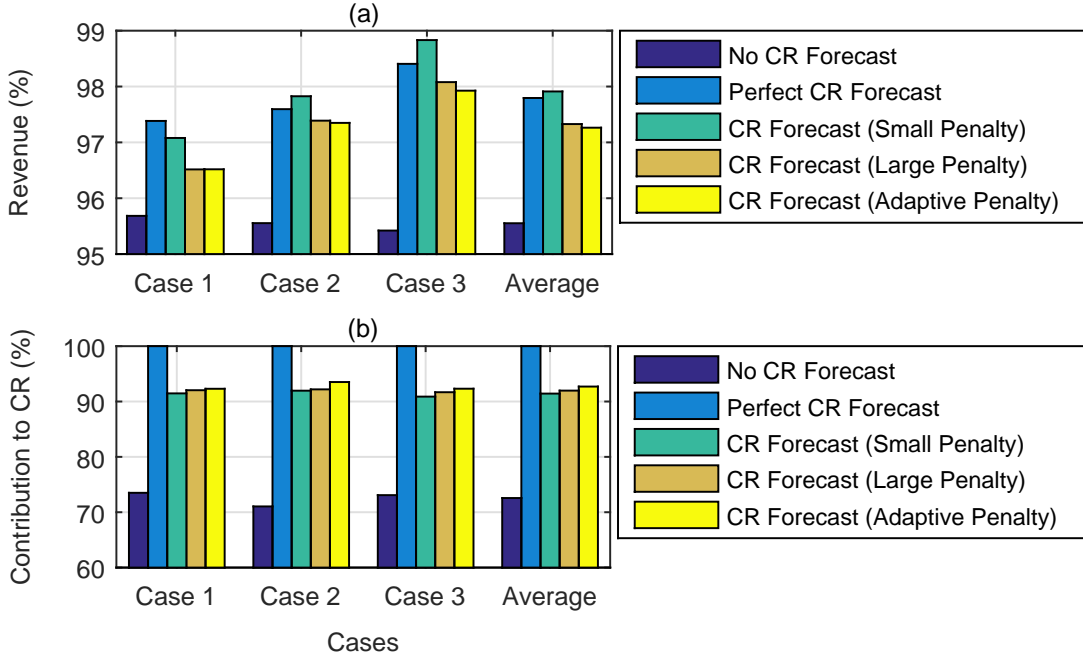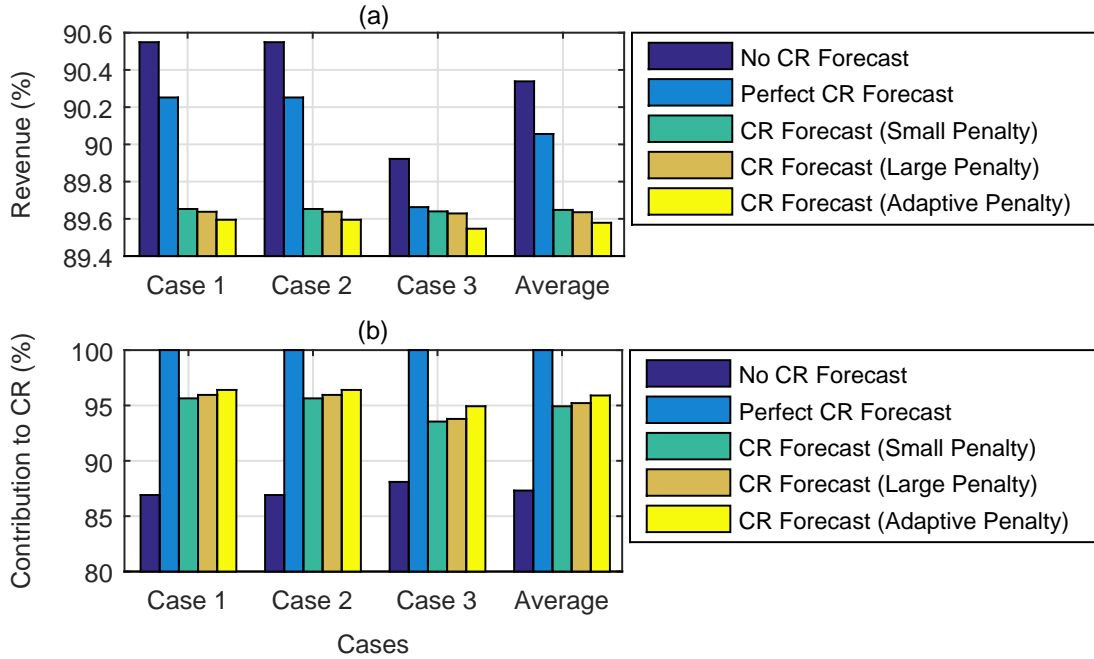
Figure 3.7: (a): Storage revenue in % of base annual revenue, (b): Storage contribution to Congestion Relief (CR) in % of actual commanded *charging* power: for *perfect* price forecast.

be used as a compensation tool, let us assume the following: The ISO purchases power virtually more expensive when the storage is discharging to respond to ISO's command; and the ISO sells power virtually less expensive to the storage when the storage is charging to respond to ISO's command. The storage could be charged/paid based on two charging and discharging compensation indices multiplied by the market price during time periods when the storage has responded to ISO's commands. The charging and discharging indices will be, therefore, smaller and larger than 1, respectively. For the case study presented in this chapter of the thesis, minimum discharging compensation indices for each case and for the average of three cases are calculated and reported in Table 3.3. As reported in Table 3.3, on average, the storage could be paid 16% and 9% more for perfect and imperfect price forecasts, respectively, when it is discharging to respond to ISO's command in order to achieve its base revenue. If the discharging index is larger than the minimum value, more profit is provided for the storage owner when it is responding to ISO's command for congestion relief.

3.4.3.2   Congestion Relief by Absorbing Power from the Grid

In the first case study presented in Section 3.4.3.1, the storage contributes to congestion relief by following ISO's discharging commands. In order to investigate the efficacy of the
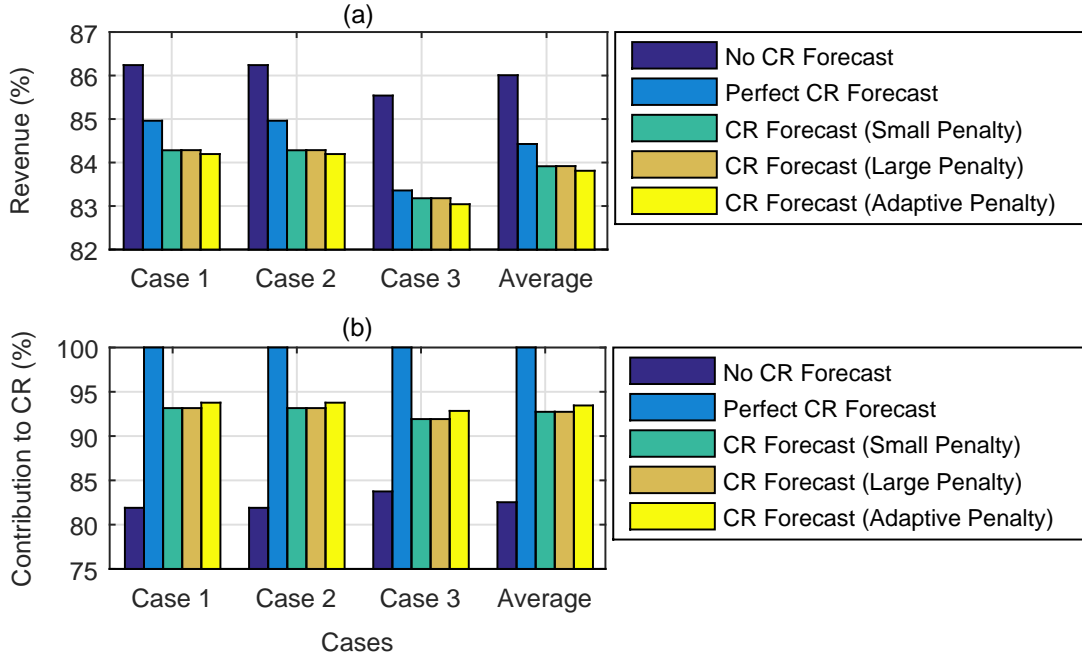
Figure 3.8: (a): Storage revenue in % of base annual revenue, (b): Storage contribution to Congestion Relief (CR) in % of actual commanded *charging* power: for *imperfect* price forecast.

proposed RTOS algorithm when the storage absorbs power from the grid, the same study is performed in this section where the storage is following the ISO's charging commands. The ISO's commands for absorbing 80–100 MW power from the grid for two hours to relieve the congestion is assumed to be issued at 10 am and 11 am.

According to the simulation results, when a storage unit with a 2000 MWh reservoir, is employed for evaluations, the storage contribution to congestion relief would be 100% in all cases. The storage reservoir with 2000 MWh capacity will have empty space and is able to follow charging commands in most time periods even if it has not been prepared for such commands prior to real-time. However, if a smaller reservoir is used, the same outcomes as the first case study will be achieved. Thus, in this section, the same CAES unit as rated in Section 3.4 has been used but with half of the reservoir capacity (i.e., 1000 MWh). In such a case, the storage base revenue would be slightly less than what is generated with a 2000 MWh reservoir. Nevertheless, the storage revenue in percentage of the base revenue has been calculated regardless of the absolute value of revenue.

The resulting revenue along with the storage contribution to congestion relief in percentage of the actual commanded power are calculated and depicted in Figs. 3.7 and 3.8 for perfect and imperfect price forecasts, respectively. Similar to the first case study carried out in Section 3.4.3.1, the results depicted in Figs. 3.7 and 3.8 reveal the im-

Table 3.4: Revenue Shortfall ($/MWh) due to Contribution to Congestion Relief by *Charging*

	Case 1	Case 2	Case 3	Average
Perfect Price Forecast	16.6608	16.6608	16.4398	16.5863
Imperfect Price Forecast	17.4522	17.4522	18.2927	17.7367

Table 3.5: The Required *Charging* Indices to Compensate Storage Revenue Shortfall

	Case 1	Case 2	Case 3	Average
Perfect Price Forecast	0.4012	0.4012	0.4135	0.4053
Imperfect Price Forecast	0.3760	0.3760	0.3496	0.3672

portance of congestion relief command forecasting and its incorporation as part of the RTOS algorithm as well as the efficacy of the proposed adaptive penalizing mechanism in providing a higher percentage of the storage contribution to congestion relief. The storage contribution to congestion relief would be up to 8.6% more compared to the case in which the command forecast is not considered. Moreover, using the adaptive penalizing mechanism, the storage contribution to congestion relief would be 1% and 0.7% higher than the methods using small and large penalty factors, respectively.

The storage revenue shortfall for the three studied cases (i.e., Cases 1 to 3) plus the average of all three are calculated and reported in Table 3.4. As reported in Table 3.4, on average, the storage owner loses $16.59 and $17.74 per 1 MWh contribution to congestion relief for perfect and imperfect price forecasts, respectively. Additionally, the minimum charging compensation indices for each case and for the average of the three cases are calculated and reported in Table 3.5. As reported in Table 3.5, on average, the storage could be charged 41% and 37% of the actual market price (=59% and 63% less) for perfect and imperfect price forecasts, respectively, when it is charging to respond to ISO's command in order to achieve its base revenue. If the charging index is smaller than the minimum value, more profit is provided for the storage owner when it is responding to ISO's command for congestion relief.

Finally, it is worth mentioning that the revenue shortfall and the required amount of financial compensation depends on how much and when the storage is required to absorb/inject power since there are different price levels during different time periods. Thus, the historical price and congestion data of each market must be studied to determine the revenue shortfall and the appropriate amount of compensation for that market.

3.5   Conclusion

In this chapter of the thesis, the concept of employing privately owned large-scale storage for long-term transmission congestion relief is investigated. It is demonstrated that in the conventional scheduling algorithms, the storage is not able to effectively contribute to congestion relief. A new Real-time Optimal Scheduling (RTOS) algorithm based on an adaptive penalizing mechanism and soft constraints is proposed. The forecast of external Independent System Operator's (ISO's) commands for congestion relief is incorporated into the optimization problem to best prepare the storage for such commands. Real data from Ontario's market are used for evaluations. It is indicated that when storage contributes to congestion relief by injecting power into the grid, using the proposed adaptive penalizing mechanism, a considerable amount of contribution to congestion relief is obtained (i.e., 93.35% and 92.7% for perfect and imperfect prices forecasts, respectively); in such a case, only a small portion of the storage base revenue (i.e., 3.25% and 2.74% for perfect and imperfect prices forecasts, respectively) is lost. This reveals the feasibility and efficacy of the proposed RTOS algorithm, which aims to optimally employ large-scale storage for congestion relief. The same conclusions are drawn when the storage contributes to congestion relief by absorbing power from the grid.

Chapter 4

Scheduling of Storage as a Dispatchable Asset

4.1   Introduction

Independently operated energy storage can exploit arbitrage opportunities available due to inter-temporal variation of electricity prices. Storage can be utilized as a dispatchable or non-dispatchable asset. In this chapter of the thesis, a new optimal scheduling algorithm is proposed to enable independently operated, locally controlled storage to accept dispatch instructions issued by ISOs. Storage in this case is referred to as *dispatchable storage*. Additionally, a new index is proposed to measure the storage dispatchability. While the operation of locally controlled storage is optimally scheduled at the owner's end, using the proposed algorithm, storage is fully dispatchable at the ISO's end. Dispatchable storage units have great potential to enhance the flexibility of electric grids and are key elements envisioned to enable smart grid realization. The proposed algorithm outperforms previous algorithms in which storage is either locally controlled at the owner's end and cannot optimally accept ISO's instructions; or storage is centrally controlled by the grid operator to achieve some technical objectives for the grid. The efficacy and feasibility of the proposed algorithm are validated using real-world data. It is demonstrated that the proposed scheduling algorithm can enable the storage to accept almost all ISO's instructions. Revenue values of dispatchable and non-dispatchable storage are also computed and compared.
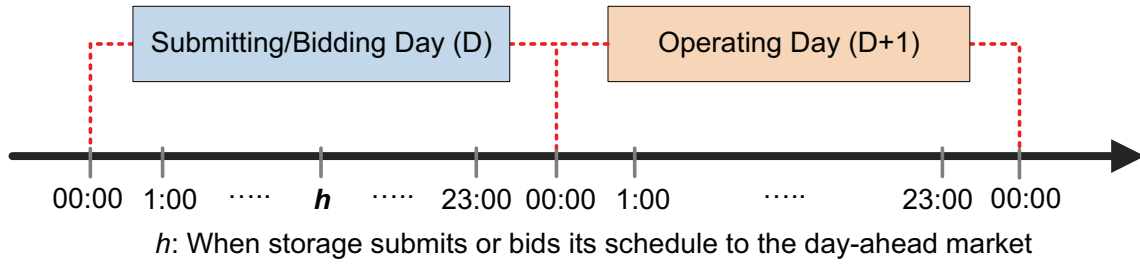
Figure 4.1: Market timeline for schedule submission of self-scheduling storage or bidding of dispatchable storage.

4.2   Non-dispatchable Storage

4.2.1   Intermittent Storage

Intermittent storage freely purchases/sells electricity from/to the market. Since the storage controller does not submit the charging/discharging schedule of storage to the DAM, the ISO does not have any direct information about the storage schedule in advance of real-time. The optimal schedule of intermittent storage is updated by rerunning the optimization calculations at every time step to account for the time-varying nature of market prices. The optimal scheduling algorithm would be, therefore, a real-time algorithm, also known as rolling time horizon or MPC method. Optimization-based models for intermittent storage units have been developed in Chapter 2 of this thesis.

4.2.2   Self-scheduling Storage

Fig. 4.1 shows the market timeline for schedule submission/bidding and operation of storage. As shown in Fig. 4.1, storage submits/bids its schedule during the day D for the DAM (i.e., $D + 1$). For instance, in Ontario's market, the window for entering daily bids opens at 6 a.m. the day before the energy will flow [74]. The charging/discharging schedule of self-scheduling storage is submitted to the DAM and simultaneously commanded to the storage unit by the storage controller. Since the storage schedule cannot be updated in real-time, the optimal scheduling algorithm would be a non-real-time algorithm. Optimization-based models for self-scheduling storage are similar to those for intermittent storage except that the storage schedule cannot be updated in real-time for intermittent storage.
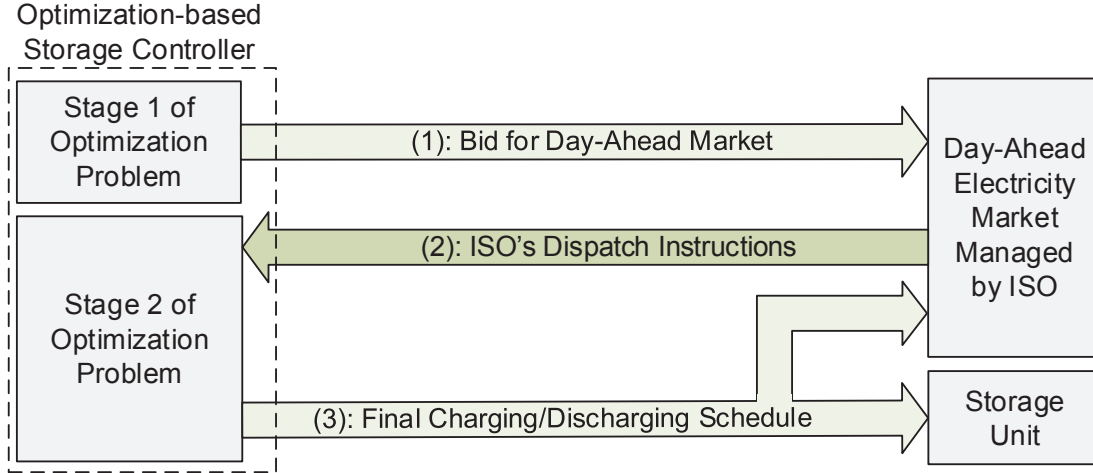
Figure 4.2: The proposed framework for operation of storage as a dispatchable asset.

4.3 Proposed Algorithm for Dispatchable Storage

In this section, based on the market policies for bidding and operation of dispatchable assets as explained in Section 1.4.3.1, a new model is proposed which enables an independently operated, locally controlled storage to accept ISO's dispatch instructions. Fig. 4.2 represents the framework of the proposed model for operation of a storage unit as a dispatchable asset in the DAM.

Optimal charging/discharging schedule of storage is initially decided by Stage 1 of the optimization problem. As shown in Fig. 4.2, this schedule along with the offered price is bid to the DAM by the storage controller. Considering the bids of all market participants including generators, loads, and storage units, the MCP is determined by the ISO [74]. In each time step, if the storage charging price (i.e., purchase price) is offered higher than or equal to the MCP, the storage charging bid is accepted by the ISO for that time step and vice versa. Additionally, if the storage discharging price (i.e., sale price) is offered lower than or equal to the MCP, the storage discharging bid is accepted by the ISO for the time step and vice versa. Based on these criteria as well as grid constraints, the dispatch schedule is determined by the ISO, and dispatch instructions (i.e., P_t^{Dsp}) are sent to the storage controller (see Fig. 4.2). Positive and negative values of P_t^{Dsp} represent charging and discharging, respectively.

In Stage 2 of the optimization problem, the charging/discharging schedule of storage is decided considering the ISO's dispatch instructions and commanded to the storage unit by the storage controller, also sent to the DAM as the final schedule. The proposed

algorithm aims to enable the storage to accept ISO's dispatch instructions regardless of how these instructions are determined. Thus, the ISO's dispatch algorithm does not affect the concepts proposed in this thesis. It is emphasized that although the final schedule of storage is decided in Stage 2, scheduling in Stage 1 is still necessary since the storage bid for the DAM is determined in Stage 1. ISO's dispatch instructions depend on the bids submitted by all market participants including energy storage units. Being dispatchable is essential for storage to be properly operated in a competitive market. Moreover, dispatchable storage helps the ISO to provide a balance between the consumption and generation of energy in the grid [74].

The proposed model is based on the following assumptions:

i) As opposed to centrally controlled storage, the storage in the proposed model is locally controlled, owned, and managed by the private investor. The storage controller aims to exploit energy price arbitrage opportunities in the DAM. It also accepts ISO's dispatch instructions, making the storage a dispatchable asset in the market.

ii) Storage may choose to submit single-block or multi-block bids to the DAM. However, this will not affect the concepts proposed in this thesis to create a dispatchable storage.

iii) Considering the bids submitted by all market participants and technical constraints of the grid, the ISO determines the dispatch instructions. However, the ISO's dispatch algorithm does not affect the concepts proposed in this thesis.

The optimization problem for optimal scheduling of dispatchable storage in two stages is presented in the following:

4.3.1   Stage 1 of the Optimization Problem

The optimization in this stage is performed without considering ISO's dispatch instructions. It aims (i) to maximize the revenue by exploiting energy price arbitrage in the DAM and (ii) to optimally adapt the storage charging/discharging capacity in order to prepare the storage to follow ISO's dispatch instructions in Stage 2. An MILP optimization problem is formulated. The objective function of the optimization problem in this stage is as follows:

$$
\operatorname*{Maximize}_{P_t^{S,Chg}, P_t^{S,Dhg}, SOC_t^{Slk,LB}, SOC_t^{Slk,UB}} \sum_{t \in \mathcal{T}} \Bigg((P_t^{S,Dhg} - P_t^{S,Chg}) \cdot E_t^{FMrk}
$$

$$
- C^{S,DhgO} \cdot P_t^{S,Dhg} - C^{S,ChgO} \cdot P_t^{S,Chg} - \rho^{Pnl,SOC} \cdot (SOC_t^{Slk,LB} + SOC_t^{Slk,UB}) \Bigg) \cdot \Delta T. \quad (4.1)
$$

This includes the following terms:

(i) Energy price arbitrage profit: $(P_t^{S,Dhg} - P_t^{S,Chg}) \cdot E_t^{FMrk} \cdot \Delta T$

(ii) Storage OPEX: $(C^{S,DhgO} \cdot P_t^{S,Dhg} + C^{S,ChgO} \cdot P_t^{S,Chg}) \cdot \Delta T$

(iii) Penalty terms: $\rho^{Pnl,SOC} \cdot (SOC_t^{Slk,LB} + SOC_t^{Slk,UB}) \cdot \Delta T$,

subject to the following operational constraints as expressed by (4.2)–(4.4):

$$b_t^{S,Chg} \cdot P_{min}^{S,Chg} \leq P_t^{S,Chg} \leq b_t^{S,Chg} \cdot P_{max}^{S,Chg} \quad \forall t \in \mathcal{T} \tag{4.2}$$

$$b_t^{S,Dhg} \cdot P_{min}^{S,Dhg} \leq P_t^{S,Dhg} \leq b_t^{S,Dhg} \cdot P_{max}^{S,Dhg} \quad \forall t \in \mathcal{T} \tag{4.3}$$

$$SOC_t^S - SOC_{t-1}^S + \left(P_t^{S,Dhg}/\eta^{S,Dhg} - \eta^{S,Chg} \cdot P_t^{S,Chg} + \eta^{S,Dsp} \cdot SOC_t^S \right) \cdot \Delta T = 0$$

$$\forall t \in \mathcal{T}, \tag{4.4}$$

subject to the following constraint to adapt the lower bound of SOC:

$$SOC_t^S \geq \beta^{LB,SOC} \cdot SOC_{min}^S - SOC_t^{Slk,LB} \quad \forall t \in \mathcal{T}, \tag{4.5}$$

subject to the following constraint to adapt the upper bound of SOC:

$$SOC_t^S \leq \beta^{UB,SOC} \cdot SOC_{max}^S + SOC_t^{Slk,UB} \quad \forall t \in \mathcal{T}, \tag{4.6}$$

and subject to constraints (4.7) and (4.8) to ensure that slack variables do not violate physical limitations of storage SOC, i.e., to keep SOC_t^S between SOC_{min}^S and SOC_{max}^S:

$$\beta^{LB,SOC} \cdot SOC_{min}^S - SOC_t^{Slk,LB} \geq SOC_{min}^S \quad \forall t \in \mathcal{T}$$

$$\therefore \quad SOC_t^{Slk,LB} \leq (\beta^{LB,SOC} - 1) \cdot SOC_{min}^S \quad \forall t \in \mathcal{T} \tag{4.7}$$

$$\beta^{UB,SOC} \cdot SOC_{max}^S + SOC_t^{Slk,UB} \leq SOC_{max}^S \quad \forall t \in \mathcal{T}$$

$$\therefore \quad SOC_t^{Slk,UB} \leq (1 - \beta^{UB,SOC}) \cdot SOC_{max}^S \quad \forall t \in \mathcal{T}, \tag{4.8}$$

where

$$SOC_t^{Slk,LB} \text{ and } SOC_t^{Slk,UB} \geq 0 \quad \forall t \in \mathcal{T}, \tag{4.9}$$

and $\mathcal{T}$ is the set of time steps for storage scheduling in the DAM, defined as follows:

$$\mathcal{T} = \{1, \ 1 + \Delta T, \ 1 + 2\Delta T, \ \ldots, \ N - \Delta T, \ N\}. \tag{4.10}$$

In (4.1)–(4.10), except E_t^{FMrk}, other parameters are non-negative (refer to nomenclature section for definitions of parameters). In (4.1), E_t^{FMrk} is a forecast for DAM prices.

The objective function, stated in (4.1), includes the financial benefit of selling electricity to the market, the cost of purchasing electricity from the market, and the storage OPEX for charging and discharging within the optimization horizon. It also includes penalty terms which will be explained in the following sections.

Equations (4.2) and (4.3) express charging and discharging constraints of storage, respectively. The energy balance of storage is expressed by (4.4), defining the relation of SOC at the two consecutive time steps t and $t - \Delta T$.

If $\beta^{LB,SOC} > 1$, the lower bound of SOC is considered higher than the physically limited lower bound (i.e., SOC_{min}^S) for energy reservation in the storage reservoir (see (4.5)). If $\beta^{LB,SOC} = 1$, there would be no reserved energy. If $\beta^{UB,SOC} < 1$, the upper bound of SOC is considered lower than the physically limited upper bound (i.e., SOC_{max}^S) for reservation of an empty space in the reservoir (see (4.6)). If $\beta^{UB,SOC} = 1$, there would be no reserved empty space.

Two slack variables $SOC_t^{Slk,LB}$ and $SOC_t^{Slk,UB}$ have been included in (4.5) and (4.6) to present soft constraints. In such a case, the optimization problem is not strictly forced to increase the lower bound or decrease the upper bound of SOC. Slack variables adapt the lower and upper bounds of SOC to decide the optimal value of reserve margin and to ensure that the optimization problem converges. As stated by (4.1), slack variables $SOC_t^{Slk,LB}$ and $SOC_t^{Slk,UB}$ are penalized using the penalty factor $\rho^{Pnl,SOC}$ to preferably prevent non-zero values. In such a case, if $SOC_t^{Slk,LB}$ or $SOC_t^{Slk,UB}$ takes any non-zero value, the value of the objective function (4.1) decreases.The optimization problem aims to maximize the value of the objective function. Thus, Slack variables are set to zero by the optimization problem unless there is a need of non-zero values for the optimal operation or convergence of the optimization problem.

4.3.2   Stage 2 of the Optimization Problem

As shown in Fig. 4.2, the ISO's dispatch instructions (i.e., P_t^{Dsp}) are inputted to Stage 2 of the optimization problem. The storage charging/discharging schedule is decided based on these instructions. As shown in Fig. 4.2, the final charging/discharging schedule which meets all of the storage constraints is commanded to the storage unit and also sent to the DAM. Later in this section, the reason for the second stage optimization is described.

The objective function of the optimization problem in this stage is formulated as follows:

$$\underset{P_t^{S,Chg}, P_t^{S,Dhg}, P_t^{Slk,DI'}, P_t^{Slk,DI''}}{\text{Maximize:}} \sum_{t\in\mathcal{T}}\Bigg((P_t^{S,Dhg} - P_t^{S,Chg}) \, . \, E_t^{FMrk}$$

$$-C^{S,DhgO} \, . \, P_t^{S,Dhg} - C^{S,ChgO} \, . \, P_t^{S,Chg} - \rho_t^{Pnl,DI} \, . \, (P_t^{Slk,DI'} + P_t^{Slk,DI''})\Bigg) \, . \, \Delta T, \quad (4.11)$$

including the arbitrage profit, the storage OPEX, and penalty terms: $\rho_t^{Pnl,DI} \, . \, (P_t^{Slk,DI'} + P_t^{Slk,DI''}) \, . \, \Delta T$, subject to the storage operational constraints expressed by (4.2)–(4.4), and (4.12) as follows:

$$SOC_{min}^S \leq SOC_t^S \leq SOC_{max}^S \quad \forall t \in \mathcal{T}, \tag{4.12}$$

and subject to the following constraint to fulfill ISO's dispatch instructions:

$$P_t^{S,Chg} - P_t^{S,Dhg} = P_t^{Dsp} + P_t^{Slk,DI'} - P_t^{Slk,DI''} \quad \forall t \in \mathcal{T}, \tag{4.13}$$

where

$$P_t^{Slk,DI'} \text{ and } P_t^{Slk,DI''} \geq 0 \quad \forall t \in \mathcal{T}. \tag{4.14}$$

In (4.11)–(4.13), except E_t^{FMrk} and P_t^{Dsp}, other parameters are non-negative (refer to the nomenclature section for definitions of parameters).

In order for the optimal scheduling algorithm to follow ISO's instructions in Stage 2, a constraint set must be added to the optimization problem. In such a case, hard constraints are not suitable since the storage controller could choose to partially deviate from these instructions in a competitive market. Additionally, infeasibility of the optimization problem might be inherent when hard constraints are considered. Thus, using slack variables $P_t^{Slk,DI'}$ and $P_t^{Slk,DI''}$, a soft constraint is formulated, stated by (4.13). In (4.13), the charging schedule minus the discharging schedule is set equal to P_t^{Dsp}. The zero value of P_t^{Dsp} means no operation to storage. A positive value of P_t^{Dsp} means zero discharging and non-zero charging power equal to $P_t^{Dsp} + P_t^{Slk,DI'} - P_t^{Slk,DI''}$. A negative value of P_t^{Dsp} translates into zero charging and non-zero discharging equal to $-(P_t^{Dsp} + P_t^{Slk,DI'} - P_t^{Slk,DI''})$. Slack variables $P_t^{Slk,DI'}$ and $P_t^{Slk,DI''}$ adapt ISO's dispatch instructions. As stated by (4.11), slack variables $P_t^{Slk,DI'}$ and $P_t^{Slk,DI''}$ are penalized using the adaptive penalty factor $\rho_t^{Pnl,DI}$ to preferably prevent non-zero values. Zero values for these slack variables might be preferred since every non-zero value means that storage is not/partially following ISO's dispatch instructions. This could result in financial

penalties imposed by the ISO for the storage owner. However, in some cases, storage might generate more revenue by partially/fully deviating from ISO's instructions even after paying the penalty cost to the ISO. Thus, the higher the ISO's penalty cost is, the higher the $\rho_t^{Pnl,DI}$ must be at each time step t. The adaptive penalty factor is an array with the following N elements:

$$\rho_1^{Pnl,Slk}, \rho_2^{Pnl,Slk}, \ldots, \rho_{N-1}^{Pnl,Slk}, \rho_N^{Pnl,Slk}.$$

Therefore, different values can be assigned to $\rho_t^{Pnl,DI}$ at different time steps for each optimization horizon. These values can be estimated based on historical penalty cost values. In other words, $\rho_t^{Pnl,DI}$ can be adapted at each time step differently, and thus, affect the optimization problem at each time step in a different fashion. In such a case, there are two different cases as follows:

i) ISO's instructions are not in violation of storage operational constraints at all time steps. Thus, these instructions may or may not be rescheduled depending on the penalty cost imposed by the ISO and storage revenue.

ii) ISO's instructions are in violation of storage constraints at one or some time steps, and thus, the optimization problem will not converge. In such a case, these instructions are optimally rescheduled to meet storage constraints at all time steps, thereby ensuring the convergence of the optimization problem.

4.3.3   Proposed Index to Measure Storage Dispatchability

In this section, using slack variables, a new index is proposed to measure the storage dispatchability, i.e., the percent of ISO's dispatch instructions accepted and followed by storage. The summation of the slack variables $P_t^{Slk,DI'}$ and $P_t^{Slk,DI''}$ when P_t^{Dsp} is non-zero, represents the total amount of dispatch instructions in MW which has not been accepted (i.e., has been canceled) by storage. The Cancellation of Dispatch Instructions (CODI) can be expressed in percent of the total dispatch instructions as defined in the following for each optimization horizon:

$$\text{Daily CODI} \% = \frac{\sum_{t \in \mathcal{T}^*} (P_t^{Slk,DI'} + P_t^{Slk,DI''})}{\sum_{t \in \mathcal{T}^*} |P_t^{Dsp}|} \times 100, \tag{4.15}$$

where $\mathcal{T}^*$ is defined as the set of time steps for storage scheduling in the DAM excluding those time steps in which P_t^{Dsp} is zero. This ensures that the right value is measured by (4.15), and that the equation would not result in a division by zero. Daily CODI is summed over the year for 365 days to express the annual CODI as follows:

$$\text{CODI}\,\% = \frac{\sum_{d=1}^{365} \left(\sum_{t \in \mathcal{T}^*} (P_{d,t}^{Slk,DI'} + P_{d,t}^{Slk,DI''}) \right)}{\sum_{d=1}^{365} \left(\sum_{t \in \mathcal{T}^*} |P_{d,t}^{Dsp}| \right)} \times 100. \qquad (4.16)$$

Thus, the percent of the annual dispatch instructions accepted and followed by the storage, referred to as *the storage dispatchability index*, is stated as follows:

$$\text{Storage Dispatchability Index}\,\% = 100\,\% - \text{CODI}\,\%. \qquad (4.17)$$

4.4 Numerical Evaluation of Storage Operation

The proposed optimal scheduling algorithm is modeled and executed in MATLAB using real-world wholesale electricity prices adopted from Ontario's market [65]. The optimization horizon of 24 h (i.e., $T = 24$) with 1 h time intervals (i.e., $\Delta T = 1$) is considered to optimally decide the charging and discharging schedules of storage. Using the perfect price forecast, the higher bound of revenue is generated. However, the perfect forecast cannot be practically realized. Using back-casting method, the lower bound of revenue is generated [40]. Any price forecast with an accuracy between the perfect forecast and imperfect forecast (using back-casting) generates a revenue level in between the two aforementioned bounds. For simulation purposes, the actual prices of the DAM are taken as MCPs, and the price forecast used for storage scheduling is taken as the price offered by storage to the DAM.

Very large finite numbers have been considered for $\rho^{Pnl,SOC}$ and $\rho_t^{Pnl,DI}$ to severely penalize any non-zero value of slack variables in the optimization problem. As explained in Section 4.3.2, in general, $\rho_t^{Pnl,DI}$ can be determined based on penalty costs that might be imposed by the ISO at each time step. In this study, however, in order to numerically examine the maximum dispatchability of storage, the storage controller is set to follow as much as ISO's instructions as possible.

As a large-scale storage option, the CAES as sized in Section 2.4 is used for evaluations. If other types of large-scale storage units are used for numerical evaluation,

Table 4.1: Annual Revenue and Dispatchability of Dispatchable Storage in Ontario's Market

Year	$\beta^{LB,SOC}$	$\beta^{LB,SOC} \times SOC^S_{min}$ (MWh)	Revenue (M\$)	Dispatchability Index (%)
	1	200	0.8911	78.60
2012	3	600	1.0181	96.94
	5	**1000**	**1.0147**	**99.84**
	7	1400	0.9340	99.97
	1	200	0.9421	77.59
2013	3	600	1.1336	92.25
	5	**1000**	**1.2217**	**98.15**
	7	1400	0.9696	99.60
	1	200	1.8414	79.25
2014	3	600	2.3192	90.92
	5	**1000**	**2.3042**	**97.64**
	7	1400	1.8334	98.97

the ultimate outcomes will not change since the validity of the proposed algorithm does not depend on the storage type. Maximum ratings of storage are as follows: $P^{S,Chg}_{max} = P^{S,Dhg}_{max} = 100\,\text{MW}$, and $SOC^S_{max} = 2000\,\text{MWh}$. The storage is modeled in MATLAB and the optimization problem is solved using GLPK package [102]. The final charging and discharging schedule of storage and actual market prices over the year are used to calculate the annual profit from electricity sale minus the annual cost for electricity purchase, and minus the annual OPEX. This results in the annual revenue.

4.4.1 Dispatchable Storage

4.4.1.1 Dispatchability and Revenue of Dispatchable Storage

For numerical studies, the factor $\beta^{UB,SOC}$ as included in (4.6) and (4.8) has been considered as 1. Based on the analyses, $\beta^{UB,SOC} = 1$ is optimal for the storage employed in this chapter of the thesis. For a smaller storage unit, however, it might be needed to use a value smaller than 1 for $\beta^{UB,SOC}$, which could be investigated.

The revenue of dispatchable storage as modeled in Section 4.3 along with the storage dispatchability index as stated by (4.17) has been calculated and reported in Table 4.1 at different values of $\beta^{LB,SOC}$ for three years.

The three-year average of the results in Table 4.1 is represented in Fig. 4.3 for different values of $\beta^{LB,SOC}$. As shown in Fig. 4.3, at $\beta^{LB,SOC} = 1$, the storage dispatchability
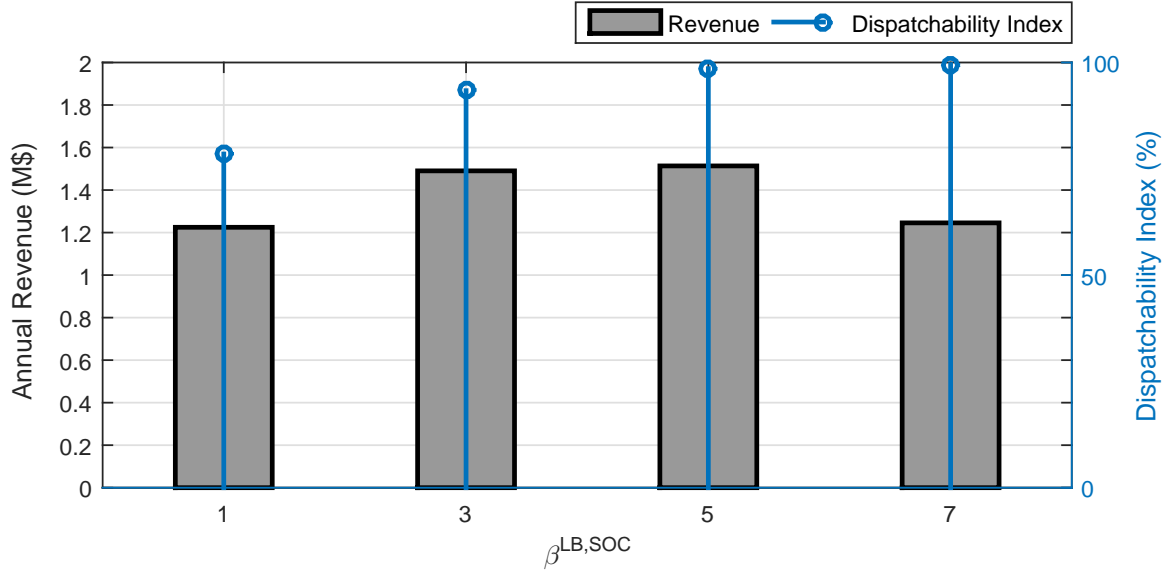
Figure 4.3: The three-year average (2012–2014) of revenue of dispatchable storage and % of the storage dispatchability index in Ontario's electricity market.

index has the lowest value (i.e., 78.48%); this represents the dispatchability index of storage when a conventional algorithm is employed since no reserved energy is available in this case. As $\beta^{LB,SOC}$ increases, the percentage of the dispatchability index increases because more reserved energy would be available for storage to accept ISO's dispatch instructions. However, the storage revenue decreases if $\beta^{LB,SOC}$ is supposed to be too large. At $\beta^{LB,SOC} = 5$, the highest level of revenue is generated, yet the storage dispatchability index would be 98.54%; this means that the storage can follow around 100% of ISO's dispatch instructions. Thus, $\beta^{LB,SOC} = 5$ is selected for the rest of the analyses.

4.4.1.2 Hourly Operation of Dispatchable Storage

Fig. 4.4 represents the simulation results of the hourly operation of the dispatchable storage for 24 h in a typical day in Ontario's electricity market.

In January 2, 2014, the optimal scheduling algorithm schedules the storage for the DAM (i.e., market in January 3). Then, the charging/discharging schedule of storage along with the offered price is bid for the DAM. Offered prices for the DAM and MCPs are shown in Fig. 4.4 (a). The bid schedule of storage, ISO's instructions, and the final schedule of storage are shown in Fig. 4.4 (b). In Fig. 4.4 (b), positive and negative powers represent charging and discharging, respectively. Fig. 4.4 (c) compares the storage SOC in Stage 1 (i.e., bid SOC) and in Stage 2 of the optimization problem (i.e., final SOC).

As shown in Fig. 4.4, since the storage offered price for energy purchase (i.e., charging)
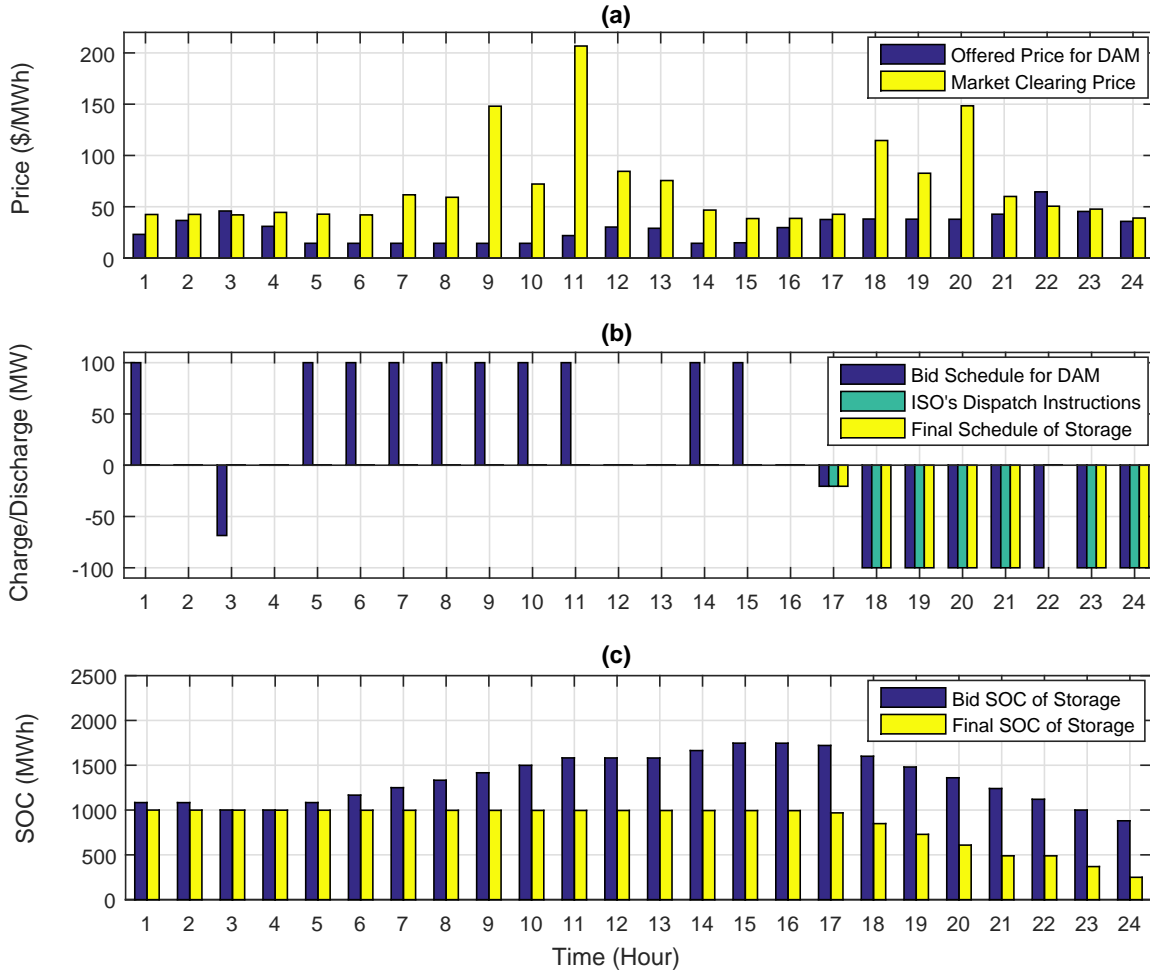
Figure 4.4: Simulation results of the hourly operation of dispatchable storage in Ontario's market. (a): Electricity market prices for a typical day, (b): Charging/discharging schedule (positive = charging, negative = discharging), and (c): State of charge.

has been less than the MCP, none of the charging bids has been accepted by the ISO on this particular day (see hours 1, 5–11, 14, and 15). However, since the offered price for energy sale (i.e., discharging) has been less than the MCP in most hours, the discharging bids have been accepted for those hours except for hours 3 and 22 in which the storage offered price has been higher than the MCP (compare bid schedule and ISO's dispatch instructions). Thus, storage has not been able to charge and store energy, but it has to follow its discharging bids (i.e., ISO's dispatch instructions) in all time steps. In a conventional optimal scheduling algorithm, this issue can make the storage cancel ISO's dispatch instructions due to insufficient stored energy, resulting in financial penalties for storage imposed by the ISO. However, as shown in Fig. 4.4 (b), ISO's dispatch instructions and the final schedule of storage are the same, meaning that storage has followed all of the ISO's dispatch instructions.
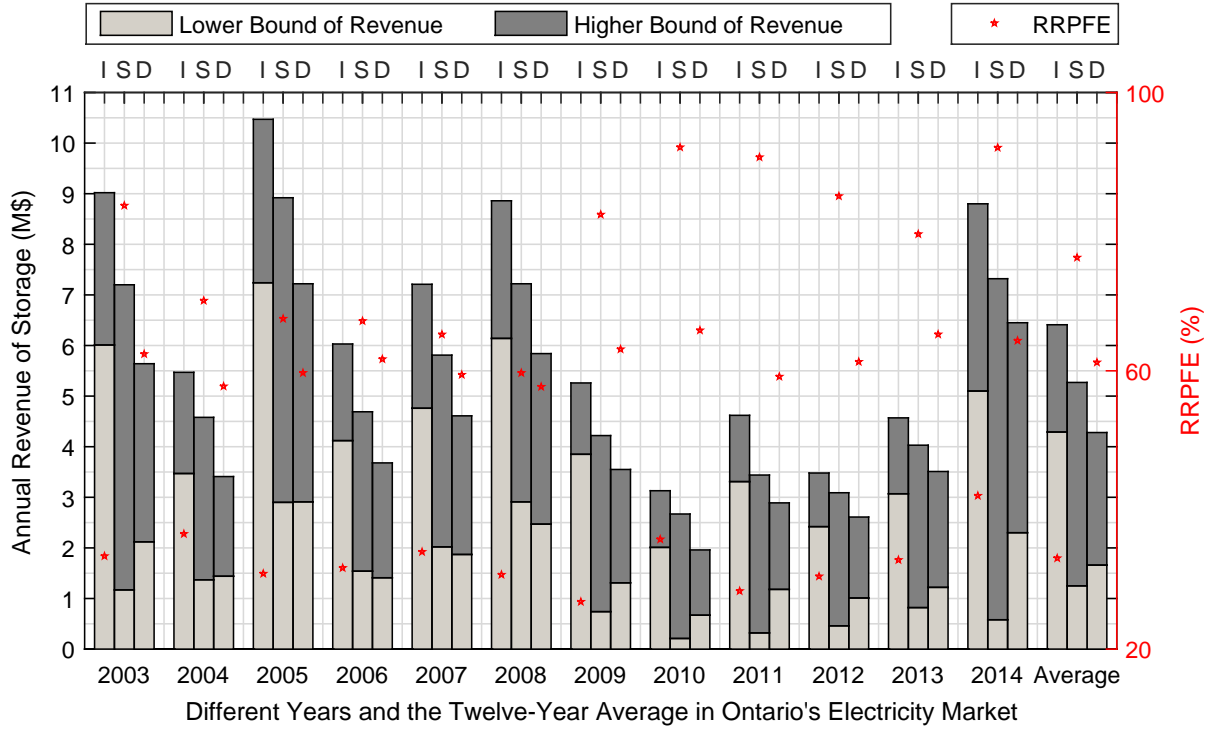
Figure 4.5: Annual revenue and Revenue Reduction due to Price Forecast Error (RRPFE) for I: intermittent storage, S: self-scheduling storage, and D: dispatchable storage.

4.4.2 Revenue of Dispatchable and Non-dispatchable Storage

This section aims to calculate and compare the revenue values of dispatchable and non-dispatchable storage using real-world market prices from 2003 to 2014. The impact of market price forecast error on the storage revenue is also examined. The storage revenue using the perfect price forecast (i.e., higher bound of revenue [40]) and an imperfect price forecast using back-casting method (i.e., lower bound of revenue [40]) is computed. The % of Revenue Reduction due to Price Forecast Error (RRPFE) is computed, as follows:

$$\text{RRPFE\%} = \frac{(\text{Higher} - \text{Lower}) \text{ Bound of Revenue}}{\text{Higher Bound of Revenue}} \times 100.$$

The RRPFE states how much the storage revenue is sensitive to the market price forecast error. Higher and lower values of RRPFE state higher and lower sensitivity values, respectively. Simulation results have been shown in Fig. 4.5 for dispatchable and non-dispatchable (i.e., intermittent and self-scheduling) storage in different years and for the average of all years.

The following outcomes are obtained by evaluation of Fig. 4.5:

- Both bounds of revenue for intermittent storage are higher than those for self-scheduling and dispatchable storage. For instance, on average, the lower and higher bounds of revenue are as follows: \$4.29 M and \$6.41 M for intermittent storage, \$1.25 M and \$5.27 M for self-scheduling storage, and \$1.66 M and \$4.28 M for dispatchable storage. Moreover, the RRPFE is the lowest for intermittent storage, meaning the storage revenue is less affected by the market price forecast error. On average, RRPFE is 33.07% for intermittent storage, 76.28% for self-scheduling storage, and 61.21% for dispatchable storage. As explained in Section 4.2.1, for intermittent storage, the storage schedule is updated in each time step. As a result, a more precise schedule is decided by the RTOS algorithm, and especially peak and off-peak prices appearing in real-time could be kept into consideration. Thus, a higher level of revenue can be generated for intermittent storage. This opportunity does not exist for self-scheduling and dispatchable storage since the optimal schedule cannot be corrected in real-time. However, intermittent storage neither submits its charging/discharging schedule to the DAM nor can accept ISO's dispatch instructions. In this case, the operation of large-scale storage can create uncertainties in the market.

- The higher bound of revenue for dispatchable storage is smaller than that for self-scheduling storage (\$4.28 M versus \$5.27 M on average). However, the lower bound of revenue for dispatchable storage is larger than that for self-scheduling storage (\$1.66 M versus \$1.25 M on average). This means that the more inaccurate the market price forecast is, the higher the revenue will be for dispatchable storage as compared to the self-scheduling storage. Due to price forecast inaccuracy in practice, dispatchable storage will generate higher revenue as compared to self-scheduling storage. Dispatchable storage submits its charging/discharging schedule along with the offered prices for each time step t (see Fig. 4.2). In case of charging, the storage will not purchase energy if the market price is higher than the price offered by the storage. Therefore, it will not overpay for purchase of energy when market prices are high. In case of discharging, storage will not sell energy if the market price is lower than the price offered by storage. Thus, it will not be underpaid for energy sale when the market prices are low. Moreover, the RRPFE is lower for dispatchable storage as compared to self-scheduling storage (61.21% versus 76.28% on average), revealing the effectiveness of dispatchable storage.
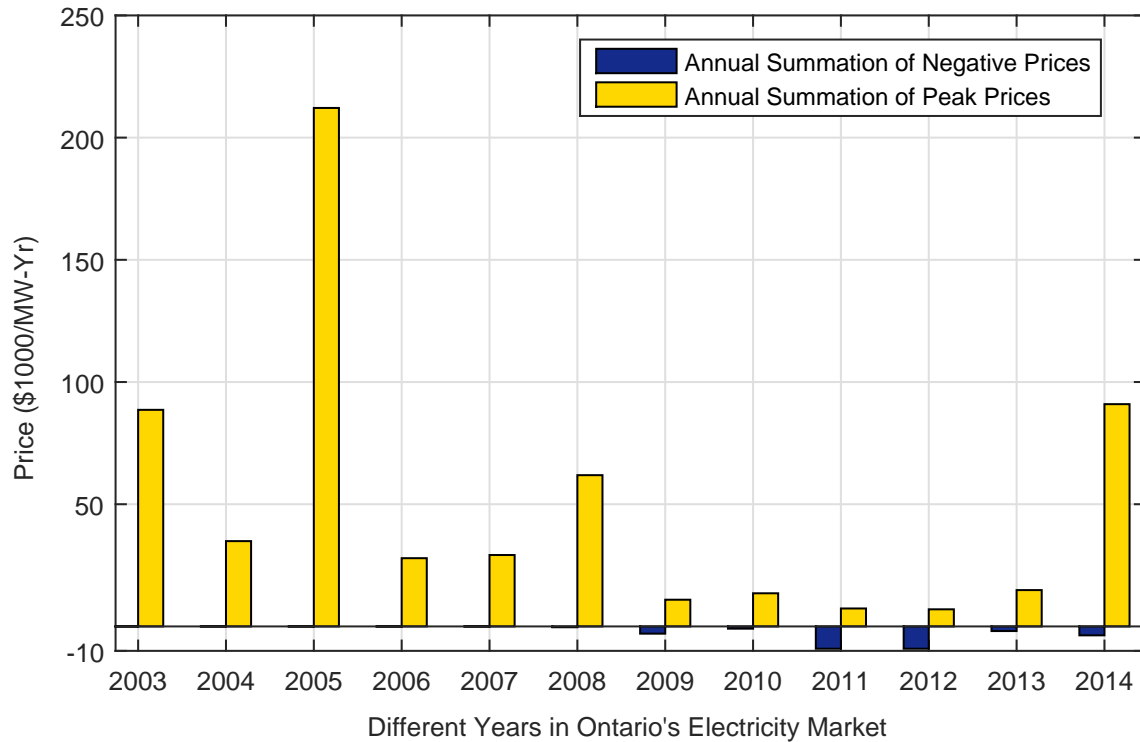
Figure 4.6: Annual summation of negative and peak (i.e., $\geq \$100\,/\,\mathrm{MWh}$) prices.

4.4.3   Annual Changes of Storage Revenue

As represented in Fig. 4.5, different levels of revenue have been generated in different years of Ontario's market. The storage revenue is generated by exploiting arbitrage opportunities. The price arbitrage is mostly dependent upon very low or negative and very high or peak prices. The annual summation of negative and peak prices (i.e., prices $\geq \$100\,/\mathrm{MWh}$) have been calculated and represented in Fig. 4.6 (in \$1000/MW-Year) for different years in Ontario's market.

By observation of Figs. 4.5 and 4.6, one can realize that, in general, the higher the peak prices are, the higher the generated revenue will be and vice versa. For instance, the peak prices are the highest in 2005 in which the highest level of revenue has been generated. The peak prices in 2003, 2008, and 2014 are moderate in which the moderate level of revenue has been generated. The peak prices in 2004, 2006, and 2007 are lower in which the lower level of revenue has been generated. Finally, the peak prices in 2009–2013 are the lowest in which the lowest level of revenue has been generated. Negative prices can also increase the storage revenue; however, their impact is not clear in Fig. 4.5 since their level is smaller than peak prices. These observations are approximate since the storage revenue is dependent upon all price values over the year.

4.5   Conclusion

In this chapter of the thesis, a new optimal scheduling algorithm for storage as a dispatchable asset in a competitive electricity market is proposed. While the operation of an independently operated, locally controlled storage unit is optimally scheduled at the owner's end, using the proposed algorithm, the storage is fully dispatchable from the Independent System Operator's (ISO's) end. In addition, a new index is proposed to measure the storage dispatchability. The efficacy of the proposed algorithm is validated using real-world data adopted from Ontario's electricity market. According to numerical studies, the storage dispatchability index equals 98.5% and 78.5% using the proposed and conventional optimal scheduling algorithms, respectively. Hence, around 100% of ISO's dispatch instructions can be followed by the storage using the proposed algorithm. Considering forecast uncertainties associated with Day-ahead Market (DAM) prices, the storage revenue for dispatchable storage is larger than that for self-scheduling storage ($1.66 M versus $1.25 M on average); moreover, the Revenue Reduction due to Price Forecast Error (RRPFE) is lower for dispatchable storage as compared to self-scheduling storage (61.2% versus 76.3% on average). Since dispatchable storage cannot be operated intermittently in the market, it generates lower revenue as compared to the intermittent storage; however, dispatchable storage units can play an essential role in preserving the reliability and security limits of the grid. For this reason, the proposed optimal scheduling algorithm can potentially open up new opportunities for profit generation for dispatchable storage.

Chapter 5

Scheduling of Load-storage Systems

5.1 Introduction

Inspired by operational practices and requisites of real-world storage applications, a new RTOS model is presented and analyzed in this chapter of the thesis to aggregate storage benefits for a large-scale load. The complete model for optimal scheduling of storage-based electrical loads considering both the CAPEX and OPEX of storage is developed. A real-time load forecaster is incorporated into the optimal scheduling algorithm using soft constraints, slack variables, and penalizing mechanisms. The application of the proposed model to a real-world large-scale institutional load in Ontario, Canada, is examined and compared with previous models. It is demonstrated that the proposed real-time model outperforms prior models by generating higher profitability of investment, lower storage OPEX, and an extended life of the storage plant.

5.2 Proposed Model

In this section, the proposed model for optimal scheduling of a load-storage system is developed and formulated. The general framework of the model is represented in Fig. 5.1. As shown in Fig. 5.1, storage is jointly operated with the large-scale load. The load is fed by storage and the grid. The load-storage system is simply a consumer since it does not inject any power to the grid. The storage controller is fed by the forecasts of load and market prices. The charging/discharging schedule of storage is decided by the RTOS model.

Optimal scheduling is performed for the next T hours with ΔT hour time steps. Forecast data and optimal decisions are updated by re-running the forecasters and the op-
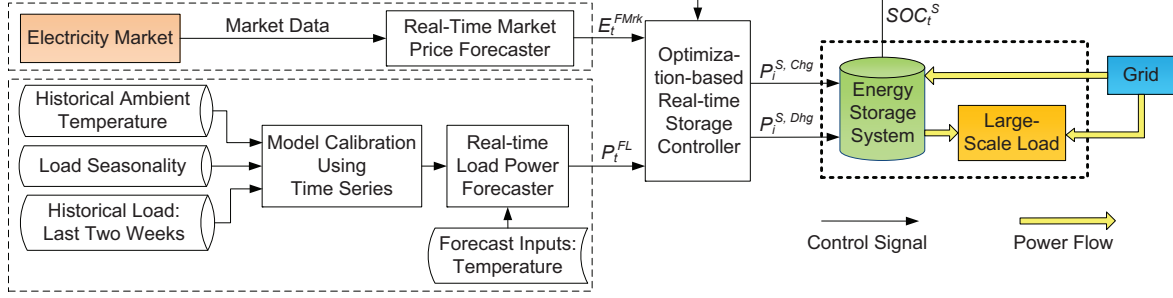
Figure 5.1: Framework of the model for real-time optimal operation of a load-storage system.

timization problem at each time step. This procedure is performed to account for the time-varying nature of load and market price data. More accurate schedules are made for storage by using real-time updates of forecast data. A real-time multi-step optimization-based model is then formulated, including variables with N elements. The real-time storage controller and load forecaster are presented in Sections 5.2.1 and 5.2.2 as follows:

5.2.1   Real-time Storage Controller

A new RTOS model for storage is formulated as an MILP problem. Its chief aim is to optimally coordinate the storage, grid, and load to minimize the electricity cost for the consumer. It also seeks to reduce storage OPEX and to adapt the storage SOC to create a reserve margin that partially feeds the load in case of grid power outages. All the objectives are integrated into a single objective function as formulated in the following:

$$\underset{P_t^{S,Chg}, P_t^{S,Dhg}, P_t^{Slk,LCr}, SOC_t^{Slk,Res}}{\text{Minimize :}} \quad \text{Cost Function} = \sum_{t \in \mathcal{N}_i} \Bigg((P_t^{FL} + P_t^{S,Chg} - P_t^{S,Dhg}) \cdot E_t^{FMrk}$$

$$+ C^{S,ChgO} \cdot P_t^{S,Chg} + C^{S,DhgO} \cdot P_t^{S,Dhg} + \rho^{Pnl,LCr} \cdot P_t^{Slk,LCr} + \rho^{Pnl,Res} \cdot SOC_t^{Slk,Res} \Bigg) \cdot \Delta T. \quad (5.1)$$

This includes the following three terms:

(i) Electricity cost: $(P_t^{FL} + P_t^{S,Chg} - P_t^{S,Dhg}) \cdot E_t^{FMrk} \cdot \Delta T$

(ii) Total OPEX: $(C^{S,ChgO} \cdot P_t^{S,Chg} + C^{S,DhgO} \cdot P_t^{S,Dhg}) \cdot \Delta T$

(iii) Penalty terms: $(\rho^{Pnl,LCr} \cdot P_t^{Slk,LCr} + \rho^{Pnl,Res} \cdot SOC_t^{Slk,Res}) \cdot \Delta T,$

subject to the following physical constraints of storage:

$$b_t^{S,Chg} \cdot P_{min}^{S,Chg} \leq P_t^{S,Chg} \leq b_t^{S,Chg} \cdot P_{max}^{S,Chg} \qquad \forall t \in \mathcal{N}_i \qquad (5.2)$$

$$b_t^{S,Dhg} \cdot P_{min}^{S,Dhg} \leq P_t^{S,Dhg} \leq b_t^{S,Dhg} \cdot P_{max}^{S,Dhg} \qquad \forall t \in \mathcal{N}_i \qquad (5.3)$$

$$SOC_t^S - SOC_{t-1}^S + \left(P_t^{S,Dhg}/\eta^{S,Dhg} - \eta^{S,Chg} \cdot P_t^{S,Chg} + \eta^{S,Dsp} \cdot SOC_t^S \right) \cdot \Delta T = 0$$

$$\forall t \in \mathcal{N}_i , \qquad (5.4)$$

subject to the following reserve-provision constraints:

$$SOC^{S,Res} + SOC_{min}^S - SOC_t^{Slk,Res} \leq SOC_t^S \leq SOC_{max}^S \qquad \forall t \in \mathcal{N}_i \qquad (5.5)$$

$$0 \leq SOC_t^{Slk,Res} \leq SOC^{S,Res} \qquad \forall t \in \mathcal{N}_i , \qquad (5.6)$$

subject to the following constraint to ensure no power is injected into the grid:

$$P_t^{S,Dhg} \leq P_t^{FL} \quad \forall t \in \mathcal{N}_i , \qquad (5.7)$$

and subject to the following constraints to fulfill the load demand in case of grid power outages:

$$P_t^{S,Dhg} = P_t^{FL} - P_t^{Slk,LCr} \quad \forall t \in \mathcal{N}_i \wedge S_t^{Grd} = 0 \qquad (5.8)$$

$$0 \leq P_t^{Slk,LCr} \qquad \forall t \in \mathcal{N}_i , \qquad (5.9)$$

where $\mathcal{N}_i$ is the set of time steps, rolling over the T–hour time notation, defined as follows:

$$\mathcal{N}_i = \{i, \ldots, i + N - 1\}, \qquad (5.10)$$

where i refers to the present time step, defined in a T–hour time notation divided by the time interval ΔT. For instance, at 5:00 am and for $\Delta T = 1$, $i = 5/1 = 5$. In (5.1)–(5.10), except E_t^{FMrk}, other parameters are non-negative (refer to the nomenclature for definitions of parameters).

The objective function, stated in (5.1), includes the cost of purchasing electricity from the market for the total load-storage system and storage OPEX for charging and discharging within the optimization horizon. It also includes penalty terms which will be explained in the following sections. In (5.1), E_t^{FMrk} is the electricity price forecast at the time step t while it is equal to the actual price at the present moment, i.e., $t = 1$. In addition, in (5.1), P_t^{FL} represents the load power forecast in the next T hours. The load power forecaster is presented in Section 5.2.2.

Equations (5.2) and (5.3) express storage charging and discharging power constraints, respectively. The storage energy balance is stated by (5.4), defining the relation of SOC at the two consecutive time steps t and $t - \Delta T$.

Equation (5.5) expresses the SOC constraint. By adding $SOC^{S,Res}$ to (5.5), the lower bound of SOC is considered higher than the physically limited SOC (i.e., SOC^S_{min}) to create reserved energy in the storage reservoir. The reserved energy $SOC^{S,Res}$ can support the load in case of grid power outages. The slack variable $SOC^{Slk,Res}_t$ is included in the constraint (5.5) to optimally decide when and how much reserved energy should be released. This is performed by adapting the lower bound of SOC using the slack variable. As stated by (5.1), this slack variable is penalized to preferably prevent non-zero values. Any non-zero value for the slack variable tends to increase the value of the objective function. The optimization problem always tends to minimize the objective function. Thus, the slack variable is set to zero by the optimization problem solver unless a non-zero value is required to feed the load in case of grid power outages. The zero value for the slack variable is preferred to ensure that the reserved energy is used only in contingencies not in the presence of the grid. Equation (5.6) ensures that the physically limited SOC constraint is not violated by the slack variable. Equation (5.7) ensures that no power is injected to the grid since the load-storage system is considered as an electricity consumer at all times in this study.

As shown in Fig. 5.1, the load power is provided by the grid and storage discharging. If the grid power is interrupted (i.e., $S^{Grd}_t = 0$), the only source of power for the load is storage. This is realized by the constraint (5.8), through which the load requirement is fulfilled as part of the optimization problem. Using the slack variable $P^{Slk,LCr}_t$, the requested power by the load can be curtailed if storage cannot completely fulfill the load requirement. $P^{Slk,LCr}_t$ is penalized in (5.1) to preferably prevent non-zero values that would minimize the load curtailment.

In order for the proper operation of the optimization problem, the following constraint should be met:

$$\rho^{Pnl,LCr} \cdot P^{Slk,LCr}_t > \rho^{Pnl,Res} \cdot SOC^{Slk,Res}_t$$
$$\forall P^{Slk,LCr}_t > 0 \quad \wedge \quad \forall SOC^{Slk,Res}_t > 0 \quad \wedge \quad \forall t \in \mathcal{N}_i. \tag{5.11}$$

The constraint (5.11) imposes a larger penalty for load curtailment than usage of reserved energy. This forces the storage controller to use the reserved energy to meet the load requirement. No load curtailment is performed unless the entire reserved energy is used or if the load requirement is higher than the maximum discharging power of storage.

Equation (5.11) can be met by (5.12), as follows:

$$\rho^{Pnl,LCr} \gg \rho^{Pnl,Res}. \tag{5.12}$$

Finally, as shown in Fig. 5.1, the charging/discharging power set-point in the present time step i is commanded to the storage unit by the storage controller.

5.2.2   Real-time Load Power Forecaster

The mathematical description of a real-time load-forecasting method, which is incorporated into the proposed scheduling model is presented here. The general load-forecasting methodology is adopted from [108], but tailored and fitted to our application (i.e., large-scale loads) in this section.

Since weather-independent and weather-dependent components of the load power are intrinsically different, they are modeled separately. Inspired by the Short-term Load Forecasting (STLF) method in [108], the load power is split into weather-independent and weather-dependent components as expressed in the following:

$$P_t^L = P_t^{WIL} + P_t^{WDL} \qquad \forall t \in \mathcal{N}_i^{\mathcal{L}}, \tag{5.13}$$

where $\mathcal{N}_i^{\mathcal{L}}$ is the set of time steps rolling over the T^L–hour time notation, as follows:

$$\mathcal{N}_i^{\mathcal{L}} = \{i, \ldots, i + N^L - 1\}; \tag{5.14}$$

the weather-independent component of the load depends on the frequently repeated factors of the system. Hence, it can be modeled using a time series-based function such as the Fourier series-based function, expressed in the following [108]:

$$P_t^{WIL} = A_0 + \sum_{k=1}^{n} \left(A_k \, Cos(\omega_k^L t) + B_k \, Sin(\omega_k^L t) \right) \qquad \forall t \in \mathcal{N}_i^{\mathcal{L}}, \tag{5.15}$$

$$\omega_k^L = 2\pi h_k f^L \qquad \forall k \in \{1, 2, 3, \ldots n\}. \tag{5.16}$$

In total, 17 harmonics are selected for model fitting, as follows:

$$h_k = \{1, \ldots, 14, 21, 28, 35\} \qquad \forall k \in \{1, 2, 3, \ldots, n = 17\}; \tag{5.17}$$

based on simulation of various cases in this study, these harmonics are selected to create an accurate model, and yet, to minimize the computation burden.

The relationship between temperature and the weather-dependent component of the load can be expressed using a third-order polynomial function as follows [108]:

$$P_t^{WDL} = \sum_{k=1}^{3} \left(C_{1k} T_t^{Avg,k} + C_{2k} T_{(t-2)}^{Avg,k} + C_{3k} T_{(t-4)}^{Avg,k} \right) \qquad \forall t \in \mathcal{N}_i^{\mathcal{L}}, \tag{5.18}$$

where $T_t^{Avg,k}$ is defined as follows:

$$T_t^{Avg,k} = \left(T_t^k + T_{(t-1)}^k \right) \Big/ 2 \quad \forall k \in \{1,2,3\} \wedge \forall t \in \mathcal{N}_i^{\mathcal{L}}. \tag{5.19}$$

The total load power is stated in the matrix form, as follows:

$$P_t^L = P_t^{WIL} + P_t^{WDL} = \vec{Y_t} \vec{M} \qquad \forall t \in \mathcal{N}_i^{\mathcal{L}}, \tag{5.20}$$

where $\vec{Y_t}$ and $\vec{M}$ are defined as follows:

$$\vec{Y_t} = [\,1 \ \ Cos(\omega_1^L t) \dots Cos(\omega_n^L t), \ \ Sin(\omega_1^L t) \dots Sin(\omega_n^L t), \ \ T_{(t)}^{Avg,1} \ \ T_{(t)}^{Avg,2} \ \ T_{(t)}^{Avg,3}$$
$$T_{(t-2)}^{Avg,1} \ \ T_{(t-2)}^{Avg,2} \ \ T_{(t-2)}^{Avg,3} \ \ T_{(t-4)}^{Avg,1} \ \ T_{(t-4)}^{Avg,2} \ \ T_{(t-4)}^{Avg,3}\,] \quad \forall t \in \mathcal{N}_i^{\mathcal{L}}, \tag{5.21}$$
$$\vec{M} = [\,A_0 \ \ A_1 \dots A_n, \ \ B_1 \dots B_n, \ \ C_{11} \ \ C_{12} \ \ C_{13} \ \ C_{21} \ \ C_{22} \ \ C_{23} \ \ C_{31} \ \ C_{32} \ \ C_{33}\,]^{tr}. \tag{5.22}$$

For every sample of historical load data (i.e., at every t), one equation is generated as stated by (5.20). For N^L samples of historical data, (5.20) is expressed as follows:

$$\underline{Y}_{(N^L,\,2n+10)} \, \vec{M}_{(2n+10,\,1)} = \vec{P}_{(N^L,\,1)}^L + \vec{\epsilon}_{(N^L,\,1)}. \tag{5.23}$$

The model parameters vector $\vec{M}$ is unknown which is to be estimated. In such a case, using a Least Error Square (LES)-based method, the aim is to estimate an $\vec{M}$ which minimizes the error vector $\vec{\epsilon}$; that $\vec{M}$ represents the optimal vector of model parameters, as stated in the following:

$$\vec{M} = \underline{Y}^{-1L} \, \vec{P}^L, \tag{5.24}$$

where $\underline{Y}^{-1L}$ is the left pseudo-inverse of $\underline{Y}$ given as follows:

$$\underline{Y}^{-1L} \triangleq \left[[\underline{Y}^{tr} \, \underline{Y}]^{-1} \, \underline{Y}^{tr} \right]. \tag{5.25}$$

The proof of obtaining (5.24) from (5.23) is stated in Appendix A.

Function matrix $\underline{Y}$ is generated by (5.21) using historical load and temperature data.

Then, $\vec{M}$ is computed by (5.26), as follows:

$$\vec{M} = \underline{Y}^{-1L}\,\vec{P}^{HL},\tag{5.26}$$

where historical load data $\vec{P}^{HL}$ is assumed to be available.

Using the temperature forecast, $\underline{Y}^F$ is generated by (5.21). Finally, forecast load $\vec{P}^{FL}$ is computed by (5.27), as follows:

$$\vec{P}^{FL} = \underline{Y}^F\,\vec{M}.\tag{5.27}$$

As shown in Fig. 5.1, the load forecast is inputted to the optimization-based storage controller where in real-time, the actual value of load substitutes for the forecast one.

5.3 Numerical Evaluation

As a real-world case study, a large-scale institutional electricity consumer in Ontario, Canada is selected. In general, a large-scale consumer may purchase the electricity from the local distribution company or wholesale electricity market. In this study, it is assumed that the selected large-scale consumer purchases the electricity directly from the wholesale market and experiences real-time pricing on an hourly basis. It is also emphasized that the calculated electricity cost for different cases in this section only includes HOEP charges. The consumer bill can include supplementary charges in addition to HOEP charges. The main purpose of electricity cost analysis in this section would be, therefore, to compare the HOEP charges for different cases. The electrical load information, ambient temperature, and HOEPs - adopted from Ontario's electricity market - in different years (i.e., 2012, 2013, and 2014) are used for numerical evaluation.

5.3.1 Modeling and Validation

The model represented in Fig. 5.1 is developed in MATLAB. As an imperfect forecasting method, back-casting has been used in this thesis to estimate DAM prices [38], [40]. In real-time, the actual value of price substitutes for the forecast one. In the RTOS model, E_t^{FMrk} is updated at every time step t. The joint execution of the GLPK package [102] and MATLAB is used to solve the optimization problem. The storage with different ratings can be used for simulation. In order to find the appropriate charge and discharge ratings for storage, different ratings have been selected, and accordingly, the storage profit against its capital cost has been examined for each set of charge/discharge rating.

Table 5.1: Modeling and Simulation Parameters

$T = 24$ (h)	$T^L = 336$ (h)
$\Delta T = 1$ (h)	$N = 24$
$N^L = 336$	$f^L = 1/168$ (h^{-1})
$P_{max}^{S,Chg} = 2.5$ (MW)	$P_{min}^{S,Chg} = 80\% \times P_{max}^{S,Chg}$
$P_{max}^{S,Dhg} = 2.5$ (MW)	$P_{min}^{S,Dhg} = 3\% \times P_{max}^{S,Dhg}$
$SOC_{max}^S = 25$ (MWh)	$SOC_{min}^S = 10\% \times SOC_{max}^S$
$SOC^{S,Res} = 10\% \times SOC_{max}^S$	$\eta^{S,Chg} = \eta^{S,Dhg} = 84\%$
$\eta^{S,Dsp} = 0.0063\% \times SOC_t^S$	Capital Cost (CC) = \$2.5 Million
Storage Age $= 40$ (Yr) $= 350400$ (h)	$C^{S,Main} = 5\% \times$ CC/Storage Age
$C^{S,ChgO} = 60\% \times C^{S,Main}/P_{max}^{Chg}$	$C^{S,DhgO} = 40\% \times C^{S,Main}/P_{max}^{Dhg}$
$\rho^{Pnl,Res} = 10^6$	$\rho^{Pnl,LCr} = 10^{12}$

Finally, a storage unit with charge and discharge ratings equal to 10% of the load daily peak, i.e., 2.5 MW has been selected. Due to its smaller footprint, CES does not occupy a large space as compared to CAES, and hence, it is more appropriate for urban locations. Thus, CES has been selected for simulation studies in this chapter of the thesis. The modeling parameters of CES along with simulation parameters are listed in Table 5.1.

To evaluate the accuracy of the load forecasting model, the mean value and standard deviation of forecast error are computed for the selected real-world case-load. The Probability Density Function (PDF) and probability of forecast error are illustrated in Fig. 5.2. According to Fig. 5.2, in most cases, the forecast error has a significantly low mean value and standard deviation, i.e., less than 5% in more than 50% of the cases. This reveals the feasibility and efficacy of the forecasting model. According to simulation results, this level of load forecast inaccuracy will not considerably affect the optimal operation of the model. Further analysis of the load forecasting algorithm is presented in Appendix B.

5.3.2 Impact of Storage on the Consumers' Electricity Cost

The annual electricity cost is calculated for both the proposed real-time and the self-scheduling models considering perfect and imperfect market price forecasts; these costs are presented in Table 5.2 along with the costs incurred without storage. As obvious from Table 5.2, in both the self-scheduling and proposed models, storage has been successful in reducing the consumers' electricity cost.
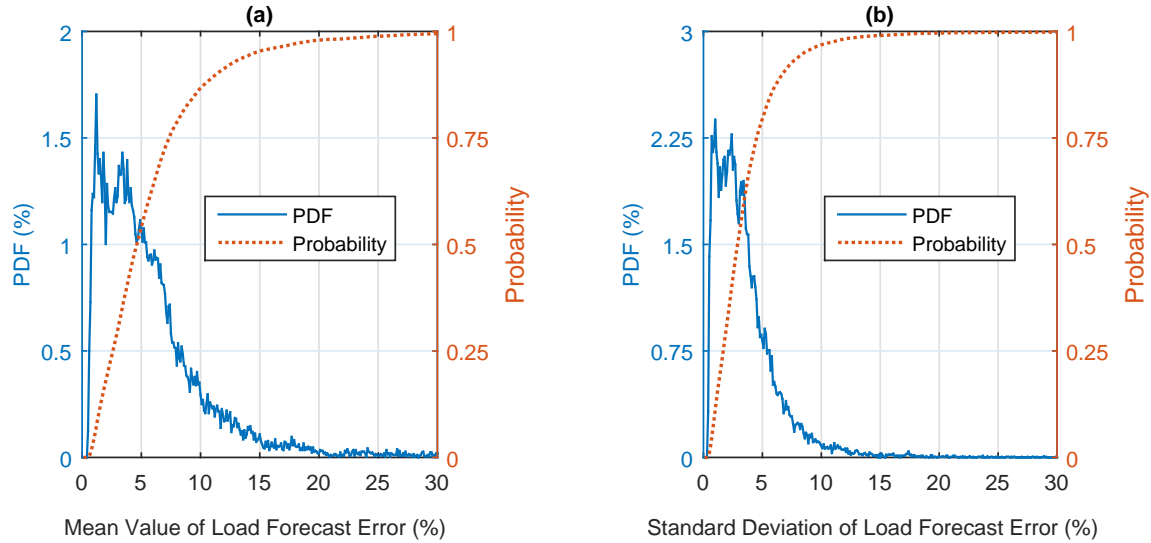
Figure 5.2: Probability density function and probability of forecast error (a): mean value and (b): standard deviation for the real-world load information from 2012 to 2014.

Table 5.2: Annual Electricity Cost (M$) for Consumer in Different Cases

Year	No Storage	Perfect Price Forecast		Imperfect Price Forecast	
		Self-Scheduling	Proposed	Self-Scheduling	Proposed
2012	2.94	2.87	2.85	2.92	2.88
2013	3.20	3.11	3.09	3.18	3.13
2014	3.85	3.69	3.65	3.82	3.74
Average	3.33	3.22	3.20	3.31	3.25

The annual reduction of the electricity cost through storage that uses the proposed real-time model has been compared with that using the self-scheduling model; the results are depicted in Fig. 5.3. Based on the three-year average results, for the perfect forecast of market prices, the electricity cost is reduced by 3.9% using the proposed model; whereas, the cost reduction is 3.3% using the self-scheduling model, previously proposed in the literature. For the imperfect price forecast, the cost reduction is 2.4% versus 0.6% using the proposed and self-scheduling models, respectively. Notably, the proposed model becomes more effective when forecast error increases.

In the proposed model, the storage schedule is updated at each time step. As a result, a more precise schedule is determined by the proposed model, where especially peak and off-peak prices appearing in real-time are kept in consideration. Thus, the electricity cost is reduced more compared to the self-scheduling model. This opportunity does not exist for the self-scheduling model since the optimal schedule cannot be corrected in real-time.
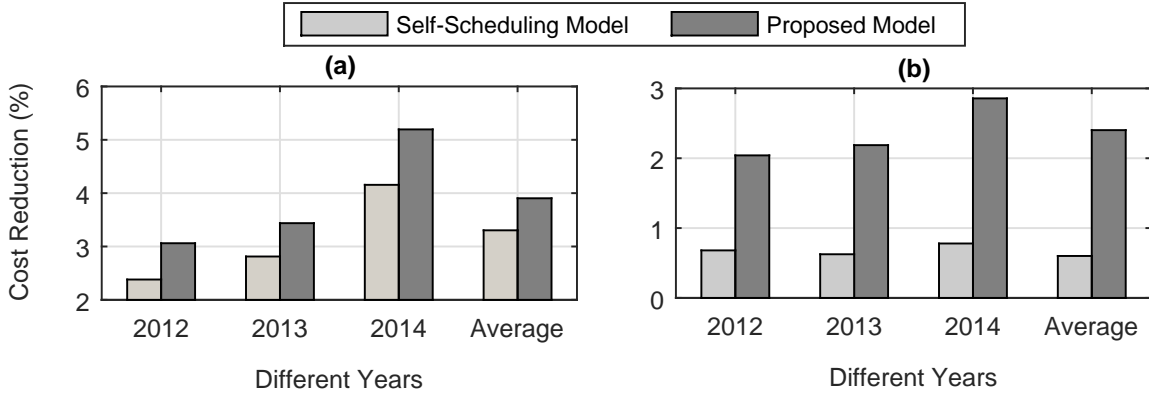
Figure 5.3: Annual reduction of electricity cost for the consumer using (a): perfect forecast, (b): imperfect forecast of Ontario's market prices in different years.

Moreover, it can be observed from Fig. 5.3 that in the most recent year (i.e., 2014), the electricity cost reduction is higher than the one in 2012. This reveals that load-storage systems will benefit more in the near future since the cost reduction has an increasing trend from 2012 to 2014.

5.3.3   Impact of Storage on Absorbed Power from the Grid

Fig. 5.4 shows the total power absorbed by the load-storage system from the grid and the scheduled charging (positive power) and discharging (negative power) of storage in a typical day (i.e., April 21, 2014) for three cases as follows:

- Case 0: load without storage.

- Case 1: load with storage using the self-scheduling model.

- Case 2: load with storage using the proposed model.

Figs. 5.4 (a) and (c) represent the result for the perfect price forecast while Figs. 5.4 (b) and (d) represent the result for the imperfect price forecast.

As shown in Fig. 5.4 (a), due to the storage operation, in both Cases 1 and 2, the load profile has flattened more compared to Case 0. However, there is a small difference between Cases 1 and 2 in the sense that in Case 2, less power has been absorbed during peak periods. It is observed from Fig. 5.4 (c) that the storage has discharged more during peak hours in Case 2 as compared to Case 1. Therefore, in Case 2 the electricity cost is reduced more as compared to Case 1 (see Fig. 5.3 (a)).
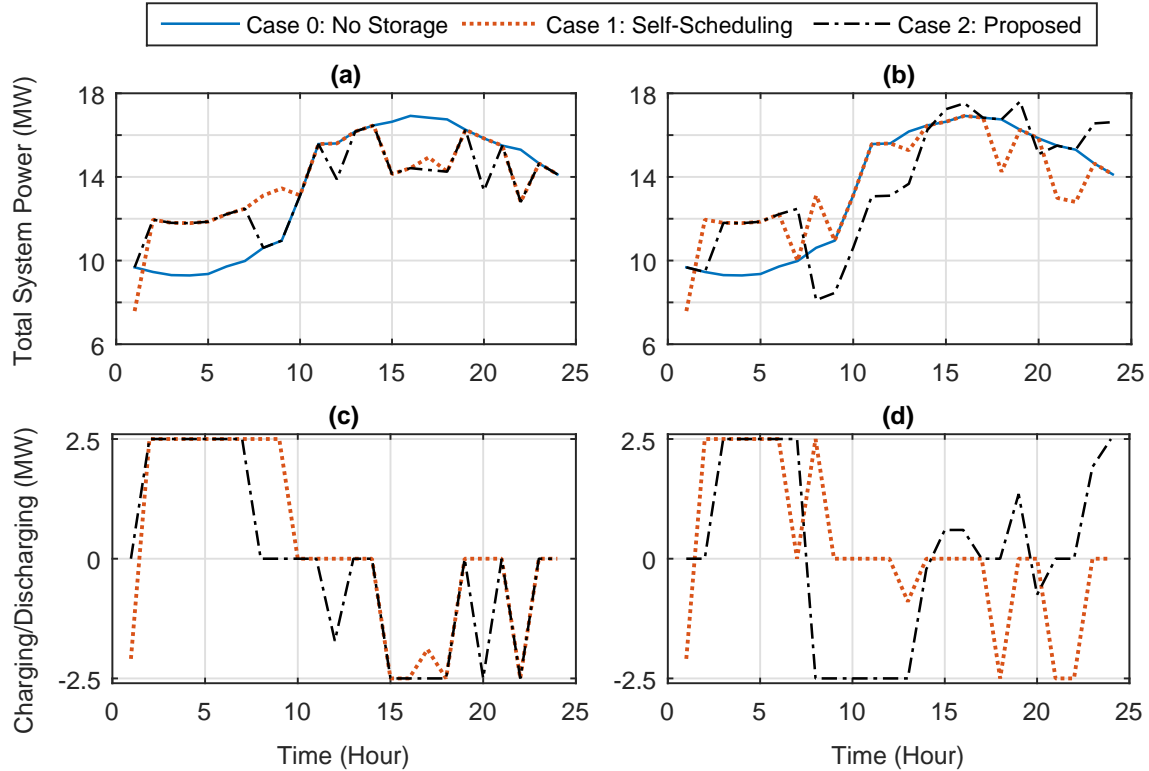
Figure 5.4: (a) & (c): System and storage power for perfect price forecast. (b) & (d): System and storage power for imperfect price forecast: in April 21, 2014.

As shown in Figs. 5.4 (b) and (d), the load profile and storage operation have been affected by market price forecast error. Since in both Cases 1 and 2, more power has been absorbed during the off-peak period, the electricity cost has been reduced when compared to Case 0. However, during the peak period, the storage operation has not been optimal due to price forecast error. In the proposed model, the adverse impact of price forecast error is reduced since the storage schedule is updated at each time step. Thus, a higher level of profit is obtained by using the proposed model (see Fig. 5.3 (b)).

It is worth mentioning that the forecast power of the adjusted load (i.e., power absorbed by the load-storage system) is submitted to the DAM. Although this forecast may change in the real-time operation, it can be useful for the ISO to better manage generation and consumption in the electricity market.

5.3.4 Served Energy by Storage and Storage Operation Hours

As reported in Table 5.2, the proposed real-time model outperforms the self-scheduling model by providing a higher reduction in the consumer's electricity cost. On a basic level,

Table 5.3: Annual Discharged Energy by Storage to the Grid (GWh)

Year	Perfect Price Forecast		Imperfect Price Forecast	
	Self-Scheduling	Proposed	Self-Scheduling	Proposed
2012	3.3474	2.9885	3.3493	2.9124
2013	4.2975	4.1999	4.2909	3.9111
2014	5.3387	5.4710	5.3304	4.6990
Average	4.3279	4.2198	4.3235	3.8408

Table 5.4: Annual Hours of Operation of the Storage Discharging Plant

Year	Perfect Price Forecast		Imperfect Price Forecast	
	Self-Scheduling	Proposed	Self-Scheduling	Proposed
2012	1562	1352	1562	1379
2013	1954	1879	1951	1832
2014	2377	2420	2374	2190
Average	1964	1884	1962	1800

the better performance of storage could be due to serving more energy or equal/less energy at more appropriate hours. As presented in Table 5.3, on average, the annual discharged energy by storage in the self-scheduling and proposed models is 4.33 GWh versus 4.22 GWh, respectively, for the perfect price forecast. The values are 4.32 GWh versus 3.84 GWh for the imperfect price forecast. Moreover, as reported in Table 5.4, on average, the annual hours of the storage operation for the self-scheduling and proposed models are 1964 versus 1884, respectively, for the perfect price forecast. These values are 1962 versus 1800 for the imperfect price forecast. Thus, the proposed model has reduced the storage discharged energy by 2.5% and 11.2% for perfect and imperfect price forecasts, respectively, as compared to the self-scheduling model (see Fig. 5.5 (a)). Additionally, the proposed model has reduced the storage operation hours by 4.1% and 8.3% for perfect and imperfect price forecasts, respectively (see Fig. 5.5 (b)).

Therefore, in the proposed real-time model, less annual energy is served by storage, and storage is operated for fewer hours as compared to the self-scheduling model; yet the proposed model benefits the load more. The superior performance of storage in the proposed model is not due to serving more energy; rather, it serves less energy at more appropriate hours. Consequently, not only does the proposed real-time model benefit the load by reducing the electricity cost more, but it also decreases the storage OPEX and increases the life of storage by reducing the hours of operation.
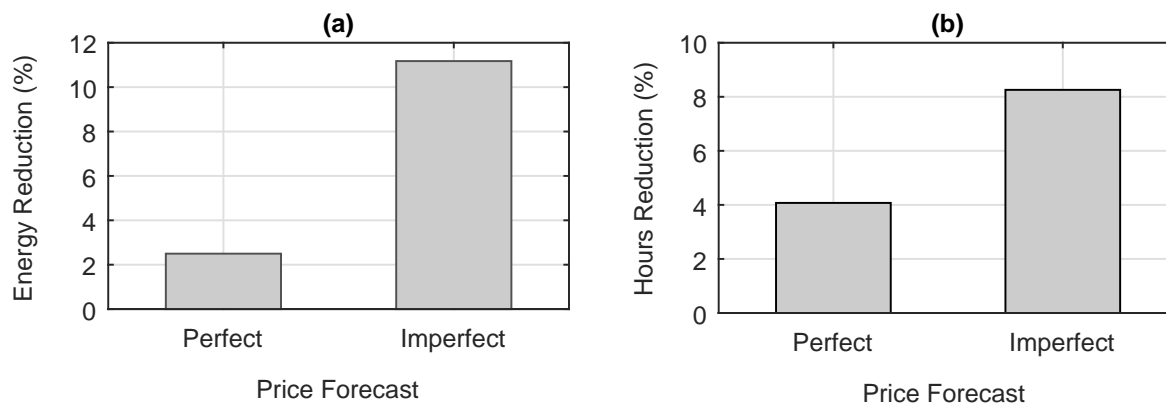
Figure 5.5: Reduction of (a): storage discharged energy and (b): storage operation hours, using the proposed model compared to the self-scheduling model.

Table 5.5: Profitability of Investment (%) and Break-even Time (Year)

	Perfect Price Forecast		Imperfect Price Forecast	
	Self-Scheduling	Proposed	Self-Scheduling	Proposed
Profitability	59	69	11	43
Break-even	22.73	19.23	125	31.25

5.3.5   Profitability of Investment and Break-even Time

In order to examine the profitability level of investment in storage, the expected ROR needs to be determined, which could be different for each project depending on its risk profile. In the following, the ability of storage operated under two studied optimization models to generate an annual net profit equal to 7.5% of the storage capital cost is investigated. This includes the storage CAPEX and the expected profit of investment over the storage life. Given that the profitability level of 100% is required for the plant to generate the expected profit, the profitability levels for self-scheduling and the proposed real-time models based on the three-year average data are calculated and compared in Table 5.5. In this table, the break-even time, which is the amount of time needed for generated profit to equal the initial capital cost, is also reported.

As indicated in Table 5.5, the proposed real-time model outperforms the self-scheduling one due to the higher profitability level (69% versus 59%) and lower break-even time (19.23 versus 22.73 years) for the perfect price forecast. As reported in Table 5.5, the proposed model is significantly more effective than the self-scheduling one when the price forecast error increases.

5.3.6   Further Benefits of Storage in the Proposed Model

As explained in Section 5.2.1, storage in the proposed model also provides reserved energy for the load in case of grid outages. The reserved energy can be used to feed the vital parts of the load similar to what emergency diesel generators do. In such a case, storage may replace some back-up diesel generators, thereby creating more financial benefits for the load. Moreover, through shifting the load from peak to off-peak periods, storage benefits the grid by reducing the possibility of congestion in both the transmission and distribution systems. This development could potentially open up opportunities for profit generation for load-storage systems.

5.4   Conclusion

A new Real-time Optimal Scheduling (RTOS) model is proposed in this chapter of the thesis to aggregate storage benefits for a large-scale electricity consumer. The application of the proposed model to a real-world large-scale institutional load in Ontario, Canada, is examined and compared with the self-scheduling model previously proposed in the literature. The electricity cost for the load is reduced by 3.9% using the proposed real-time model; whereas, the cost reduction is 3.3% based on the self-scheduling model, thereby 0.6% increase in savings. Considering uncertainties associated with Day-ahead Market (DAM) prices, the cost reduction is 2.4% versus 0.6% using the proposed and self-scheduling models, respectively, thereby 1.8% increase in savings. The annual electricity cost for a large-scale electricity consumer could be several millions of dollars. For this reason, the percentage of the increased savings multiplied by the annual cost leads to substantial savings in terms of dollars. The proposed model will, therefore, result in higher profitability of investment and lower break-even time. Additionally, the proposed model has reduced the storage operation hours by 4.1% and 8.3% for perfect and imperfect price forecasts, respectively, compared to the self-scheduling model. Consequently, not only does the proposed real-time model benefit the load by reducing the electricity cost more, but it also decreases the storage Operating Expenditure (OPEX) and increases the life of storage by reducing the hours of operation. It is indicated that the electricity cost reduction by storage has an increasing trend from 2012 to 2014. As a result, it is expected that the profitability of investment in storage will increase for large-scale consumers in the near future.

Chapter 6

Conclusion

The increase in renewable energy penetration into Ontario's electricity market has adversely altered the overall behaviour of the energy market, with negative electricity prices even starting to appear. Negative prices represent a greater supply than the market demands, mostly appearing at night and during off-peak periods. Energy storage can be deployed in Ontario for peak shaving and energy shifting from off-peak to peak periods to address the above-mentioned issues. This is also the concern of many other system operators across the world. Several market operators around the world have already started setting regulatory policies to facilitate storage deployment in the market.

This thesis is mainly focused on developing optimization-based models for scheduling of energy storage units. At first, a Real-time Optimal Scheduling (RTOS) algorithm is developed seeking to maximize the storage revenue by exploiting arbitrage opportunities available due to the inter-temporal variation of electricity prices. Comparative studies are performed to investigate the value and benefit of storage optimized to utilize wholesale and contract-based electricity prices The electricity price modulation is proposed as an approach to competitively offer incentive by the utility regulator to storage to fill the gap between current and a stable rate of return.

Subsequently, the application of large-scale storage for congestion relief in transmission systems as an ancillary service to the grid is investigated. An algorithm is proposed for the following objectives: (i) to generate revenue primarily by exploiting electricity price arbitrage opportunities and (ii) to optimally prepare the storage to maximize its contribution to transmission congestion relief. An analysis is presented regarding the appropriate amount of financial compensation for the storage owner due to its contribution to congestion relief.

In addition, an algorithm is proposed to enable independently operated, locally controlled storage to accept dispatch instructions issued by Independent System Operators

(ISOs). Storage in this case is referred to as *dispatchable storage.* A new index is proposed to measure the storage dispatchability. While the operation of locally controlled storage is optimally scheduled at the owner's end, using the proposed algorithm, storage is fully dispatchable at the ISO's end.

Finally, a model is proposed and analyzed to aggregate storage benefits for a large-scale load. The complete model for optimal operation of storage-based electrical loads considering both the capital and operating expenditures of storage is developed.

The applications of the proposed algorithms and models are examined using real-world market data adopted from Ontario's electricity market and actual load information from a large-scale institutional electricity consumer in Ontario.

6.1   Outcomes

The main outcomes of this thesis are presented as follows:

- It is indicated that the overall behaviour of the energy market has been altered, with negative electricity prices even starting to appear. The application of large-scale energy storage units independently operated in the market is considered for substantial energy shifting to deal with negative price issues.

- It is demonstrated that both Time of Use (TOU) and wholesale market prices cannot offer an attractive Rate of Return (ROR) to make investments in large-scale independently operated storage appealing for private investors; however, the profitability of investment in storage operated in the wholesale market is significantly higher compared to storage utilizing TOU rates. Using the back-casting method, the five-year average revenue of storage for Ontario's wholesale market prices equals $4.43 M, whereas the annual revenue of storage for the TOU rates equals $1.92 M.

- It is presented that the ideal profitability level using the perfect price forecast is 77%. The profitability level obtained by utilizing a forecast of wholesale market prices and TOU rates are 53% and 23%, respectively. The storage revenue increases and becomes closer to the ideal revenue if the error of the price forecast decreases.

- It is indicated that for the perfect price forecast in Ontario's market, it is required to modulate electricity prices by 1.3 to meet the expected revenue for storage owners. It is demonstrated that the price forecast inaccuracy reduces the storage revenue, and thus, a higher price modulation factor (i.e., 1.87) would be required to fill the gap between current and a stable expected ROR.

- When storage injects power to the grid for congestion relief using the proposed adaptive penalizing mechanism, a considerable contribution to congestion relief is obtained (i.e., 93.35% and 92.7% for perfect and imperfect price forecasts, respectively); in such a case, only a small portion of the storage base revenue (i.e., 3.25% and 2.74% for perfect and imperfect prices forecasts, respectively) is lost. This reveals the feasibility and efficacy of the proposed RTOS algorithm, which aims to optimally employ large-scale storage for congestion relief. In addition, the efficacy of the proposed algorithm is validated when storage contributes to congestion relief by absorbing power from the grid.

- When storage is scheduled as a dispatchable asset in the market, the storage dispatchability index equals 98.5% and 78.5% using the proposed and conventional optimal scheduling algorithms, respectively. Hence, around 100% of ISO's dispatch instructions can be followed by the storage using the proposed algorithm. Considering forecast uncertainties associated with Day-ahead Market (DAM) prices, the storage revenue for dispatchable storage is larger than that for self-scheduling storage ($1.66 M versus $1.25 M on average); moreover, the Revenue Reduction due to Price Forecast Error (RRPFE) is lower for dispatchable storage as compared to self-scheduling storage (61.2% versus 76.3% on average). It is observed that the largest levels of revenue are associated with the operation of non-dispatchable intermittent storage ($4.29 M and $6.41 M for lower and higher bounds, respectively).

- It is demonstrated that the proposed real-time model for scheduling of load-storage systems outperforms the self-scheduling model by generating a higher level of profit for the load-storage system. The electricity cost for the load is reduced by 3.9% using the proposed real-time model; whereas, the cost reduction is 3.3% based on the self-scheduling model proposed in the literature, thereby 0.6% increase in savings. Considering uncertainties associated with DAM prices, the cost reduction is 2.4% versus 0.6% using the proposed and self-scheduling models, respectively, thereby 1.8% increase in savings. The annual electricity cost for a large-scale electricity consumer could be several millions of dollars. For this reason, the percentage of the increased savings multiplied by the annual cost leads to substantial savings in terms of dollars. The proposed model will, therefore, result in higher profitability of investment and lower break-even time. Additionally, the proposed model reduces the storage operation hours by 4.1% and 8.3% for perfect and imperfect price forecasts, respectively, compared to the self-scheduling model.

6.2 Contributions and Significance of the Thesis

The contributions and significance of this thesis are presented below.

6.2.1 Scheduling of Storage for Exploiting Arbitrage

i) An RTOS algorithm has been developed by formulating a Mixed Integer Linear Programming (MILP) optimization problem which aims to generate revenue by utilizing arbitrage opportunities available due to the volatility of electricity prices.

ii) A new mechanism for storage incentivisation has been proposed. The electricity price modulation has been incorporated as part of the optimization algorithm to competitively offer incentive by utility regulators to storage owners.

iii) The economic viability of the operation of large-scale energy storage technologies in electricity markets has been studied.

Adopting the proposed mechanism in this thesis for storage incentivisation will bring value for both the utility regulator/system operator and storage investor. This is because the more the storage is operated to support the power grid by means of energy shifting/peak shaving, the more incentives it can receive from the utility regulator. The storage owner profits by receiving more incentive, and the utility regulator/system operator benefits by less demand during peak periods.

6.2.2 Scheduling of Storage for Congestion Relief

i) Based on a new adaptive penalizing mechanism, an algorithm has been proposed which optimally prepares the storage to follow external congestion relief commands.

ii) The required amount of financial compensation for the storage owner due to its contribution to congestion relief has been examined.

By implementing the proposed algorithm in this thesis, a considerable amount of contribution to congestion relief is obtained, e.g., 93.35% and 92.7% for perfect and imperfect prices forecasts, respectively. In such a case, storage contribution to congestion relief would be 15.88% and 20.14% higher for perfect and imperfect prices forecasts, respectively, when compared to a conventional algorithm. This reveals that the proposed algorithm is superior to presently employed techniques.

6.2.3 Scheduling of Storage as a Dispatchable Asset

i) A new optimal scheduling algorithm has been proposed aiming to enable an independently operated, locally controlled storage unit to accept external dispatch instructions issued by the ISO.

ii) Using slack variables, a new index has been proposed to measure the storage dispatchability in a competitive electricity market.

iii) Using real-world market data, the efficacy and feasibility of the proposed algorithm to enable a locally controlled storage unit to accept ISO's dispatch instructions have been validated.

According to numerical studies, the storage dispatchability index equals 98.5% and 78.5% using the proposed and conventional optimal scheduling algorithms, respectively. Hence, around 100% of ISO's dispatch instructions can be followed by the storage using the proposed algorithm. Thus, the proposed algorithm outperforms previous algorithms by increasing the storage dispatchability. Dispatchable storage units have great potential to enhance the flexibility of electric grids and are key elements envisioned to enable smart grid realization.

6.2.4 Scheduling of Load-storage Systems

i) A new real-time multi-step optimization-based model has been proposed and formulated to optimally schedule the joint operation of a large-scale load and a storage unit.

ii) A real-time load forecasting model, suitable for large-scale loads, has been incorporated into the optimal scheduling algorithm using soft constraints, slack variables, and penalizing mechanisms.

iii) Using a real-world case study, the operation of the proposed model has been examined and compared with the self-scheduling model proposed in the literature.

The proposed real-time model outperforms prior models by generating higher profitability of investment, lower storage Operating Expenditure (OPEX), and an extended life of the storage plant. The electricity cost for the load is reduced by 3.9% using the proposed real-time model; whereas, the cost reduction is 3.3% based on the previously proposed models in the literature. The proposed model also reduces the storage operation hours by 4.1% and 8.3% for perfect and imperfect price forecasts, respectively, compared to prior models.

6.3   Publications

The content of this thesis has also appeared in the following publications:

6.3.1   Peer-Reviewed Journals

1. **H. Khani**, R. K. Varma, M. R. D. Zadeh, and A. H. Hajimiragha, "A Real-Time Multi-Step Optimization-Based Model for Scheduling of Storage-Based Large-Scale Electricity Consumers in a Wholesale Market," *IEEE Trans. Sustain. Ener.*, Under Revision, Jun. 2016.

2. **H. Khani**, M. R. D. Zadeh, and R. K. Varma, "Optimal Scheduling of Independently Operated, Locally Controlled Energy Storage Systems as Dispatchable Assets in a Competitive Electricity Market," *IET Gener. Transm. Distrib.*, Under Revision, Aug. 2016.

3. **H. Khani**, M. R. D. Zadeh, and A. H. Hajimiragha, "Transmission Congestion Relief Using Privately Owned Large-Scale Energy Storage Systems in a Competitive Electricity Market," *IEEE Trans. Power Syst.*, vol. 31, no. 2, pp. 1449-1458, Mar. 2016.

4. **H. Khani** and M. R. D. Zadeh, "Online Adaptive Real-Time Optimal Dispatch of Privately Owned Energy Storage Systems Using Public-Domain Electricity Market Prices," *IEEE Trans. Power Syst.*, vol. 30, no. 2, pp. 930-938, Mar. 2015.

5. **H. Khani** and M. R. D. Zadeh, "Real-Time Optimal Dispatch and Economic Viability of Cryogenic Energy Storage Exploiting Arbitrage Opportunities in an Electricity Market," *IEEE Trans. Smart Grid*, vol. 6, no. 1, pp. 391-401, Jan. 2015.

6.3.2   Refereed Conferences

1. **H. Khani** and M. R. D. Zadeh, "Energy Storage in an Open Electricity Market with Contribution to Transmission Congestion Relief," in *Proc. 2014 IEEE PES General Meeting*, Washington DC, USA *(Best Conference Papers Session on Markets, Economics, Planning)*.

2. **H. Khani**, M. R. D. Zadeh, and R. Seethapathy, "Large-Scale Energy Storage Deployment in Ontario Utilizing Time-of-Use and Wholesale Electricity Prices: An Economic Analysis," in *Proc. 2014 Cigre Conference*, Toronto, ON, Canada.

3. **H. Khani**, M. R. D. Zadeh, and A. H. Hajimiragha, "Loss of Data Management in Real-Time Short-Term Forecasting Algorithms," in *Proc. 2013 IEEE International Conference on Smart Grid Engineering*, Oshawa, ON, Canada.

6.4 Future Work

The following topics are suggested for future work:

- Based on the analyses conducted throughout this thesis, storage operation is adversely affected by uncertainties associated with DAM prices. The stochastic programming approach can be employed to deal with price forecast inaccuracy to some extent. However, stochastic models are computationally challenging due to the large number of scenarios that have to be considered. The model also requires knowledge of the probability distribution of uncertain variables, which may not be available. Developing scheduling algorithms for storage which are less sensitive to market price forecast uncertainties is suggested for future work.

- Comprehensive mechanisms can be developed for storage compensation when it provides ancillary services to the grid, such as congestion relief. These mechanisms should comply with the rules and regulations of the electricity markets.

- In order to increase the profitability level of investment in storage, different sources of revenue and profit generation should be provided for storage. In this thesis, storage is utilized for exploiting arbitrage and for congestion relief at the same time. One of the application of large-scale storage is for Transmission and Distribution (T & D) upgrade deferral. Storage can also be operated in the reserve market in order to generate more profit. While these applications of storage have been investigated in the literature, incorporating all the applications into a single optimal scheduling algorithm would be a useful topic for future research in this area.

- Dispatchable storage units play a crucial role in preserving the reliability and security limits of the grid; they are also key elements envisioned to enable smart grid realization. Appropriate policies for financial support of locally controlled dispatchable storage units by utility regulators/ISOs can be investigated in the future; the objectives of this financial support would be to encourage deployment of storage units as dispatchable assets in electricity markets.

- Numerical evaluation of several benefits of storage both for the load and for the grid, such as providing reserved energy for the load and decreasing the possibility of congestion in the grid is suggested for future research in this area.

Appendix A

Proof of Theorem for Load Forecasting

The proof of obtaining (5.24) from (5.23) is presented in this section. Based on (5.23), the load power is stated as follows:

$$\underline{Y}\,\vec{M} = \vec{P}^L + \vec{\epsilon}. \tag{A.1}$$

Equation (A.1) can be written as follows:

$$\underline{Y}\,\vec{M} - \vec{P}^L = \vec{\epsilon} \tag{A.2}$$

$$(\underline{Y}\,\vec{M} - \vec{P}^L)^{tr}(\underline{Y}\,\vec{M} - \vec{P}^L) = \vec{\epsilon}^{tr}\vec{\epsilon} \tag{A.3}$$

$$(\vec{M}^{tr}\,\underline{Y}^{tr} - \vec{P^L}^{tr})\,(\underline{Y}\,\vec{M} - \vec{P}^L) = \vec{\epsilon}^{tr}\vec{\epsilon} \tag{A.4}$$

$$\vec{M}^{tr}\underline{Y}^{tr}\underline{Y}\vec{M} - \vec{M}^{tr}\underline{Y}^{tr}\vec{P}^L - \vec{P^L}^{tr}\underline{Y}\vec{M} + \vec{P^L}^{tr}\vec{P}^L = \vec{\epsilon}^{tr}\vec{\epsilon}. \tag{A.5}$$

Considering (A.6) in the following:

$$\vec{M}^{tr}\underline{Y}^{tr}\vec{P}^L = (\vec{P^L}^{tr}\underline{Y}\vec{M})^{tr}\ \&\ (\vec{P^L}^{tr}\underline{Y}\vec{M})^{tr} = \vec{P^L}^{tr}\underline{Y}\vec{M}, \tag{A.6}$$

equation (A.5) is simplified as expressed in the following:

$$\vec{M}^{tr}\,\underline{Y}^{tr}\,\underline{Y}\,\vec{M} - 2\,\vec{M}^{tr}\,\underline{Y}^{tr}\,\vec{P}^L + \vec{P^L}^{tr}\,\vec{P}^L = \vec{\epsilon}^{tr}\,\vec{\epsilon}. \tag{A.7}$$

The optimal solution for $\vec{M}$ in (A.7) can be obtained when the values of elements in $\vec{M}$ minimize the error vector $\vec{\epsilon}$. Thus,

$$\frac{d}{d\vec{M}}\left(\vec{M}^{tr}\,\underline{Y}^{tr}\,\underline{Y}\,\vec{M} - 2\vec{M}^{tr}\,\underline{Y}^{tr}\,\vec{P}^{L} + \vec{P^{L}}^{tr}\,\vec{P}^{L}\right) = 0 \tag{A.8}$$

$$2\,\underline{Y}^{tr}\,\underline{Y}\,\vec{M} - 2\,\underline{Y}^{tr}\,\vec{P}^{L} = 0. \tag{A.9}$$

Finally, the model parameters vector $\vec{M}$ as expressed by (5.24) is given in the following:

$$\vec{M} = \underline{Y}^{-1L}\,\vec{P}^{L}, \qquad \underline{Y}^{-1L} \triangleq \left[[\underline{Y}^{tr}\,\underline{Y}]^{-1}\,\underline{Y}^{tr}\right]. \tag{A.10}$$

Appendix B

Analysis of the Load Forecaster

B.1 Real-time Load Forecasting Algorithm

In this appendix, the aim is to further analyze the STLF algorithm used in Chapter 5 for scheduling of load-storage systems. Fig. B.1 shows the block diagram of a Real-time Short-term Forecasting (STF) algorithm. As shown in this figure, the historical data including load, generation, price, weather data (mostly temperature data), seasonality, and any other required data depending on the type of forecaster are first provided for the calibrator to create the forecasting model. The model can be made by the calibrator based on different methods such as time series or artificial intelligent-based methods. A calibration report is required to evaluate the performance of the model in order to ensure that it is accurate. After the model is made, the parameters of the forecasting model is fed into the forecaster. The forecaster is also provided with other input data, such as weather forecast data or any other required parameter to perform accurate forecasting. The output forecast data in a STF algorithm can include electric load, electric power generation, or energy price data for the next several hours, such as 24 hours. The forecast data is inputted to the controller in real-time in order for the controller to be able to run the RTOS algorithm every several minutes, thereby providing optimal set-points for energy storage units.

B.2 Two Forecasting Methods

In case of load and electricity price forecasts, STF algorithms can fall into two general categories. In the first category, weekdays, weekends, and holidays are forecast together using the same algorithm and historical data, which is called Method 1 in this thesis.
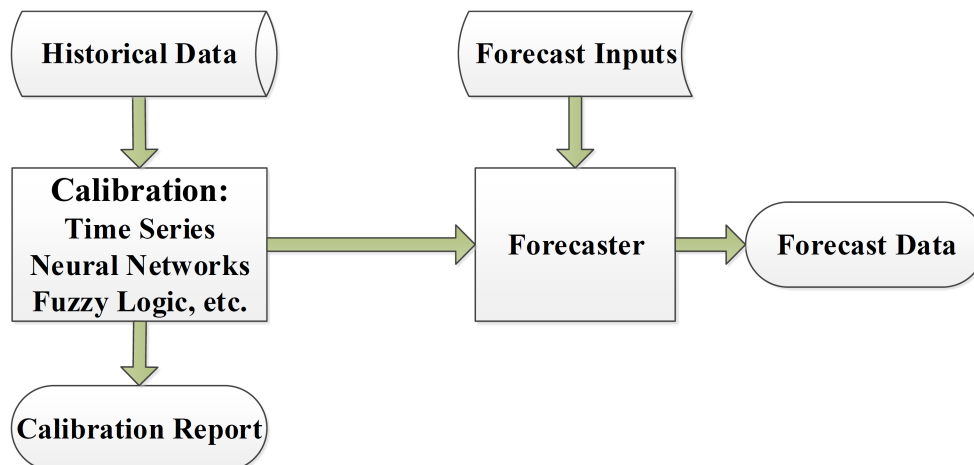
Figure B.1: General block diagram of a real-time short-term forecasting algorithm.

However, in the second category called Method 2 in this thesis, separate forecasters are created for weekdays, weekends, and holidays. It is also possible to combine weekend and holiday forecasting to minimize the number of forecasters since the pattern of electric consumption in holidays is similar to the one in weekends. The second method is more complicated and require more processing power as compared to the first method since Method 2 uses multiple forecasters. In the following sections, the application of the model represented in Fig. B.1 is specifically examined for load forecasting.

B.3   Analysis of the Load Forecasting Algorithm

This section aims to investigate the load forecasting of large-scale electricity consumers in details. The aim is to come up with parameters needed for accurate modeling of the load forecaster. Several cases are studied in order to investigate the details of the forecasting problem. The main objectives of the studies in this section are as follows: (i) to evaluate the effect of window length on historical load data and (ii) to examine the effect of resolution (i.e., the sampling rate) of load data.

Different cases can be considered for STLF. In the following, each case is evaluated through simulation. There are some figures for each case showing the load and temperature curves. For all the figures, figure x-a shows the historical and fitted load on the left side of the vertical line; it shows actual and forecast load on the right side of the vertical line. The historical and actual loads are represented in blue; the fitted and forecast loads
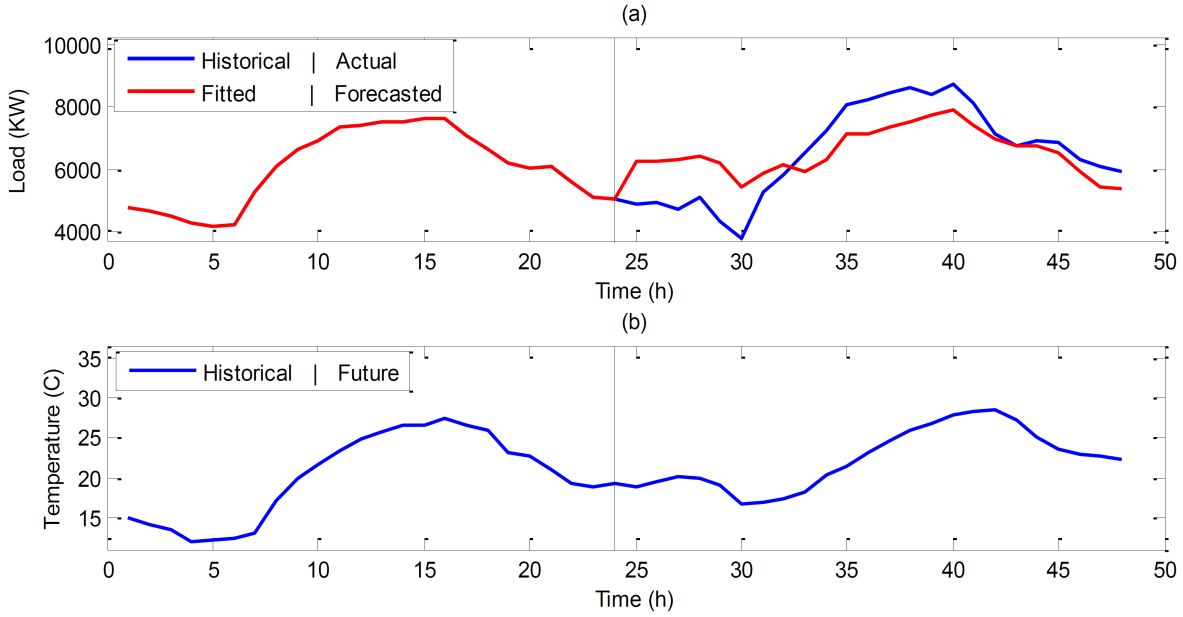
Figure B.2: (a): Load power and (b): ambient temperature for a one-day window length.

are shown in red. Furthermore, figure x-b shows the historical ambient temperature on the left side of the vertical line, and future ambient temperature on the right side of the vertical line.

B.3.1   One-day Window Length, One-day Frequency

In this case, the forecasting window length (i.e., T^L) and the fundamental frequency (i.e., f^L) of historical data are selected as one day (i.e., 24 hours). Fig. B.2 shows the result of forecasting as well as the ambient temperature for a forecast weekday. As shown in Fig. B.2, the forecast error is significant since the forecast and actual data do not look similar. This is mainly due to the fact that the weekly pattern cannot be taken into considerations when the window length is only one day. The difference in patterns of the load in different weekdays increases the forecast error. In the next case, the window length will increase to two days.

Figure B.3: (a): Load power and (b): ambient temperature for a two-day window length.

B.3.2   Two-day Window Length, One-day Frequency

In this case, the window length is considered as two days, and the fundamental frequency is taken as one day. Fig. B.3 shows the simulation result for this case. As shown in Fig. B.3, there is still considerable forecast error observed in load forecasting. For a two-day window length, the forecasting model cannot follow the weekly pattern. The model cannot detect if the load changes are due to temperature changes or due to the regular pattern of that specific day. Therefore, in the next sections, the window length will be considered longer than two days.
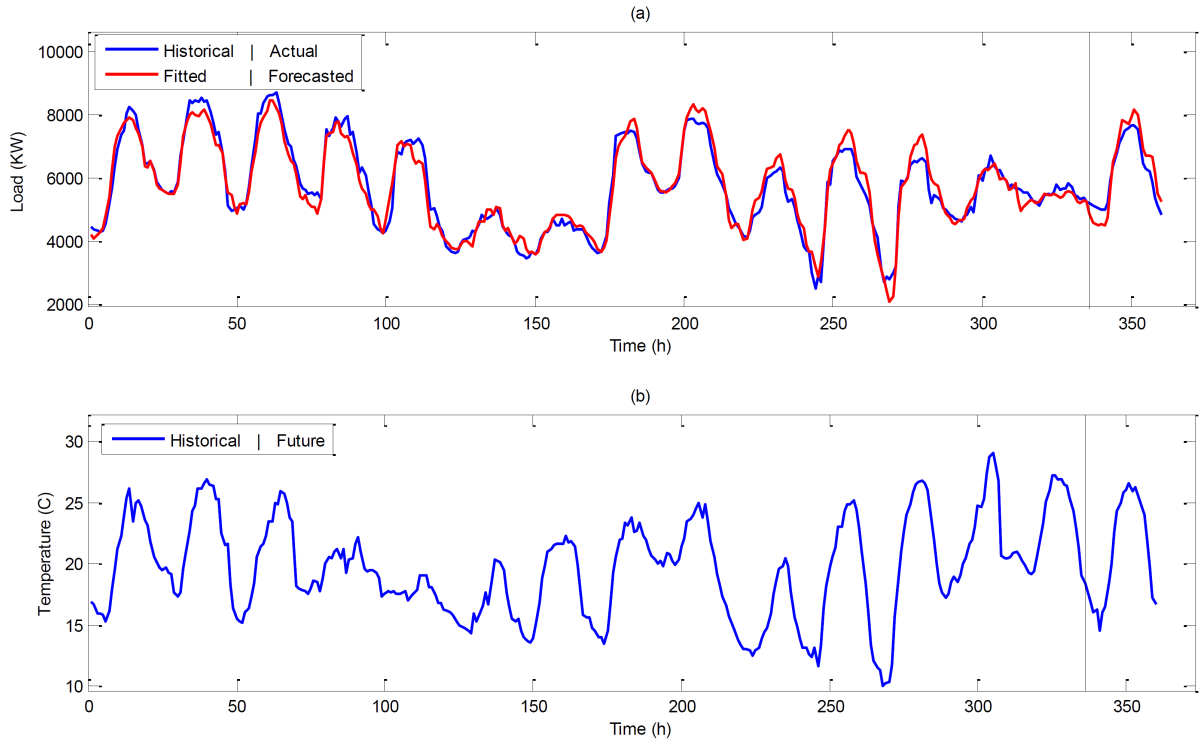
Figure B.4: (a): Load power and (b): ambient temperature for a two-week window length.

B.3.3   Two-week Window Length, One-week Frequency

In this case, the window length is considered as two weeks and the fundamental frequency is taken as one week. Fig. B.4 shows the results. As shown in Fig. B.4, the forecast error is relatively small since the forecast and actual data look similar. In this case, the weekly pattern of weekdays and weekends can be considered. The window length is large enough to account for the weekly pattern. In the next section, the window length will increase to indicate if the forecast accuracy can be further improved.
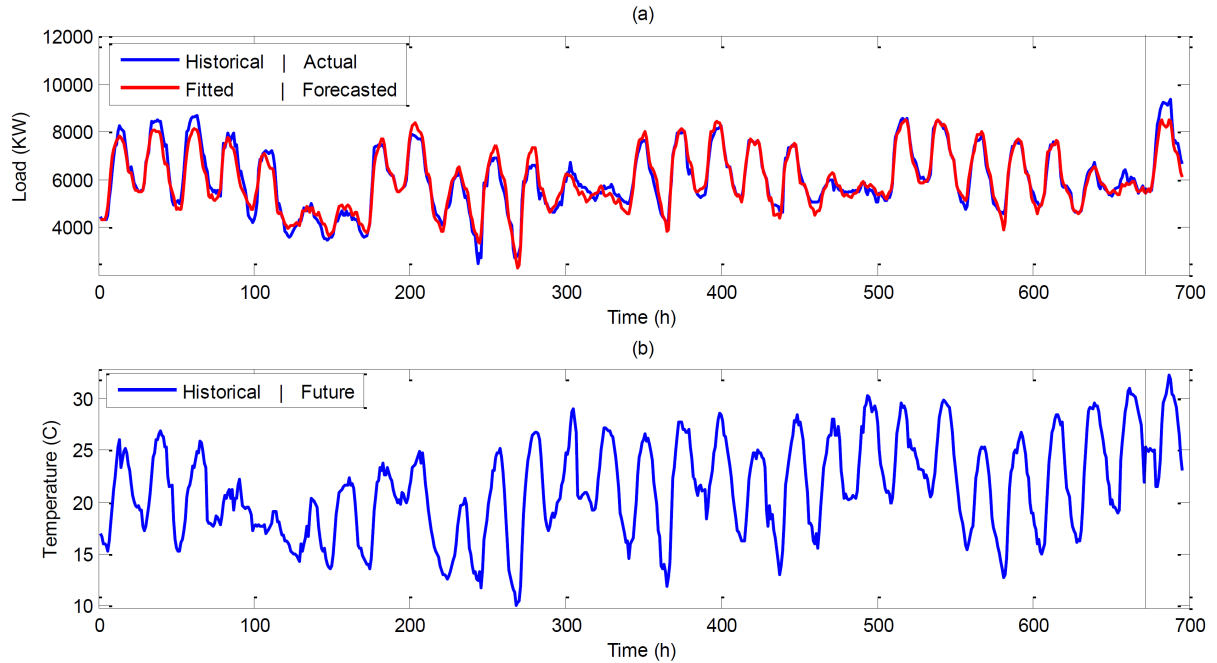
Figure B.5: (a): Load power and (b): ambient temperature for a four- week window length.

B.3.4   Four-week Window Length, One-week Frequency

In this case, the window length is considered as four weeks and the fundamental frequency is taken as one week. Fig. B.5 shows the results.

By comparison of Figs. B.4 and B.5, it can be observed that increasing the window length beyond two weeks cannot increase the forecast accuracy; this is because the model does not consider any monthly and sub-monthly patterns. Thus, for the rest of analyses, the window length will be limited to two weeks.
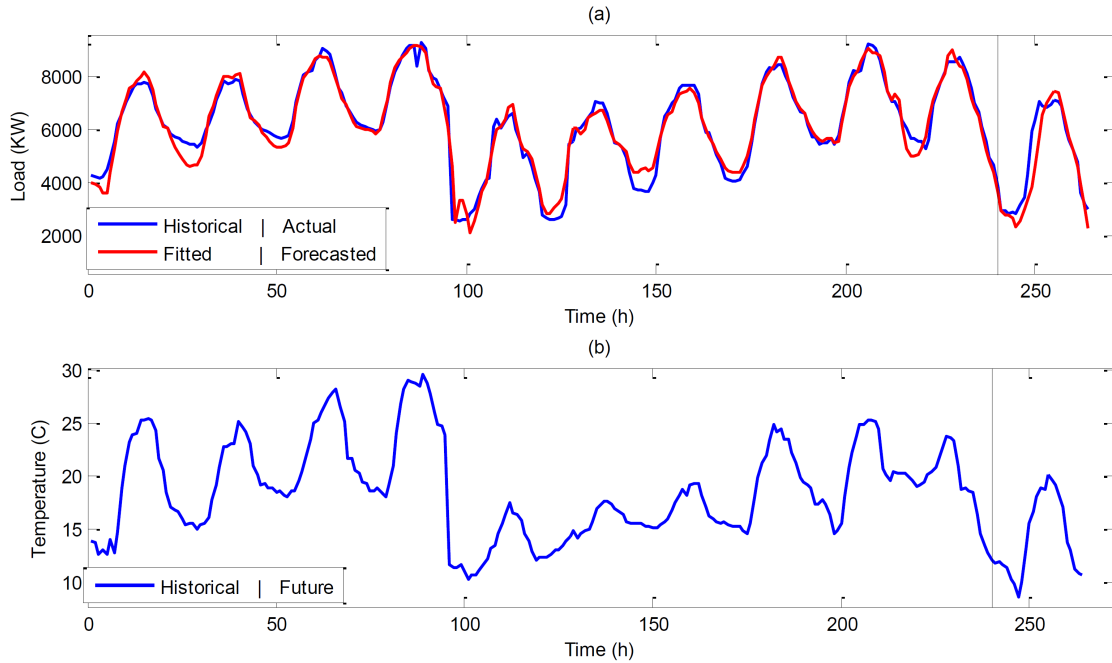
Figure B.6: (a): Load power and (b): ambient temperature for a ten-day window length.
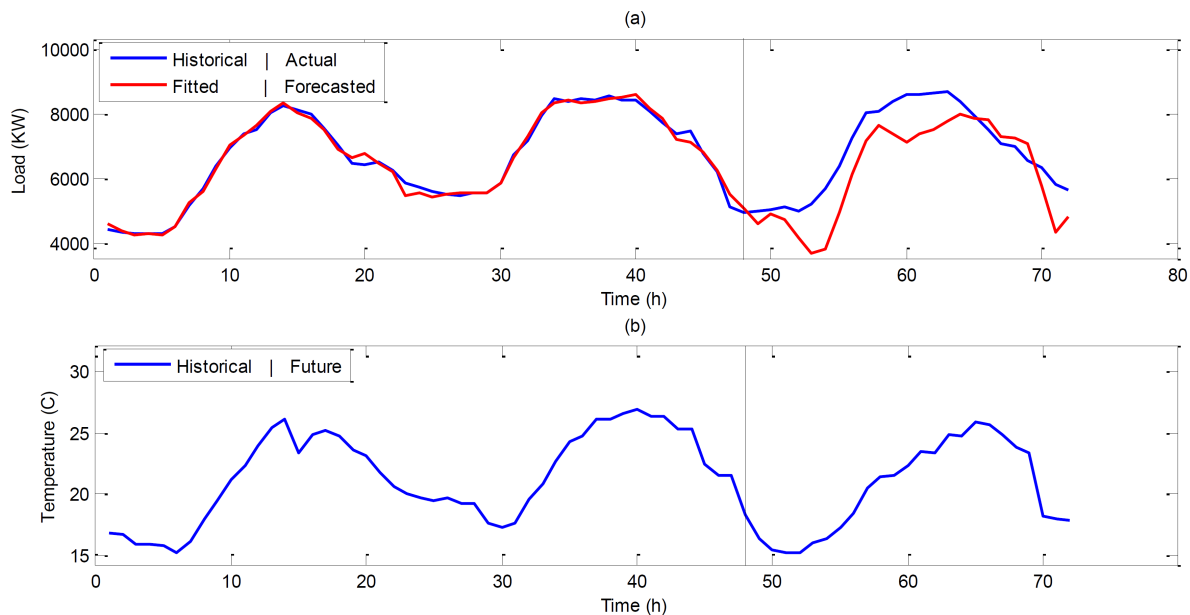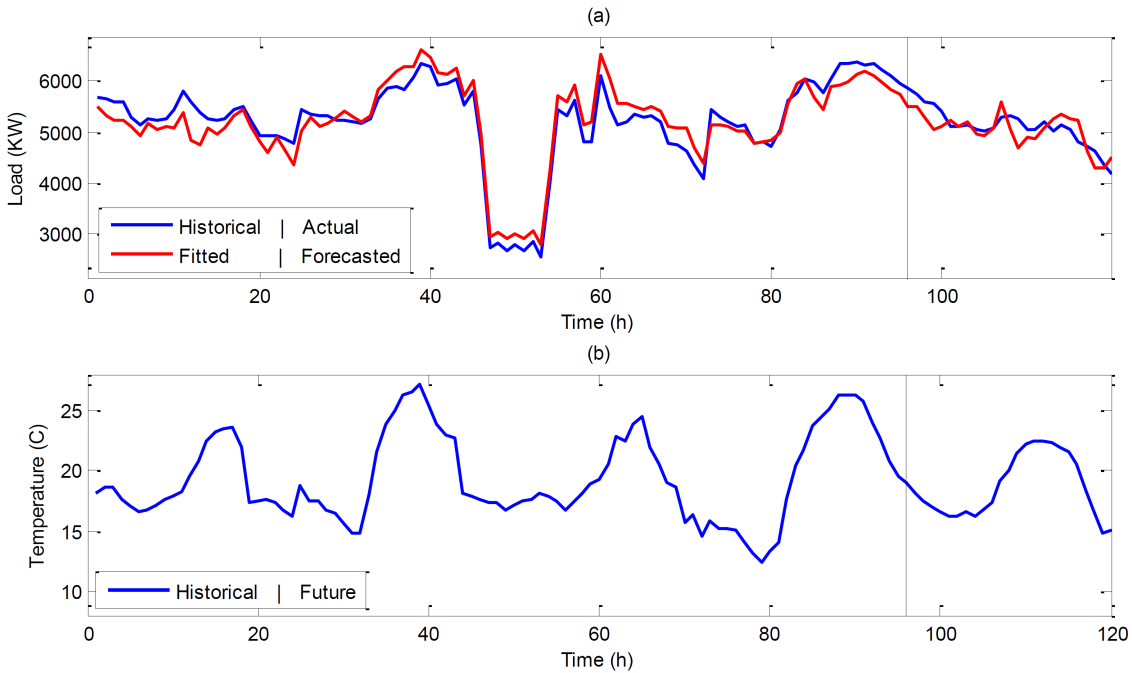

Figure B.7: (a): Load power and (b): ambient temperature for a four-day window length.

B.3.5   Ten/Four-day Window Length, Five/Two-day Frequency

In this case, the window length is considered as ten weekdays for weekday forecasting and four weekends for weekend and holiday forecasting. The fundamental frequency is
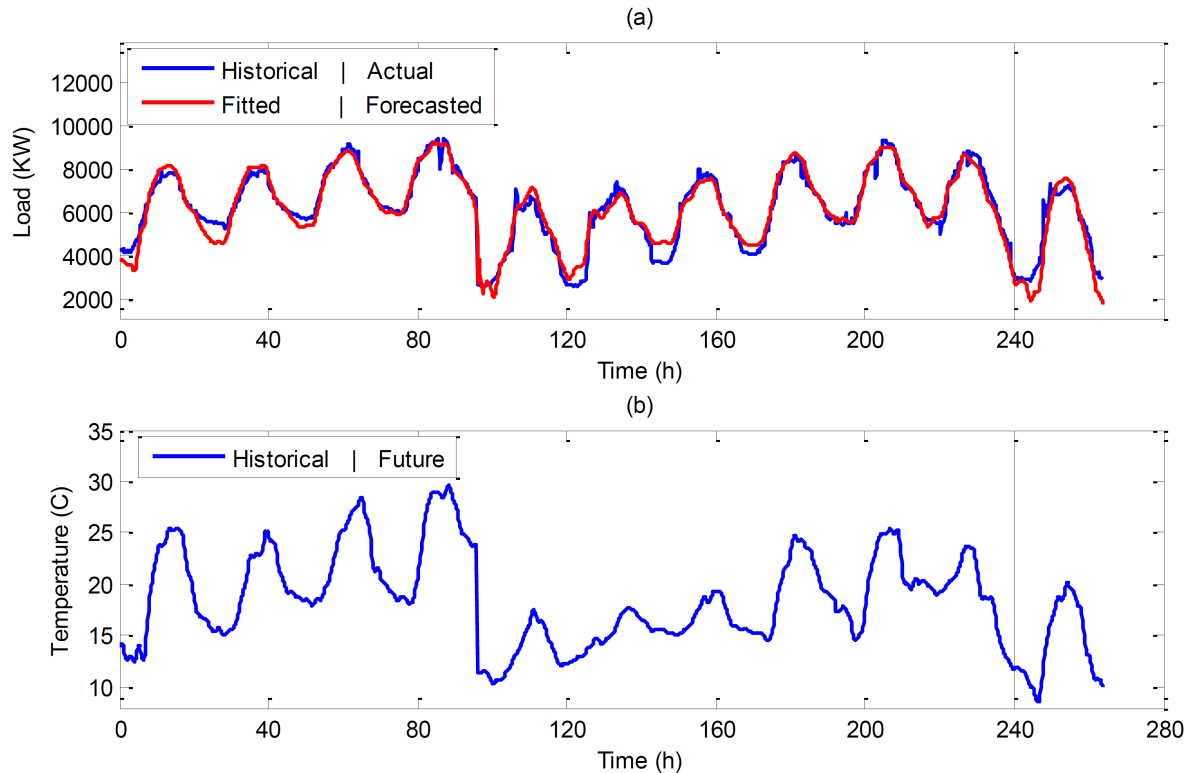
Figure B.8: (a): Load power and (b): ambient temperature for 12-minute sampling rate.

taken as half of the window length in each case. Figs. B.6 and B.7 show a weekday and a weekend forecasting, respectively.

As shown in Figs. B.6 and B.7, the load forecast of both the weekday and weekend are similar to the actual load. In this case, the weekly pattern of weekdays and weekends can be considered. Weekdays are separated from weekends and holidays; thus, the model can be well fitted for each case. Weekdays are forecast by weekday forecaster; weekends and holidays are forecast by weekend forecaster.

B.3.6   Impact of Load Data Resolution

The above-mentioned analyses were conducted over the load data while the sampling rate were taken as 1 hour. In this section, the sampling rate or the resolution of the load data increases to investigate if the forecast accuracy can increase. Figs. B.8 and B.9 show two cases with 12-minute and 5-minute sampling rate, respectively, for a ten-day window length.

By comparison of Figs. B.8 and B.9 with Fig. B.6, it can be observed that in-
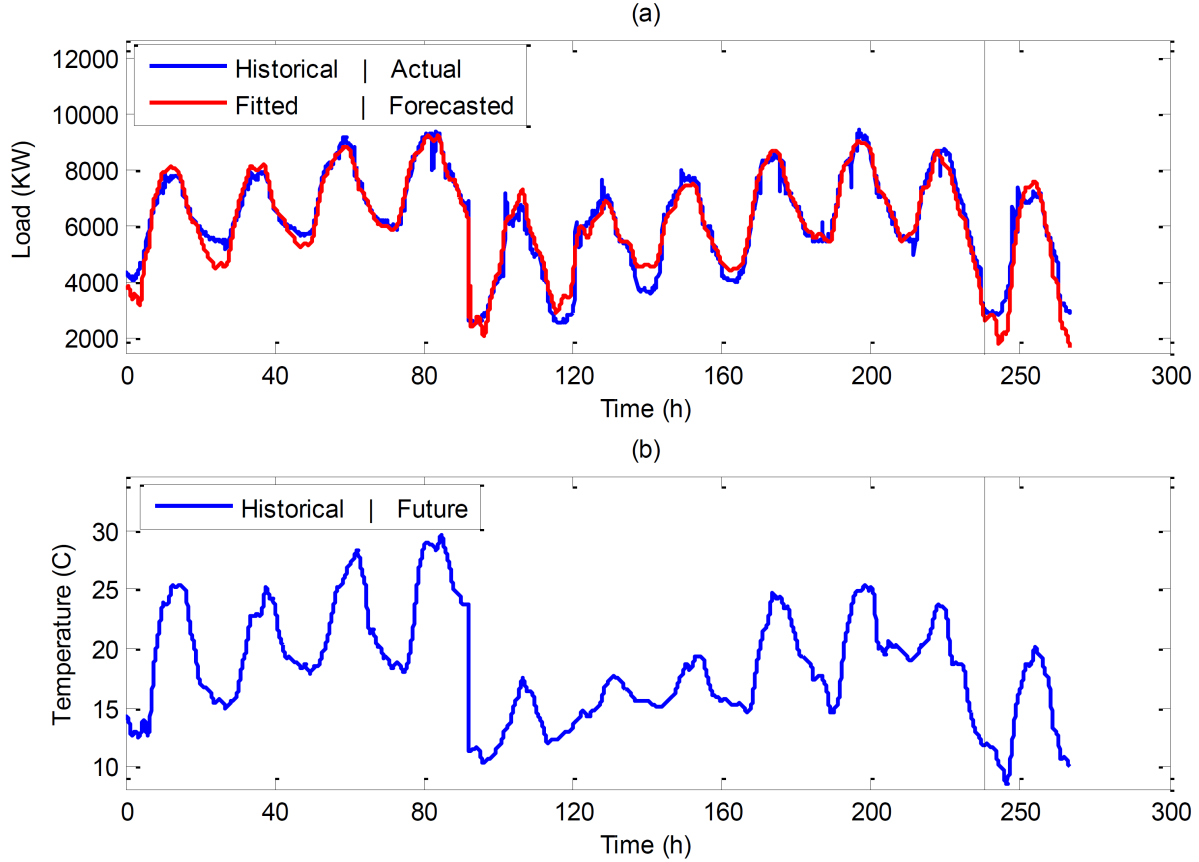
Figure B.9: (a): Load power and (b): ambient temperature for 5-minute sampling rate.

Table B.1: Matrix Dimension at Different Sampling Rates

Sampling Rate	1 Hour	12 Minutes	5 Minutes
Dimension of Matrix $\underline{Y}$ to be Pseudo Inversed	240×80	1200×80	2880×80

creasing the sampling rate to more than 1 sample per hour cannot considerably increase the forecast accuracy. Instead, the size of Matrix $\underline{Y}$, which is to be inversed, substantially increases at higher than 1-hour sampling rate; this results in higher computation requirements which is not appropriate.

Table B.1 reports the dimension of Matrix $\underline{Y}$, which is to be pseudo inversed, at different sampling rates. As reported in Table B.1, the matrix dimension for 12-minute and 5-minute sampling rates are considerably larger as compared to the case of 1- hour sampling rate.

B.4 Forecast Error Analysis

B.4.1 Load Forecasting Using Method 1

As pointed out in Section B.2, Method 1 uses two complete weeks (i.e., 14 days) of window length for weekday, weekend, and holiday load forecasting; Due to its pattern, each holiday can be considered either as a Saturday or as a Sunday. According to the literature, holiday loads are more similar to Sundays than Saturdays [108]. Thus, holidays are forecast as Sundays.

The fundamental frequency is considered as one week. Then, the load in the next 24 hour is forecast using the forecasting model considering the forecast temperature. The load of each forecast day is compared with the actual load of that day and their difference is considered as the forecast error. The percent of the forecast error in comparison with the actual load is then calculated. The simulation is rerun at each hour and the forecast error is calculated for the entire data. Then, the mean value and standard deviation of the error for each hour is calculated. To evaluate the performance of the forecasting algorithm, the PDF and probability of the mean values of error and the standard deviation of error are calculated.

A PDF is a function that indicates the relative likelihood for a random variable to take on a given value. The PDF is non-negative, and its integral over the entire space would be equal to one. For instance, if for the error value of 5%, the PDF is 0.01, it means that the probability that the 5% error occurs is 1%. In addition, the probability for the random variable to fall within a particular region is given by the integral of the PDF over that region. For instance, if the probability of the 5% error is 0.35, it means that the probability that the 5% error falls in the region of 0 to 5% is 35%. In other words, with the probability of 35%, the error values are less than or equal to 5%.

B.4.2 Load Forecasting Using Method 2

The second method in this section uses ten-weekday window length for weekday forecasting and four-weekend window length for weekend and holiday forecasting. With the same process as mentioned in section B.4.1 for Method 1, the PDF and probability for the mean values and standard deviation of forecast error are calculated for this case.

B.4.3 Numerical Results Using Real-world Data

In this section, the historical load and ambient temperature information of a substation at a large-scale institutional electricity consumer for the year of 2011 is used for simulation
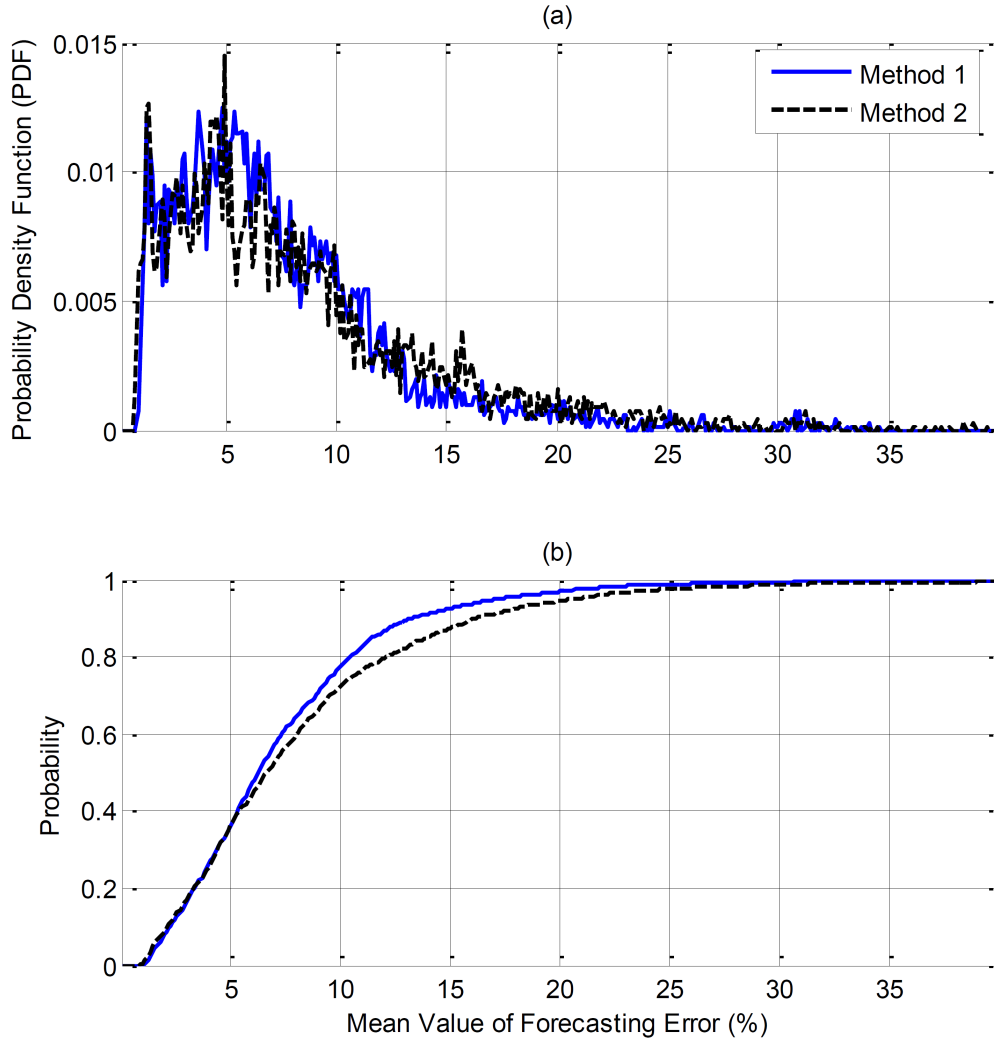
Figure B.10: (a): Probability density function and (b): probability of mean values of forecast error for Methods 1 and 2.

studies of the load forecasting methods. The real-time simulation is used for analyses of the two forecast methods (i.e., Methods 1 and 2) as defined earlier in this appendix.

Figs. B.10 and B.11 show the PDF and probability of the mean values and standard deviation of the forecast error for the two methods, respectively. As shown in Fig. B.10 (a), the PDFs for the two methods are different for each mean value of error; however, their overall trends are approximately the same. Moreover, as shown in Fig. B.10 (b), at a specific value of probability, the mean value of error is larger for Method 2. This reveals that the forecast accuracy of Method 1 is higher than that of Method 2 for the given load and temperature pattern.

As shown in Fig. B.11 (a), the PDFs in two different methods are different for
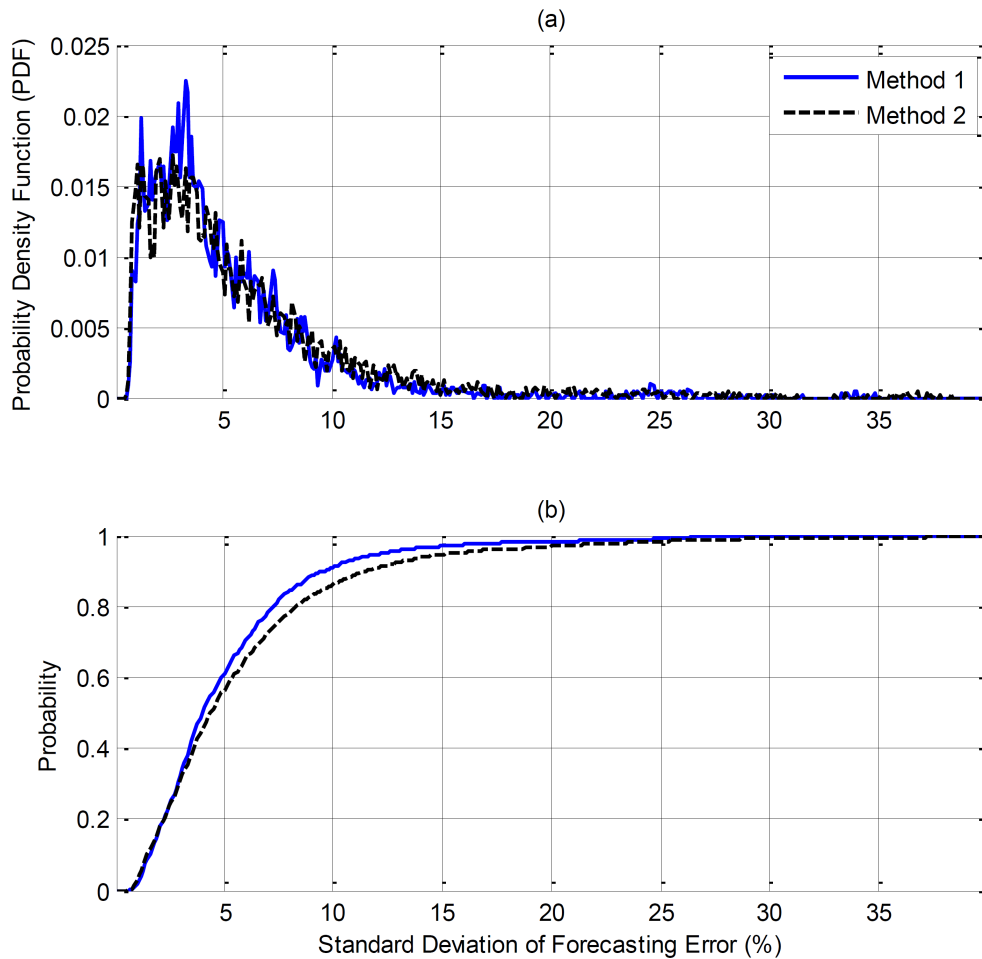
Figure B.11: (a): Probability density function and (b): probability of the standard deviation of forecast error for Methods 1 and 2.

each mean value of error; however, their overall shapes are approximately the same. In addition, as shown in Fig. B.11 (b), at a specific value of probability, the standard deviation of error is larger in Method 2. Since the standard deviation in Method 1 is smaller than that in Method 2, the values of errors are closer to the mean value in Method 1. Thus, Method 1 would be more effective than Method 2.

Table B.2 reports the mean value and standard deviation of forecast error in Methods 1 and 2 at probability of 0.8. As reported in Table B.2, both the mean value and standard deviation of forecast error in Method 1 are smaller than those in Method 2. A large standard deviation means that the value of forecast error in different hours is far below or above the mean value which may not be acceptable. Based on the results in Table B.2, Method 1 is more effective than Method 2.

Table B.2: Mean Value and Standard Deviation of Forecast Error at the Probability of 0.8

Type of Forecaster	Mean Value of Forecast Error	Standard Deviation of Forecast Error
Method 1	10.45	7.25
Method 2	12	8.3

The outcomes of the studies in this appendix are summarized as follows:

- In forecasting with one-day or two-day window lengths, the weekly pattern of the load cannot be considered; therefore, the forecast error would be significant. However, when the window length increases to two weeks, the weekly pattern of weekdays and weekends are taken into considerations. Thus, the forecast error significantly decreases.

- By increasing the window length to more than two weeks, e.g., such as four weeks, the forecast accuracy will not increase.

- Increasing the sampling rate to higher than 1 sample per hour does not have a substantial impact on forecast accuracy, but rather increases the amount of computation required for model fitting and forecasting.

- By examining and comparing Methods 1 and 2 using real-world load data, it is indicated that Method 1 is more effective than Method 2 due to lower forecast error.

Appendix C

Implementation of the Load Forecaster

C.1 Introduction

In this thesis, real-time models are proposed and developed for controlling the operation of storage as a single entity or joint operation of a large-scale load and a storage unit. A large-scale load together with a storage unit can be considered as a microgrid. Microgrids are essential parts of smart grids which will be vital in the trend towards integrating Distributed Energy Resources (DERs) [109]. A microgrid supervisory control system is necessary to efficiently monitor and optimally operate a microgrid with DERs and/or energy storage devices [8], [110]. This control system needs to measure different parameters such as demands, generations, and the status of each microgrid asset in real-time at various locations across the microgrid network. Since DERs, loads, and storage devices are likely to be dispersed across the microgrid, a communication network is required to carry data across the various resources [111].

An appropriate supervisory control system should be able to interact with possible operators and remote clients, such as a distribution automation system to demonstrate and archive the microgrid real-time data and receive required commands and information. In order for a microgrid supervisory control system to have all the mentioned specifications, each microgrid asset or a combination of them should be provided with a local controller. Supervisory controllers are also required to run scheduling algorithms (e.g., those that are developed in this thesis) every several minutes to provide optimal set-points for the microgrid assets, e.g., storage units. This supervisory controller requires several inputs, including forecasts of electrical load, power generations, and energy price to be able to re-

liably and optimally supervise the entire microgrid and to determine the optimal power set-points for the microgrid. Moreover, a reliable and robust communication network should be set up to provide data communication from local controllers to the supervisory controller and vice versa in order to provide all the required input information for the supervisory controller [112]. The performance of such a microgrid controller depends highly upon the accuracy of the forecast information. The more accurate the forecast data are, the more optimal the microgrid supervisory controller can dispatch its DERs [112].

In practice, it is desired to have a single device as a microgrid supervisory controller, which automatically monitors the microgrid asset's information, buffers the information for a short-time interval such as two weeks; performs various forecasting algorithms such as load and generation; executes optimal scheduling algorithm; and commands local asset controllers. This supervisory controller may be installed in a substation that should comply with electric substation standards. This means that the controller's central processing unit should be a fan-less chip that tolerates harsh environmental conditions, such as high and low temperatures. In such a controller, use of extrapolation and interpolation is not an ideal solution to tackle data loss issue due to its complexity and the limitation in the controller's processing power and memory space. Several studies have proposed different real-time STF algorithms; however, practical challenges such as loss of data for a period of time with the above-mentioned limitations have not been adequately investigated. In this appendix, a method for loss of data management is proposed.

The recorded data concerning holidays should be excluded from the historical buffer of a regular day load and electricity price forecasting due to the considerable difference in the profiles of a holiday and a regular weekday. As a result, 24-hour holiday data should be replaced with appropriate data to ensure an accurate forecast for future hours and days. This challenge is similar to the data loss issue; as a result, the proposed method in this thesis is extended to address this challenge as well. The proposed method is simple yet effective and can be applied to any real-time STF, such as electrical load, electric power generation, and energy price forecasting with insignificant additional computation.

As described in Appendix A, all real-time STLF algorithms need to have a window of historical data in order to forecast the future load. This data window is what is monitored and recorded by the microgrid controller in real-time. Whenever the electric load/generation data is not available, e.g., due to communication loss, during the normal working of the microgrid controller, no data exist to be recorded into the buffer. If that is the case, the real-time forecaster loses a time period of data in its buffer; therefore, it does not have all the required historical data for model calibration and forecasting. This problem should be solved through real-time implementations since the forecaster

should provide real-time forecast data in order for the microgrid supervisory controller to be able to work properly. As mentioned earlier, extrapolation and interpolation-based methods can be used to create data for the outage period. However, these methods add considerable computation and impose more complexity on the forecasting algorithm.

In addition to loss of data management, the following challenges are discussed: forecasting in the presence of a holiday, lack of historical data in first time utilization, management of limited memory and processing capability, and time shift for daylight savings.

C.2   Handling the Issue of Data Loss

In this section, a simple yet effective method is proposed to address the challenge of data loss by adding an insignificant amount of additional computation. The real-time STLF algorithm, used in Chapter 5 and analyzed in Appendix A, is selected to which the proposed method for handing loss of data issue is applied to verify the efficacy and feasibility of the proposed method. Using the same concept of the proposed method for handling data loss issue, a technique is proposed for addressing the challenges of forecasting during holidays. Although the performance of the proposed method is evaluated only on a real-time STLF algorithm, the method can be used in any real-time STF algorithm.

The proposed method employs the recent historical forecast data to fill in the lost data in case of a failure in data communication. As explained in Appendix A, in a real-time STF algorithm, a window of historical data such as two-weeks is used to calibrate and construct the forecasting model. This window of data contains the most recent historical data. For instance, in the case of a two-week window length, in order to forecast the data in the next 24 hours, data in the last two weeks (i.e., in the last 336 hours) is picked up and used to create the model. Then, the model is recalibrated at the next time interval using the last 336 hours. Therefore, the present data should be monitored and recorded into the buffer for at least two weeks to calibrate the forecasting model.

If for any reason, such as communication loss, the actual input data are interrupted, the above-mentioned window will not have enough historical data; hence, the forecaster cannot perform accurately for two weeks. For example, in the case of real-time STLF, if the actual load data are interrupted for 5 hours in each week, then the forecaster will have only $336 - 5 \times 2 = 326$ hours; thus, the two-week window of data is not complete. This causes load forecasting to be significantly inaccurate from the moment of data interruption till 336 hours later when the window of data reaches to two full weeks. Accordingly, in order to address this challenge, one could find a way to provide data in the outage period in such a way that these data are equal or similar to the actual data.
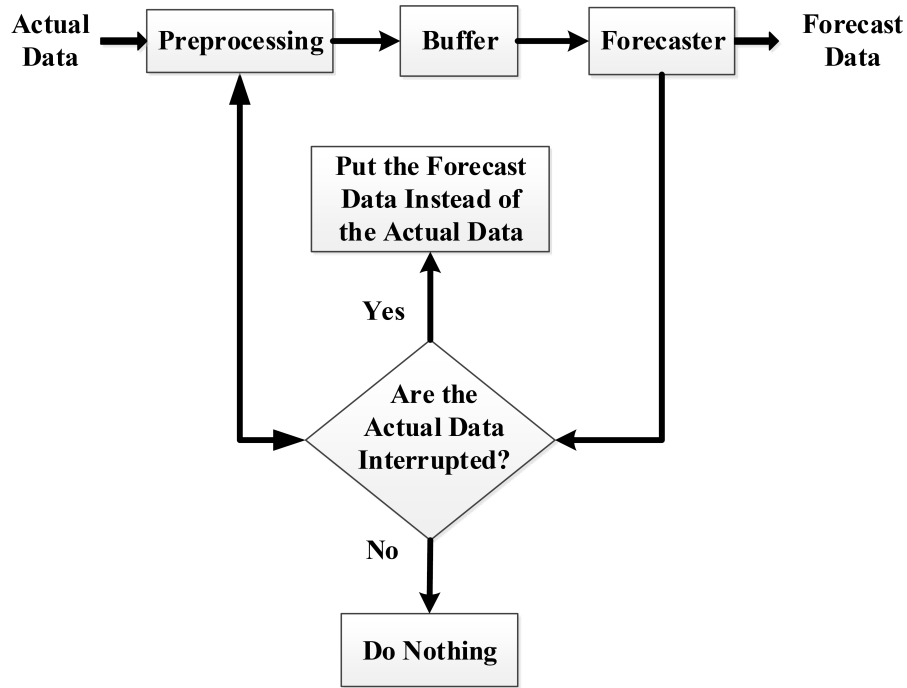
Figure C.1: The basic diagram showing how to handle the issue of data loss.

At each time interval, the forecaster estimates the forecast data from the present time till 24 hours ahead; at the time of data interruption, the forecast data after the last instance when the data monitoring was available are proposed to be used instead of the actual data and saved into the historical buffer until the interruption problem is cleared. Since the forecast data are supposed to be similar to the actual data, it is appropriate to use the forecast data in place of the lost data. This process continues until there are actual data available for the forecaster. Fig. C.1 shows the flowchart of the proposed method for handling loss of data issue. As shown in Fig. C.1, there is a feedback system that can transfer the forecast data from the output to the input. It is continually checked to see if the actual input data fed to the buffer are interrupted or not; if the input data are interrupted, the forecast data is substituted for the actual ones until the data interruption problem is cleared. As illustrated in Fig. C.1, the proposed method is very simple and can be implemented easily by only considering a buffer to store the forecast data. This will not add significant cost and computation to the forecasting algorithm since the forecast data are already available for the device and no additional computation is required to obtain the data.

In Section C.4.1, simulation results will prove that this method is effective and can perform load forecasting with relatively high accuracy during actual data interruption. Moreover, after the outage period when the actual data monitoring is resumed, the
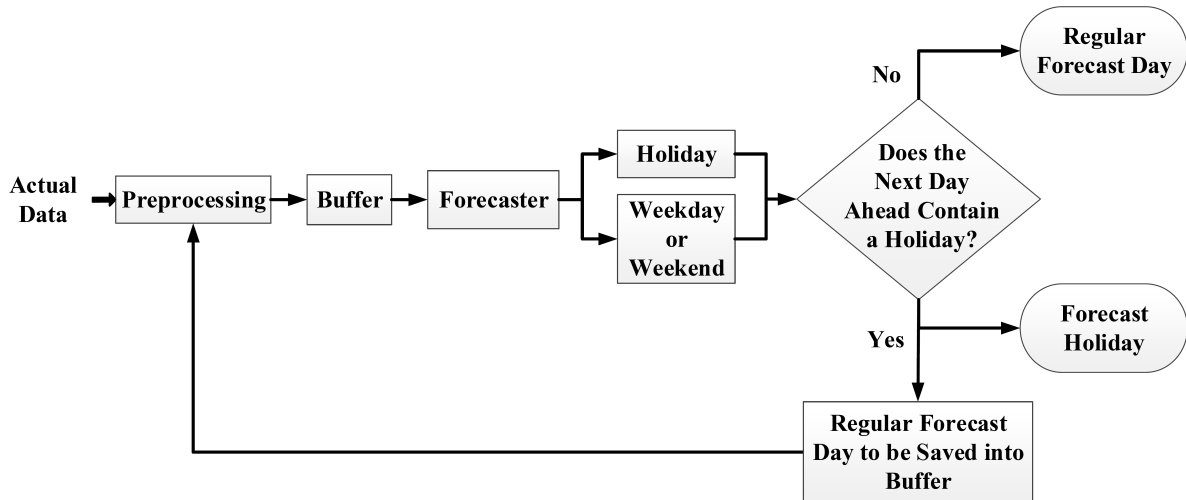
Figure C.2: The basic diagram for management of holiday forecasting.

forecasting device automatically returns to normal operations and performs its regular load forecasting. The same concept used for handling data loss issue, which uses the forecast data instead of actual data, can be used to manage data forecasting when there is a holiday in a week. This will be described in the following paragraph.

In case of load forecasting, the pattern of the data in a holiday is different from the one in a regular weekday since the consumption behaviour during holidays and regular weekdays are different. Therefore, there should be special considerations in forecasting when the week contains a holiday. Accordingly, the holiday data should not be recorded in the weekday or weekday-weekend buffer since this creates error in the model calibration and forecasting of future data. On the other hand, exclusion of a specific day from the historical buffer requires several adjustments in the forecasting algorithm that makes it very difficult for real-time implementation. In this appendix, a simple method is proposed to address this challenge using the same technique used to manage data loss issue. In this technique, to prevent the creation of forecast error, it is proposed to use forecast weekdays instead of holidays and record them into the buffer.

C.3 Load Forecasting in the Presence of a Holiday

Fig. C.2 shows the flowchart of the proposed method for managing holiday forecasting. This technique can be applied to both load and energy price forecasting or any other cases in which the pattern of data in holidays is different from the one in regular weekdays. Based on this method, first, the holiday dates during the year should be acquired from the user as settings. Then, when the holiday arrives, during the first hour of the holiday,

two forecasts are performed as follows: one regular weekday forecast and one holiday forecast. Then, the forecast holiday appears at the output of the forecaster, and the forecast weekday is saved into the weekday buffer instead of the actual data of the holiday. As shown in Fig. C.2, the proposed method for managing holiday data forecasting uses the same concept as handling loss of data issue. This method is simple yet effective and does not impose a heavy computation burden on the forecasting device.

C.4   Numerical Results

In this section, the two load forecasting methods studied in Appendix A are selected for numerical evaluation of the proposed method in Section C.2 for handling the issue of data loss. Although the case study in this thesis deals only with STLF, the proposed method can be used in any real-time STF algorithm, such as electricity price and renewable power generation forecasting, e.g., solar and wind. The real-time simulation is used for implementing the two forecasting methods, by day-ahead load forecasting with one-hour time intervals for data updating. The window length for historical data is selected as two weeks. Thus, for the first method of STLF, the window length is two complete weeks for weekday and weekend/holiday load forecasting; for the second method, it is ten weekdays for weekday forecasting and four weekends for weekend/holiday load forecasting since the weekdays and weekends are separated in the two-week-length window of data.

The simulations are run through the real-world electricity load and ambient temperature data of a substation at a large-scale institutional electricity consumer for the year of 2011 during wintertime. It is clarified that during wintertime, the electrical load is not directly dependent upon the temperature since colling systems are not operated. In such a case, the load follows a more predictable trend as opposed to the load during summertime, and thus, the forecast error decreases. For this reason, the load forecast error in this section is less than the forecast error of the case studies in Section B.4.3. Nevertheless, the same load has been used to comparatively evaluate the forecast error with and without data loss. In both of the implemented STLF methods, the proposed strategy for addressing the challenge of data loss is verified by comparing the probability values of forecast error in two operating conditions of the load forecaster as follows:

(i) When there is no data loss, and therefore, the forecaster is provided with the actual input data all the time.

(ii) There is a 5-hour period of data loss in each week, and thus, the forecaster will have to use the forecast data instead of the actual ones during these hours.
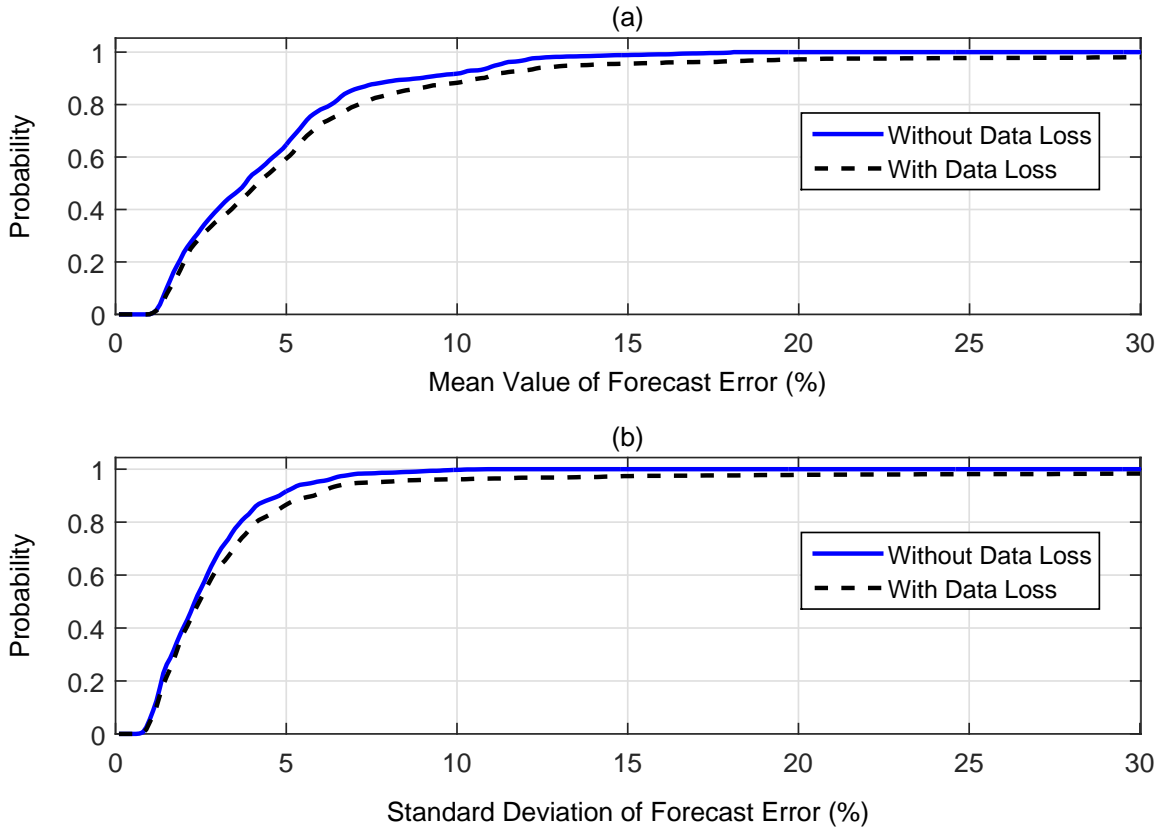
Figure C.3: Probability of forecast error (a): mean value & (b): standard deviation for Method 1.

Based on the above-mentioned operating conditions, the forecast and actual load data of each day in the year are compared, and their differences are considered as the forecast error. The percent of this error in comparison with the actual load data is then calculated. The simulation is rerun every hour, and the forecast error is calculated for the entire load data at each hour. Then, the mean value and standard deviation of the error at each hour are calculated. To evaluate the performance of the proposed method, the probability values of mean and standard deviation of error is calculated for both operating conditions, i.e., with and without occurring data loss. In the following, the method for handling data loss issue is applied to Methods 1 and 2 of STLF.

C.4.1   Handling Data Loss Issue for Method 1

In this section, the proposed approach to solve the data loss problem is applied to the first method of STLF, i.e., only one forecaster for weekday, weekend, and holiday load forecasting with a two-week window of historical data. The probability values of the mean and standard deviation of the forecast error for two operating conditions, i.e., with and
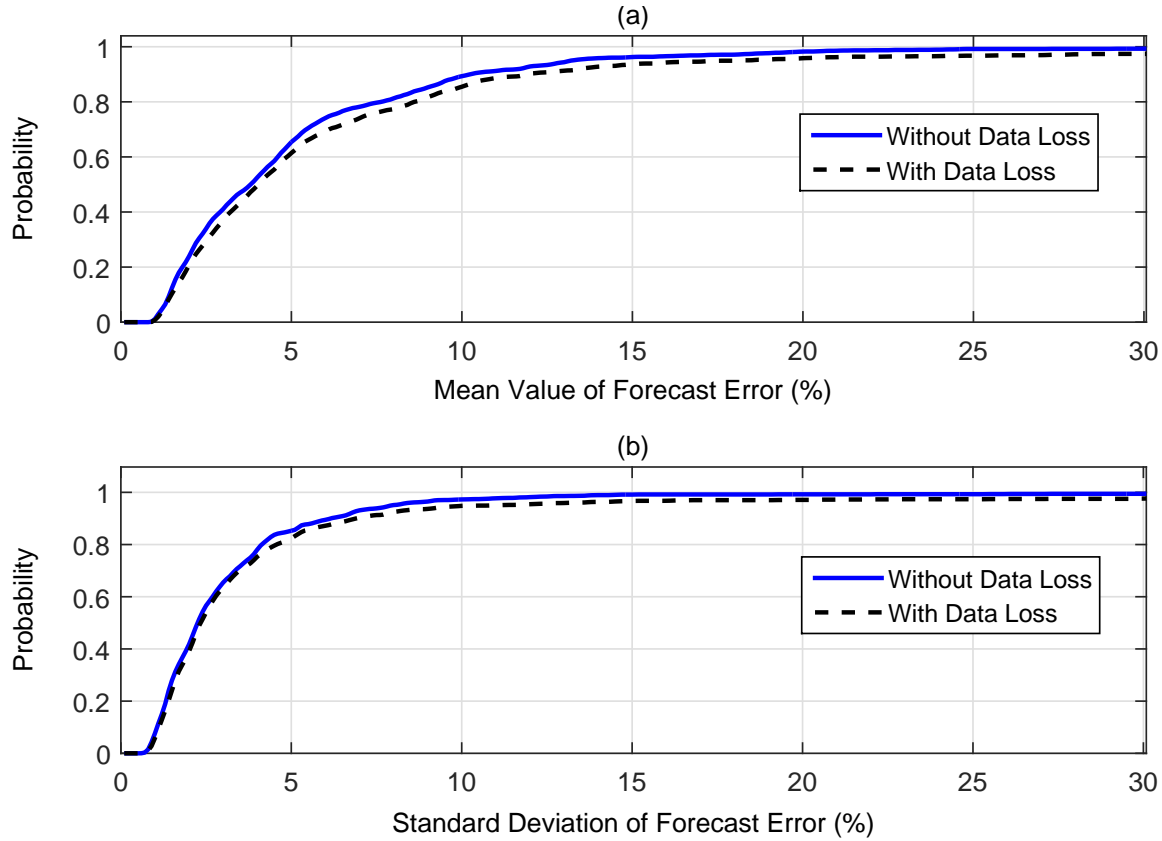
Figure C.4: Probability of forecast error (a): mean value & (b): standard deviation for Method 2.

without occurring data loss, are calculated and represented in Fig. C.3. In this study, in order to simulate loss of data monitoring, the actual input load data are interrupted in a real-time simulation for a 5-hour period in each week, and therefore, substituted with related forecast data based on the proposed technique. Fig. C.3 (a) shows the probability of the mean value of forecast error. For instance, if the probability of the 5% forecast error is 0.65, it means that the probability that this value of error falls less than or equal to 5% is 65%. In other words, with the probability of 65%, the error values are less than or equal to 5%. Therefore, if the large probability values occur for small error values, the forecaster will be more accurate. In other words, the more the curve peak moves towards the left, the more accurate the forecaster will be. The same concept is valid for the curves shown for the standard deviations. If the curve peak moves towards the left, the high probability values occur for small values of standard deviation. The smaller the standard deviation is, the less the error values are scattered around the mean value, indicating that the forecaster is more accurate; this is because it is not appropriate if the values of forecast error are considerably lower or higher than the mean value.

As shown in Fig. C.3, the probability values of error and standard deviation for

Table C.1: Mean Value (MV) & Standard Deviation (SD) of Forecast Error at Probability of 0.8

Method 1 of STLF				Method 2 of STLF			
Without Data Loss		With Data Loss		Without Data Loss		With Data Loss	
MV	SD	MV	SD	MV	SD	MV	SD
6.4%	3.7%	7.2%	4.2%	7.7%	4.2%	8.7%	4.6%

the two operating conditions are similar; the small difference between the curves of two operating conditions is due to the difference between the forecast and actual data in the historical buffer since the actual data are substituted with the forecast ones when the data is interrupted. Nevertheless, the forecast accuracy for both cases is almost identical-showing the efficacy of the proposed method for managing data loss issue.

C.4.2   Handling Data Loss Issue for Method 2

In this section, the proposed technique is applied to the second method of STLF, i.e., one forecaster for weekday load forecasting with a ten-weekday window of historical load data and another forecaster for combined weekend and holiday load forecasting with a four-weekend window of historical load data. The probability values of the mean value and standard deviation of forecast error for the two operating conditions, i.e., with and without data loss, are calculated and illustrated in Fig. C.4. Similar to Fig. C.3, in Fig. C.4, both the probability of error mean value and probability of error standard deviation are similar for the two the operating conditions. The small difference between the results in two operating conditions is due to the difference between the forecast and actual data in the buffer. Nevertheless, the forecast accuracy for both cases is almost identical.

Table C.1 presents the error mean value and standard deviation at the probability of 0.8. As reported in Table C.1, in both methods, the error mean value and standard deviation are similar for both the operating conditions of with and without data loss. This proves that when there is a small period of data loss in real-time implementation of STF algorithms, the use of forecast data to fill in the outage period does not significantly impact the forecast results. Thus, the method proposed in this thesis can be employed to keep the forecaster from being stopped at the time of actual data interruption. If, for any reason, such as communication loss, the actual data are not provided for the forecaster, the microgrid supervisor controller can continue working with the acceptable accuracy until the data loss problem is cleared and actual data monitoring for the device is resumed. Moreover, based on the results indicated in Table C.1, Method 1 is more effective than Method 2 due to lower mean value and standard deviation of forecast error.

C.4.3   Managing Holidays in Forecasting Algorithms

For the purpose of simulation, the load of a typical weekday, i.e., Monday (March 7, 2011), is forecast using the two-week window of historical data. Since this window of data contains two weeks of load data, it has two Mondays. In this case, the first Monday is a holiday, i.e., February 21, 2011 (Family day in Canada). Therefore, it has a load pattern significantly different from a regular Monday. The holiday load is normally significantly smaller than the regular weekday load. Since the forecasting model is significantly affected by the pattern of the holiday in two weeks ago, the load forecast for Monday on March 7, 2011 is mostly like a holiday, not a regular weekday even though it is not a holiday. Thus, the forecast data are significantly underestimated. This causes tremendous amount of forecast error. In fact, the source of this error originated from the holiday data recorded in the buffer two weeks ago appearing in the window of historical data. Thus, if these holiday data are kept from being recorded into the buffer, and instead the data of a regular weekday are recorded, this source of error will be removed.

The regular weekday data which are to be recorded into the buffer instead of the holiday data should be an estimation of the data at the time of holiday with the assumption that the holiday is a regular weekday. Accordingly, in this study, when the holiday is supposed to be forecast, an additional forecast is performed considering that this holiday were a regular Monday, and recorded into the buffer instead of the holiday data. In such a case, two sets of forecast data are performed as follows: one set is the holiday forecast and the other set is the regular weekday forecast; the regular forecast data is recorded into the buffer instead of the actual holiday data; this prevents creation of forecast errors in the next two weeks (see Fig. C.2).

To evaluate the above-mentioned approach, the mentioned Monday is first forecast without holiday management, and then it is forecast based on the method proposed. The forecast and actual data as well as the forecast error for both cases are shown in Fig. C.5. As shown in Fig. C.5, when the forecasting is performed without holiday management, there is a significant amount of forecast error, up to 17.5%, while the forecast error is very small, up to 6%, in the case of holiday management using the proposed method.

C.5   Lack of Historical Data in First Time Utilization

In this section, the case of first time utilization of the forecaster is investigated. When the device is installed for the first time, there is no historical information recorded in the buffer of the device, and therefore, the device is not able to follow the regular forecasting.
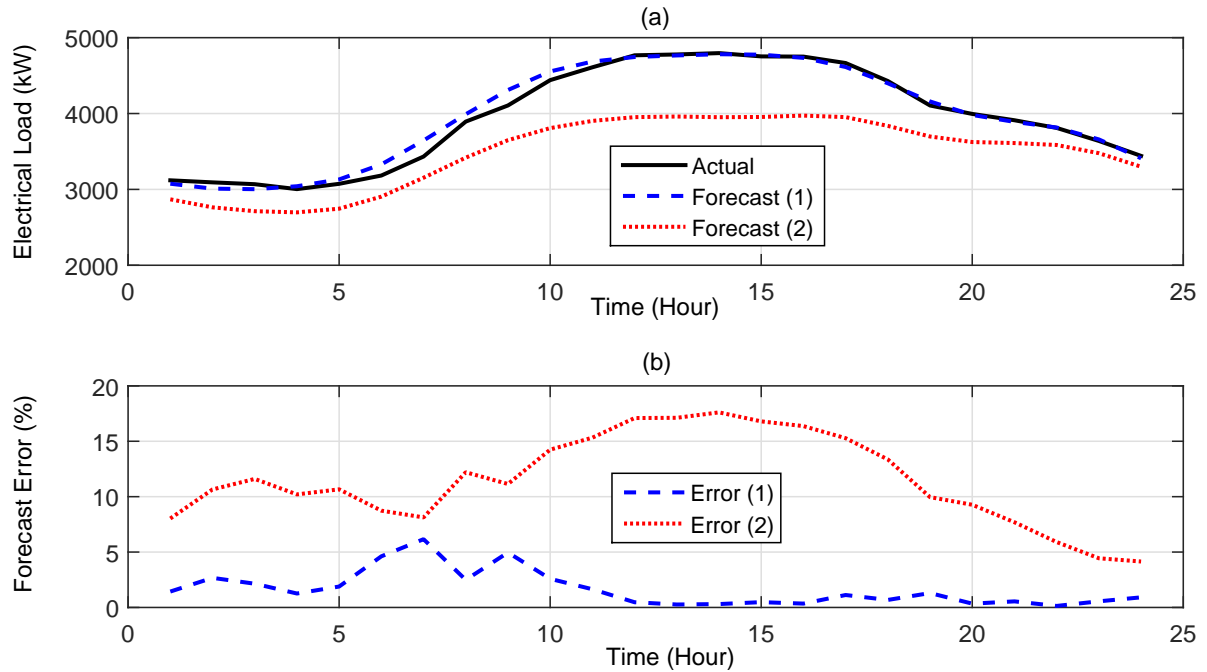
Figure C.5: (a): (1) Forecast load with holiday management and (2) forecast load without holiday management; (b): (1) forecast error with holiday management and (2) forecast error without holiday management: all for Method 1.

According to the studies conduced in Appendix A, two weeks of historical load data are required for the forecaster. If there are historical data from the microgrid before the first time utilization of the device, two weeks of historical load and temperature data can be imported to the device, and the device can perform its regular forecasting from the moment it is installed in the system.

However, if no historical data are available to provide for the device, the device cannot accurately perform any forecasting until it works in the system and records some historical data into the buffer. If that is the case, the following options can be taken into considerations at the first time utilization of the device:

i) The device works in the system for two weeks without performing any load forecasting until it saves two weeks of historical load and temperature data; after that the system will be able to perform its regular forecasting.

ii) The device saves the data of the first week without any forecasting until it has one week of temperature and load data into the buffer. Then, the forecasting of the next week will be considered as the duplication of the first week. When there are two weeks of data in the buffer, the system will be able to perform its regular forecasting.

Table C.2: Appropriate Harmonics Selected for Different Forecasters

Type of Forecaster	Harmonics for Model Fitting
Mixed Weekdays and Weekends/Holidays (Method 1)	1-14, 21, 28, 35
Only Weekdays (Weekday Forecaster of Method 2)	1-10, 15, 20, 25
Only Weekends and Holidays (Weekend/Holiday Forecaster of Method 2)	1-10

iii) The device works in the system for one day to save 24 hours of load and temperature data; the next day forecasting will be duplication of the day before, until the end of the first two weeks. When there are two weeks of data in the buffer, the system will be able to perform its regular forecasting.

iv) The device works in the system for one day to save 24 hours of load and temperature data; the next day forecasting will be duplication of the day before, until the end of the first week. The next week is then considered as duplication of the first week. When there are two weeks of data in the buffer, the system will be able to perform its regular forecasting.

Among the available options mentioned above, the first one would be the best if there are historical data available before the first time utilization of the device; this is because by using this method the device can perform its regular forecasting from the first time of installation. However, if no historical data are available before the first time utilization, the fourth option is suggested since the device can start inaccurate forecasting from the second day of installation and then follow the regular forecasting after the first two weeks.

C.6   Managing Limited Memory and Processing

Since the forecasting algorithm is implemented on a device with limited processing speed and limited memory space, the amount of calculations and required memory should be limited as possible. In order to do so, the number of harmonics which are selected for model fitting using the LES-based algorithm modeled in Chapter 5 should be reduced appropriately. Based on the analyses conducted on the historical load and ambient temperature information of a large-scale institutional electricity consumer, the proper harmonics for different forecasters are as indicated in Table C.2. These harmonics are extracted by applying Fast Fourier Transform (FFT) on the historical load data. If these

harmonics cannot be well fitted with the forecasting model, some king of settings can be considered for the device to enter the appropriate harmonics manually for each specific microgrid. Consequently, if the appropriate harmonics are determined by applying FFT on the historical load of the microgrid and are entered manually to the device, the amount of calculations and required memory is reduced by preventing extra and unnecessary harmonics and at the same time, maintaining the accuracy of model fitting.

C.7 Time Shift for Daylight Saving

In addition to the above-mentioned practical challenges, daylight saving can also be considered to increase the forecast accuracy. Daylight saving is the practice of advancing clocks during the lighter months, so that evenings have more daylight and mornings have less. Typically clocks are adjusted forward for 1-hour near the start of spring and are adjusted backward in autumn.

When the time is shifted due to the daylight saving, the pattern of the load approximately follows the new time since electricity consumers are likely to consume the electricity according to the new time. For instance, a peak in the load signal at 8am in a university is due to the fact that the university employees and students start working at 8am. Thus, no matter the time is shifted or not, at 8am in a weekday, the load has a peak; this is because the people follow the official time, and thus, the load consumption is mostly dependent on the time of the day. Therefore, in order to consider the effect of time shift for daylight saving in time-dependent load forecasting, two cases are considered as presented in Sections C.7.1 and C.7.2 in the following:

C.7.1 Daylight Saving in Spring

In a specific day of spring, the clocks are adjusted forward for 1-hour at 12am (00:00); in this case, the time suddenly changes from 12am to 1am; thus, one hour from 12am to 1am is lost; in order to consider this time shift in load forecast, when the next 24 hours contain the moment of time shifting (at 12am), the forecast load from 12am to 1am should not appear at the forecaster output, and the forecast load at this hour would be null. Thus, only the forecast of 23-hour-ahead is available whereas the forecast of 24-hour-ahead is needed; in order to address this issue, two forecasters in the following are required to forecast the two different parts of the load: one to forecast the load in the period before the time shifting moment (till 11pm), and the other one to forecast the load in the period after time shifting moment (from 1am) (forecast of the second part of
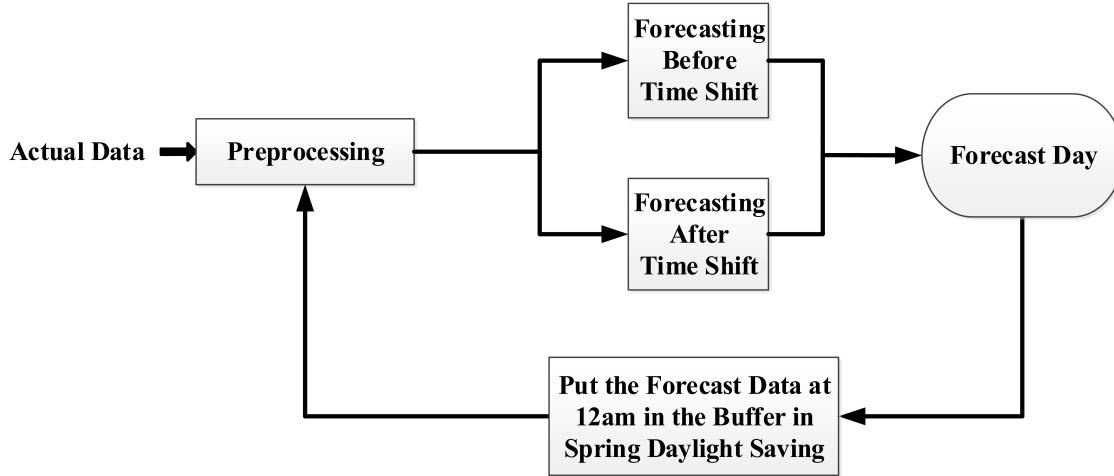
Figure C.6: Flowchart to address the challenge of daylight savings in spring.

the load can be performed by shifting the historical window of data forward for 1-hour); then the forecast load for the next 24-hour will be a combination of these two forecast parts. When the actual time reaches to the moment of time shift at 12am, the forecast data at 12am is saved into the buffer to complete the two-week historical data in order for the forecaster to have all required data to forecast the load in the next days. The forecast load at 12am should be used rather than the actual data because the period from 12am to 1am does not exist, and thus, there is no actual load consumption assigned for this 1-hour period. When the present time passes from the time shifting moment, the regular forecasting can be performed.

Fig. C.6 shows the flowchart of the proposed method to address the challenge of daylight savings in spring. In 24 hours before the moment of time shift, there should be two forecasting as follows: one to forecast the load before the moment of time shift and the other one to forecast the load after that. When the present time passes the moment of time shift (at 12:00am) the forecaster performs regular forecasting.

C.7.2   Daylight Saving in Autumn

In a specific day in autumn, the formal clock is adjusted backward for 1-hour at 12am; in this case, the time suddenly changes from 12am to 11pm; thus, one hour from 11pm to 12am is repeated; in order to consider this time shift in load forecast, when the next 24-hour contains the moment of time shifting (at 12am), two forecasters are needed to forecast two different parts of the load: one to forecast the load in the period before the time shifting moment (till 11pm), and the other one to forecast the load in the period

after time shifting moment (from 12am) (forecast of the second part of the load can be performed by shifting the historical window of data backward for 1-hour); then the forecast load for the next 24-hour will be a combination of these two forecast parts of the load. When the present time passes from the time shifting moment, then the regular forecasting can be performed. The flowchart for handling the issue of daylight savings in autumn is similar to the one represented in Fig. C.6; however, there is no need to put the forecast data at 12am in the buffer in this case.

References

[1] Market Surveillance Panel, "Monitoring Report on the IESO-Administered Electricity Markets," Apr. 2015. [Online]. Available: http://www.ontarioenergyboard.ca/oeb/_Documents/MSP/MSP_Report_Nov2013-Apr2014_20150420.pdf.

[2] M. Kintner-Meyer, "Regulatory Policy and Markets for Energy Storage in North America," *IEEE Proceed.*, vol. 102, No. 7, pp. 1065-1072, Jul. 2014.

[3] Y. Li, H. Cao, S. Wang, Y. Jin, D. Li, X. Wang, and Y. Ding, "Load Shifting of Nuclear Power Plants Using Cryogenic Energy Storage Technology," *Appl. Energy J., Elsevier*, vol. 113, pp. 1710-1716, Jan. 2014.

[4] Z. Shu and P. Jirutitijaroen, "Optimal Operation Strategy of Energy Storage System for Grid-Connected Wind Power Plants," *IEEE Trans. Sustain. Energy*, vol. 5, no. 1, pp. 190-199, Jan. 2014.

[5] H. Akhavan-Hejazi and H. Mohsenian-Rad, "Optimal Operation of Independent Storage Systems in Energy and Reserve Markets With High Wind Penetration," *IEEE Trans. Smart Grid*, vol. 5, no. 2, pp. 1088-1097, Mar. 2014.

[6] E. D. Castronuovo and J. A. P. Lopes, "On The Optimization of the Daily Operation of A Wind-Hydro Power Plant," *IEEE Trans. Power Syst.*, vol. 19, no. 3, pp. 1599-1606, Aug. 2004.

[7] P. Mercier, R. Cherkaoui, and A. Oudalov, "Optimizing a Battery Energy Storage System for Frequency Control Application in an Isolated Power System," *IEEE Trans. Power Syst.*, vol. 24, no. 3, pp. 1469-1477, Aug. 2009.

[8] C. Chen, S. Duan, T. Cai, B. Liu, and G. Hu, "Smart Energy Management System for Optimal Microgrid Economic Operation," *IET Renew. Power Gener.*, vol. 5, no. 3, pp. 258-267, May 2011.

[9] H. Oh, "Optimal Planning to Include Storage Devices in Power Systems," *IEEE Trans. Power Syst.*, vol. 26, no. 3, pp. 1118-1128, Aug. 2011.

[10] A. Hajimiragha and M. R. D. Zadeh, "Practical Aspects of Storage Modeling in the Framework of Microgrid Real-Time Optimal Control," in *Proc. 2011 IET RPG*, pp. 1-6.

[11] W. Du, H. F. Wang, J. Cao, and L. Y. Xiao, "Robustness of an Energy Storage System-Based Stabiliser to Suppress Inter-Area Oscillations in a Multi-Machine Power System," *IET Gener. Transm. Distrib.*, vol. 6, no. 4, pp. 339-351, Apr. 2012.

[12] D. Zhu and G. Hug-Glanzmann, "Coordination of Storage and Generation in Power System Frequency Control Using an Hα Approach," *IET Gener. Transm. Distrib.*, vol. 7, no. 11, pp. 1263-1271, Nov. 2013.

[13] Y. Levron, J. M. Guerrero, and Y. Beck, "Optimal Power Flow in Microgrids With Energy Storage," *IEEE Trans. Power Syst.*, vol. 28, no. 3, pp. 3226-3234, Aug. 2013.

[14] T. Jen-Hao, C. Chia-Yen, and I. C. Martinez, "Utilising Energy Storage Systems to Mitigate Power System Vulnerability," *IET Gener. Transm. Distrib.*, vol. 7, no. 7, pp. 790-798, Jul. 2013.

[15] I. Wasiak, R. Pawelek, and R. Mienski, "Energy Storage Application in Low-Voltage Microgrids for Energy Management and Power Quality Improvement," *IET Gener. Transm. Distrib.*, vol. 8, no. 3, pp. 463-472, Mar. 2014.

[16] A. S. A. Awad, T. H. M. EL-Fouly, and M. M. A. Salama, "Optimal ESS Allocation for Load Management Application," *IEEE Trans. Power Syst.*, vol. 30, no. 1, pp. 327-336, Jan. 2015.

[17] E. Liegmann and R. Majumder, "An Efficient Method of Multiple Storage Control in Microgrids," *IEEE Trans. Power Syst.*, Jan. 2015.

[18] A. Damiano, G. Gatto, I. Marongiu, M. Porru, and A. Serpi, "Real-Time Control Strategy of Energy Storage Systems for Renewable Energy Sources Exploitation," *IEEE Trans. Sustain. Energy*, vol. 5, no. 2, pp. 567-576, Apr. 2014.

[19] C. Brunetto and G. Tina, "Optimal Hydrogen Storage Sizing for Wind Power Plants in Day Ahead Electricity Market," *IET Renew. Power Gener.*, vol. 1, no. 4, pp. 220-226, Dec. 2007.

[20] J. Garcia-Gonzalez, R. M. R. de la Muela, L. M. Santos, and A. M. Gonzalez, "Stochastic Joint Optimization of Wind Generation and Pumped-Storage Units in an Electricity Market, *IEEE Trans. Power Syst.*, vol. 23, no. 2, pp. 460-468, May 2008.

[21] M. Dicorato, G. Forte, M. Pisani, and M. Trovato, "Planning and Operating Combined Wind-Storage System in Electricity Market," *IEEE Trans. Sustain. Energy*, vol. 3, no. 2, pp. 209-217, Apr. 2012.

[22] E. Perez, H. Beltran, N. Aparicio, and P. Rodriguez, "Predictive Power Control for PV Plants With Energy Storage," *IEEE Trans. Sustain. Energy*, vol. 4, no. 2, pp. 482-490, Apr. 2013.

[23] H. Beltran, E. Perez, N. Aparicio, and P. Rodriguez, "Daily Solar Energy Estimation for Minimizing Energy Storage Requirements in PV Power Plants," *IEEE Trans. Sustain. Energy*, vol. 4, no. 2, pp. 474-481, Apr. 2013.

[24] A. Khatamianfar, M. Khalid, A. V. Savkin, and V. G. Agelidis, "Improving Wind Farm Dispatch in the Australian Electricity Market With Battery Energy Storage Using Model Predictive Control," *IEEE Trans. Sustain. Energy*, vol. 4, no. 3, pp. 745-755, July 2013.

[25] J. Teng, S. Luan, D. Lee, and Y. Huang, "Optimal Charging/Discharging Scheduling of Battery Storage Systems for Distribution Systems Interconnected With Sizeable PV Generation Systems," *IEEE Trans. Power Syst.*, vol. 28, no. 2, pp. 1425-1433, May 2013.

[26] S. Gill, E. Barbour, I. A. G. Wilson, and D. Infield, "Maximising Revenue for Non-Firm Distributed Wind Generation with Energy Storage in an Active Management Scheme," *IET Renew. Power Gener.*, vol. 7, no. 5, pp. 421-430, Sep. 2013.

[27] A. A. Thatte, Le Xie, D. E. Viassolo, and S. Singh, "Risk Measure Based Robust Bidding Strategy for Arbitrage Using a Wind Farm and Energy Storage," *IEEE Trans. Smart Grid*, vol. 4, no. 4, pp. 2191-2199, Dec. 2013.

[28] J. Dhillon, A. Kumar, and S. K. Singal, "Optimization Methods Applied for Wind–PSP Operation and Scheduling under Deregulated Market: A Review," *Renew. Sustain. Energy Review. J, Elsevier*, vol. 30, pp. 682-700, Feb. 2014.

[29] Y. Ghiassi-Farrokhfal, F. Kazhamiaka, C. Rosenberg, and S. Keshav, "Optimal Design of Solar PV Farms With Storage," *IEEE Trans. Sustain. Energy*, vol. 6, no. 4, pp. 1586-1593, Oct. 2015.

[30] B. Cleary, A. Duffy, A. O. Connor, M. Conlon, and V. Fthenakis, "Assessing the Economic Benefits of Compressed Air Energy Storage for Mitigating Wind Curtailment," *IEEE Trans. Sustain. Energy*, vol. 6, no. 3, pp. 1021-1028, Jul. 2015.

[31] J. Zou, C. Peng, J. Shi, X. Xin, and Z. Zhang, "State-of-Charge Optimising Control Approach of Battery Energy Storage System for Wind Farm," *IET Renew. Power Gener.*, vol. 9, no. 6, pp. 647-652, Aug. 2015.

[32] H. Ding, Z. Hu, and Y. Song, "Rolling Optimization of Wind Farm and Energy Storage System in Electricity Markets," *IEEE Trans. Power Syst.*, vol. 30, no. 5, pp. 2676-2684, Sep. 2015.

[33] Lu Ning, J. H. Chow, and A. A. Desrochers, "Pumped-Storage Hydro-Turbine Bidding Strategies in a Competitive Electricity Market," *IEEE Trans. Power Syst.*, vol. 19, no. 2, pp. 834-841, May 2004.

[34] F. C. Figueiredo and P. C. Flynn, "Using Diurnal Power Price to Configure Pumped Storage," *IEEE Trans. Energy Convers.*, vol. 21, no. 3, pp. 804-809, Sep. 2006.

[35] P. Kanakasabapathy and K. S. Swarup, "Evolutionary Tristate PSO for Strategic Bidding of Pumped-Storage Hydroelectric Plant," *IEEE Trans. Syst., Man, Cybern.*, vol. 40, no. 4, pp. 460-471, Jul. 2010.

[36] D. Connolly, H. Lund, P. Finn, B. V. Mathiesen, and M. Leahy, "Practical Operation Strategies for Pumped Hydroelectric Energy Storage (PHES) Utilising Electricity Price Arbitrage," *Energy Policy J., Elsevier*, vol. 37, no. 7, pp. 4189-4196, Jul. 2011.

[37] R. Sioshansi, P. Denholm, T. Jenkin, and J. Weiss, "Estimating the Value of Electricity Storage in PJM: Arbitrage and Some Welfare Effects," *Energy Econ. J., Elsevier*, vol. 31, no. 2, pp. 269-277, Mar. 2009.

[38] E. Drury, P. Denholm, and R. Sioshansi, "The Value of Compressed Air Energy Storage in Energy and Reserve Markets," *Energy J., Elsevier*, vol. 36, no. 8, pp. 4959-4973, Aug. 2011.

[39] R. Sioshansi, P. Denholm, and T. Jenkin, "A Comparative Analysis of the Value of Pure and Hybrid Electricity Storage," *Energy Econ. J., Elsevier*, vol. 33, no. 1, pp. 56-66, Jan. 2011.

[40] H. Safaei and D. W. Keith, "Compressed Air Energy Storage with Waste Heat Export: An Alberta Case Study," *Energy Convers. Manage. J., Elsevier*, vol. 78, pp. 114-124, Feb. 2014.

[41] R. Walawalkar, J. Apt, and R. Mancini, "Economics of Electric Energy Storage for Energy Arbitrage and Regulation in New York," *Energy Policy J., Elsevier*, vol. 35, no. 4, pp. 2558-2568, Apr. 2007.

[42] X. He, E. Delarue, W. D'haeseleer, and J. M. Glachant, "A Novel Business Model for Aggregating the Values of Electricity Storage," *Energy Policy J., Elsevier*, vol. 39, no. 3, pp. 1575-1585, Mar. 2011.

[43] T. Muche, "Optimal Operation and Forecasting Policy for Pump Storage Plants in Day-Ahead Markets," *Appl. Energy J., Elsevier*, vol. 113, pp. 1089-1099, Jan. 2014.

[44] B. Steffen, "Prospects for Pumped-Hydro Storage in Germany," *Energy Policy J., Elsevier*, vol. 45, pp. 420-429, Jun. 2012.

[45] C. K. Ekman and S. H. Jensen, "Prospects for Large Scale Electricity Storage in Denmark," *Energy Convers. Manage. J., Elsevier*, vol. 51, no. 6, pp. 1140-1147, Jun. 2010.

[46] A. Yucekaya, "The Operational Economics of Compressed Air Energy Storage Systems under Uncertainty," *Renew. Sustain. Energy Rev. J., Elsevier*, vol. 22, pp. 298-305, Jun. 2013.

[47] E. M. Smith, "Storage of Electrical Energy Using Supercritical Liquid Air," *in Proc. 1977 Inst. Mech. Eng.*, pp. 289-298.

[48] K. Kenji, H. Keiichi, and A. Takahisa, "Development of Generator of Liquid Air Storage Energy System," *Tech. Rev. Mitsubishi Heavy Industries, Ltd.* vol. 35. pp. 4, 1998.

[49] K. Chino and H. Araki, "Evaluation of Energy Storage Method Using Liquid Air," *Heat Transfer–Asian Resear. J., Wiley Library*, vol. 29, pp. 347-357, 2000.

[50] D. Vandor, "System and Method for Liquid Air Production, Power Storage and Power Release," *US States Patent ed. Expansion Energy, LLC*, 2011.

[51] H. Chen, Y. Ding, T. Peters, and F. Berger, "Energy Storage and Generation," *Highview Enterprises Limited*, pp. 70, [USPA Publication ed.], 2009.

[52] Y. Li, Y. Jin, H. Chen, C. Tan, and Y. Ding, "An Integrated System for Thermal Power Generation Electrical Energy Storage and CO2 Capture," *Int. J. Energy Resear., Wiley Library*, vol. 35, pp. 1158-1167, 2011.

[53] H. Chen, T. N. Cong, W. Yang, C. Tan, Y. Li, and Y. Ding, "Progress in Electrical Energy Storage System: A Critical Review," *Prog. Nat. Sci. J., Elsevier*, vol. 19, pp. 291-312, 2009.

[54] Y. Li, X. Wang, and Y. Ding, "A Cryogen-Based Peak-Shaving Technology: Systematic Approach and Techno-Economic Analysis," *Int. J. Energy Resear., Wiley Library*, Nov. 2011.

[55] Y. Hu, X. Li, H. Li, and J. Yan, "Peak and Off-Peak Operations of the Air Separation Unit in Oxy-Coal Combustion Power Generation Systems," *Appl. Energy J., Elsevier*, vol. 112, pp. 747-754, Jan. 2013.

[56] Y. Li, H. Chen, and Y. Ding, "Fundamentals and Applications of Cryogen as a Thermal Energy Carrier: A Critical Assessment," *Int. J. Therm. Sci., Elsevier*, vol. 49, pp. 941-949, Jun. 2010.

[57] Y. Li, H. Chen, X. Zhang, C. Tan, and Y. Ding, "Renewable Energy Carriers: Hydrogen or Liquid Air/Nitrogen?," *Appl. Therm. Eng. J., Elsevier*, vol. 30, pp. 1985-1990, Oct. 2010.

[58] G. Brett, "Cryogenic Energy Storage: Introduction," *Highview Power Storage*, 2011.

[59] H. Zareipour, C. Canizares, and K. Bhattacharya, "Economic Impact of Electricity Market Price Forecasting Errors: A Demand-Side Analysis," *IEEE Trans. Power Syst.*, vol. 25, no. 1, pp. 254-262, Feb. 2010.

[60] P. W. Parfomak, "Energy Storage for Power Grids and Electric Transportation: A Technology Assessment", *CRS Report for Congress*, Mar. 2012. [Online]. Available: https://www.fas.org/sgp/crs/misc/R42455.pdf.

[61] S. Vazquez, S. M. Lukic, E. Galvan, L. G. Franquelo, and J. M. Carrasco, "Energy Storage Systems for Transport and Grid Applications," *IEEE Trans. Ind. Electron.*, vol. 57, no. 12, pp. 3881-3895, Dec. 2010.

[62] A. D. Del Rosso and S. W. Eckroad, "Energy Storage for Relief of Transmission Congestion," *IEEE Trans. Smart Grid*, vol. 5, no. 2, pp. 1138-1146, Mar. 2014.

[63] G. Salgi and H. Lund, "System Behaviour of Compressed-Air Energy-Storage in Denmark with a High Penetration of Renewable Energy Sources," *Appl. Ener. J., Elsevier*, vol. 85, no. 4, pp. 182-189, Apr. 2008.

[64] R. S. Fang and A. K. David, "Transmission Congestion Management in an Electricity Market," *IEEE Trans. Power Syst.*, vol. 14, no. 3, pp. 877-883, Aug. 1999.

[65] The Ontario Independent Electricity System Operator (IESO), 2014. [Online]. Available: http://www.ieso.ca.

[66] "Analytical Studies to Demonstrate Additional FACTS Technologies on the New York State Transmission System," EPRI, Palo Alto, CA, USA, 1996, TR-106464.

[67] "West Coast Utility Transmission Benefits of Superconducting Magnetic Energy Storage," EPRI, Palo Alto, CA, USA, 1996, TR-104803.

[68] "Evaluation of Superconducting Magnetic Energy Storage for San Diego Gas & Electric," EPRI, Palo Alto, CA, USA, 1997, TR-106286.

[69] "Reassessment of Superconducting Magnetic Energy Storage (SMES) Transmission System Benefits," EPRI, Palo Alto, CA, USA, 2002, 1006795.

[70] "Use of Energy Storage to Increase Transmission Capacity," EPRI, Palo Alto, CA, USA, 2011, 1024586.

[71] "Application of Storage Technology for Transmission System Support: Interim report," EPRI, Palo Alto, CA, USA, 2012, 1025418.

[72] A. S. A. Awad, J. D. Fuller, T. H. M. EL-Fouly, and M. M. A. Salama, "Impact of Energy Storage Systems on Electricity Market Equilibrium," *IEEE Trans. Sustain. Energy*, vol. 5, no. 3, pp. 875-885, Jul. 2014.

[73] Y. Gu, J. Bakke, Z. Zhou , D. Osborn, T. Guo, and R. Bo, "A Novel Market Simulation Methodology on Hydro Storage," *IEEE Trans. Smart Grid*, vol. 5, no. 2, pp. 1119-1128, Mar. 2014.

[74] IESO Training Group. Introduction to Ontario's Physical Markets. IESO, Toronto, ON, Canada, 2014 [Online]. Available: http://www.ieso.ca/imoweb/pubs/training/IntroOntarioPhysicalMarkets.pdf.

[75] G. He, Q. Chen, C. Kang, P. Pinson, and Q. Xia, "Optimal Bidding Strategy of Battery Storage in Power Markets Considering Performance-Based Regulation and Battery Cycle Life," *IEEE Trans. Smart Grid*, May 2015.

[76] F. Zhang, Z. Hu, and Y. Song, "Mixed-Integer Linear Model for Transmission Expansion Planning with Line Losses and Energy Storage Systems," *IET Gener. Transm. Distrib.*, vol. 7, no. 8, pp. 919-928, Aug. 2013.

[77] Y. Cheng, M. Tabrizi, M. Sahni, A. Povedano, and D. Nichols, "Dynamic Available AGC Based Approach for Enhancing Utility Scale Energy Storage Performance," *IEEE Trans. Smart Grid*, vol. 5, no. 2, pp. 1070-1078, Mar. 2014.

[78] C. O'Dwyer and D. Flynn, "Using Energy Storage to Manage High Net Load Variability at Sub-Hourly Time-Scales," *IEEE Trans. Power Syst.*, vol. 30, no. 4, pp. 2139-2148, Jul. 2015.

[79] A. D. Lamont, "Assessing the Economic Value and Optimal Structure of Large-Scale Electricity Storage," *IEEE Trans. Power Syst.*, vol. 28, no. 2, pp. 911-921, May 2013.

[80] U. S. Department of Energy, "Grid Energy Storage," Dec. 2013. [Online]. Available: http://energy.gov/sites/prod/files/2014/09/f18/Grid%20Energy%20Storage%20December%202013.pdf.

[81] U. S. Department of Energy, "The Value of Energy Storage for Grid Applications," Tech. Rep. NREL/TP-6A20-58465, Dec. 2013. [Online]. Available: http://www.nrel.gov/docs/fy13osti/58465.pdf.

[82] D. Papadaskalopoulos, D. Pudjianto, and G. Strbac, "Decentralized Coordination of Microgrids With Flexible Demand and Energy Storage," *IEEE Trans. Sustain. Energy*, vol. 5, no. 4, pp. 1406-1414, Oct. 2014.

[83] S. A. Arefifar and Y.A.-R.I. Mohamed, "DG Mix, Reactive Sources and Energy Storage Units for Optimizing Microgrid Reliability and Supply Security," *IEEE Trans. Smart Grid*, vol. 5, no. 4, pp.1835-1844, Jul. 2014.

[84] K. Rahbar, J. Xu, and R. Zhang, "Real-Time Energy Storage Management for Renewable Integration in Microgrid: An Off-Line Optimization Approach," *IEEE Trans. Smart Grid*, vol. 6, no. 1, pp.124-134, Jan. 2015.

[85] A. K. Barnes, J. C. Balda, and A. Escobar-Mejía, "A Semi-Markov Model for Control of Energy Storage in Utility Grids and Microgrids With PV Generation," *IEEE Trans. Sustain. Energy*, vol. 6, no. 2, pp. 546-556, Apr. 2015.

[86] M. Mahmoodi, P. Shamsi, and B. Fahimi, "Economic Dispatch of a Hybrid Microgrid with Distributed Energy Storage," *IEEE Trans. Smart Grid*, vol. 6, no. 6, pp. 2607-2614, Nov. 2015.

[87] A. A. Hussein, N. Kutkut, Z. J. Shen, and I. Batarseh, "Distributed Battery Micro-Storage Systems Design and Operation in a Deregulated Electricity Market," *IEEE Trans. Sustain. Energy*, vol. 3, no. 3, pp. 545-556, Jul. 2012.

[88] Y. Wang, X. Lin, and M. Pedram, "Adaptive Control for Energy Storage Systems in Households With Photovoltaic Modules," *IEEE Trans. Smart Grid*, vol. 5, no. 2, pp. 992-1001, Mar. 2014.

[89] F. Adamek, M. Arnold, and G. Andersson, "On Decisive Storage Parameters for Minimizing Energy Supply Costs in Multicarrier Energy Systems," *IEEE Trans. Sustain. Energy*, vol. 5, no. 1, pp. 102-109, Jan. 2014.

[90] M. Liu, W. Lee, and L. K. Lee, "Financial Opportunities by Implementing Renewable Sources and Storage Devices for Households Under ERCOT Demand Response Programs Design," *IEEE Trans. Indust. Appl.*, vol. 50, no. 4, pp.2780-2787, Jul.-Aug. 2014.

[91] K. Worthmann, C. M. Kellett, P. Braun, L. Grune, and S. R. Weller, "Distributed and Decentralized Control of Residential Energy Systems Incorporating Battery Storage," *IEEE Trans. Smart Grid*, vol. 6, no. 4, pp. 1914-1923, Jul. 2015.

[92] Y. Wang, X. Lin, and M. Pedram, "A Near-Optimal Model-Based Control Algorithm for Households Equipped With Residential Photovoltaic Power Generation and Energy Storage Systems," *IEEE Trans. Sustain. Energy*, vol. 7, no. 1, pp. 77-86, Jan. 2016.

[93] Z. Wang, C. Gu, F. Li, P. Bale, and H. Sun, "Active Demand Response Using Shared Energy Storage for Household Energy Management," *IEEE Trans. Smart Grid*, vol. 4, no. 4, pp. 1888-1897, Dec. 2013.

[94] P. M. van de Ven, N. Hegde, L. Massoulie, and T. Salonidis, "Optimal Control of End-User Energy Storage," *IEEE Trans. Smart Grid*, vol. 4, no. 2, pp. 789-797, Jun. 2013.

[95] L. Dusonchet, M. G. Ippolito, E. Telaretti, and G. Graditi, "Economic Impact of Medium-Scale Battery Storage Systems in Presence of Flexible Electricity Tariffs for End-User Applications," in *Proc. 2012 9th Inter. Conf. Europ. Ener. Market (EEM)*, pp. 1-5.

[96] Y. Xu and L. Tong, "On the Operation and Value of Storage in Consumer Demand Response," in *Proc. 2014 IEEE 53rd Annual Conf. Decision and Contr. (CDC)*, pp. 205-210.

[97] G. Carpinelli, S. Khormali, F. Mottola, and D. Proto, "Demand Response and Energy Storage Systems: An Industrial Application for Reducing Electricity Costs. Part I: Theoretical aspects," in *Proc. 2014 Power Electron., Electr. Drives, Autom. Motion (SPEEDAM)*, pp. 167-172.

[98] G. Carpinelli, S. Khormali, F. Mottola, and D. Proto, "Demand Response and Energy Storage Systems: An Industrial Application for Reducing Electricity Costs. Part II: Numerical Application," in *Proc. 2014 Power Electron., Electr. Drives, Autom. Motion (SPEEDAM)*, pp. 1038-1042.

[99] M. Parvania, M. Fotuhi-Firuzabad, and M. Shahidehpour, "Comparative Hourly Scheduling of Centralized and Distributed Storage in Day-Ahead Markets," *IEEE Trans. Sustain. Energy*, vol. 5, no. 3, pp. 729-737, Jul. 2014.

[100] E. F. Camacho and C. Bordons, "Model Predictive Control," 2nd ed. London: Springer-Verlag, 2002.

[101] L. Xie and M. D. Ilic, "Model Predictive Dispatch in Electric Energy Systems with Intermittent Resources," in *Proc. 2008 IEEE Int. Conf. Syst. Man Cybern.*, pp. 42-47.

[102] Andrew Makhorin, GUSEK (GLPK Under Scite Extended Kit), 2015. [Online]. Available: http://gusek.sourceforge.net/gusek.html.

[103] Imre P. Gyuk. (2003, Dec.). EPRI-DOE Handbook of Energy Storage for Transmission and Distribution Applications. EPRI, Washington, D.C., WA, USA. [Online]. Available: http://www.sandia.gov/ess/publications/ESHB%201001834%20reduced%20size.pdf.

[104] X. Luo, J. Wang, M. Dooner, and J. Clarke, "Overview of Current Development in Electrical Energy Storage Technologies and the Application Potential in Power System Operation," *Appl. Energy J.*, vol. 137, pp. 511-536, Jan. 2015.

[105] The Ontario Hydro One Electricity Company, 2014. [Online]. Available: www.hydroone.com/.

[106] Q. Zhou, L. Tesfatsion, and L. Chen-Ching, "Short-Term Congestion Forecasting in Wholesale Power Markets," *IEEE Trans. Power Syst.*, vol. 26, no. 4, pp. 2185-2196, Nov. 2011.

[107] G. Li, C. C. Liu, and H. Salazar, "Forecasting Transmission Congestion Using Day-Ahead Shadow Prices," in *Proc. 2006 PSCE* , pp. 1705-1709.

[108] J. Y. Fan and J. D. McDonald, "A Real-Time Implementation of Short-Term Load Forecasting for Distribution Power Systems," *IEEE Trans. Power Syst.*, vol. 9, no. 2, pp. 988-994, May 1994.

[109] Y Li, D. M. Vilathgamuwa, and P. C. Loh, "Design, Analysis, and Real-Time Testing of a Controller for Multibus Microgrid System," *IEEE Trans. Power Electron.*, vol. 19, no. 5, pp. 1195-1204, Sep. 2004.

[110] S. Conti, R. Nicolosi, S. A. Rizzo, and H. H. Zeineldin, "Optimal Dispatching of Distributed Generators and Storage Systems for MV Islanded Microgrids," *IEEE Trans. Power Deliv.*, vol. 27, no. 3, pp. 1243-1251, Jul. 2012.

[111] M. R. D. Zadeh, A. Hajimiragha, M. Adamiak, A. Palizban, and S. Allan, "Design and Implementation of a Microgrid Controller," in *Proc. 2011 64th Annual Conf. Protec. Relay Engin.,* pp. 137-145.

[112] N. Amjady, F. Keynia, and H. Zareipour, "Short-Term Load Forecast of Microgrids by a New Bilevel Prediction Strategy," *IEEE Trans. Smart Grid*, vol. 1, no. 3, pp. 286-294, Dec. 2010.

Curriculum Vitae

Name: *HADI KHANI*

Post-Secondary Education and Degrees:
University of Western Ontario
London, ON, Canada
2016, Ph.D. in Electrical Engineering

University of Western Ontario
London, ON, Canada
2014, M.E.Sc. in Electrical Engineering

Isfahan University of Technology
Isfahan, Iran
2009, M.Sc. in Electrical Engineering

Shiraz University
Shiraz, Iran
2006, B.Sc. in Electrical Engineering

Honours and Awards:
USC Teaching Honour Roll, Award of Excellence
University of Western Ontario, Canada, for the 2015-16 academic year.

Excellence in Research Award
University of Western Ontario, Canada, 2016.

Hydro One Research Program Award
University of Western Ontario, Canada, 2015.

Best Conference Papers Session on Markets, Economics, and Planning
IEEE PES General Meeting, Washington DC, USA, 2014.

Second Best Poster
Sustainability and Environment Research Showcase
University of Western Ontario, Canada, 2014.

Best M.Sc. Thesis of the Year Award
Isfahan University of Technology, Isfahan, Iran, 2009.

Top Three B.Sc. Graduates Award
Shiraz University, Shiraz, Iran, 2006.

Selected Gifted Undergraduate Student
Shiraz University, Shiraz, Iran, from 2004 to 2006.

Related Work	Course and Lab Preparation Assistant
Experience:	University of Western Ontario
	Jul. - Aug., 2016.

Sessional Lecturer
University of Western Ontario
2015 - 2016.

Research Assistant
University of Western Ontario
2012 - 2016.

Teaching Assistant
University of Western Ontario
2014 - 2015.

Consulting Engineer
Pajoohandeh-Niroo Consult. Indust. Resear. Comp., Isfahan, Iran
2009 - 2012.

Publications:

Peer-Reviewed Journals:

1. **H. Khani**, R. K. Varma, M. R. D. Zadeh, and A. H. Hajimiragha, "A Real-Time Multi-Step Optimization-Based Model for Scheduling of Storage-Based Large-Scale Electricity Consumers in a Wholesale Market," *IEEE Trans. Sustain. Ener.*, Under Revision, Jun. 2016.

2. **H. Khani**, M. R. D. Zadeh, and R. K. Varma, "Optimal Scheduling of Independently Operated, Locally Controlled Energy Storage Systems as Dispatchable Assets in a Competitive Electricity Market," *IET Gener. Transm. Distrib.*, Under Revision, Aug. 2016.

3. **H. Khani**, "CIGRE HVDC Benchmark System for Power Transfer Control and its Impact on the Quality, Strength, and Stability of Power Systems," *Renew. Sustain. Energy Rev. J., Elsevier*, Under Review, Jan. 2016.

4. **H. Khani**, M. R. D. Zadeh, and A. H. Hajimiragha, "Transmission Congestion Relief Using Privately Owned Large-Scale Energy Storage Systems in a Competitive Electricity Market," *IEEE Trans. Power Syst.*, vol. 31, no. 2, pp. 1449-1458, Mar. 2016.

5. **H. Khani** and M. R. D. Zadeh, "Online Adaptive Real-Time Optimal Dispatch of Privately Owned Energy Storage Systems Using Public-Domain Electricity Market Prices," *IEEE Trans. Power Syst.*, vol. 30, no. 2, pp. 930-938, Mar. 2015.

6. **H. Khani** and M. R. D. Zadeh, "Real-Time Optimal Dispatch and Economic Viability of Cryogenic Energy Storage Exploiting Arbitrage Opportunities in an Electricity Market," *IEEE Trans. Smart Grid*, vol. 6, no. 1, pp. 391-401, Jan. 2015.

7. S. Shojaeian, E. S. Naeeni, M. Dolatshahi, and **H. Khani**, "A PSO-DP Based Method to Determination of the Optimal Number, Location, and Size of FACTS Devices in Power Systems," *Advan. Elect. Comp. Eng.*, vol. 14, no. 1, pp. 109-114, 2014.

8. **H. Khani**, M. Moallem, S. Sadri, and M. Dolatshahi, "A New Method for Online Determination of the Location of Switched Capacitor Banks in Distribution Systems," *IEEE Trans. Power Deliv.*, vol. 26, no. 1, pp. 341-351, Jan. 2011.

Refereed Conferences:

1. **H. Khani** and M. R. D. Zadeh, "Energy Storage in an Open Electricity Market with Contribution to Transmission Congestion Relief," in *Proc. 2014 IEEE PES General Meeting*, Washington DC, USA *(Best Conference Papers Session on Markets, Economics, and Planning)*.

2. **H. Khani**, M. R. D. Zadeh, and R. Seethapathy, "Large-Scale Energy Storage Deployment in Ontario Utilizing Time-of-Use and Wholesale Electricity Prices: An Economic Analysis," in *Proc. 2014 Cigre Conf.*, Toronto, ON, Canada.

3. **H. Khani**, M. R. D. Zadeh, and A. H. Hajimiragha, "Loss of Data Management in Real-Time Short-Term Forecasting Algorithms," in *Proc. 2013 IEEE Int. Conf. Smart Grid Eng.*, Oshawa, ON, Canada.

4. **H. Khani**, M. R. D. Zadeh, and R. Seethapathy, "Optimal Weekly Usage of Cryogenic Energy Storage in an Open Retail Electricity Market," in *Proc 2013 IEEE PES General Meeting*, Vancouver, BC, Canada.

5. **H. Khani**, M. Moallem, M. Dolatshahi, A. Davari, and S. Sadri, "A New Index for Online Tracking of the Switched Capacitor Bank Location in Distribution Systems," in *Proc. 2010 18th Iranian Conf. Elec. Eng. (ICEE)*, Isfahan, Iran.

6. M. Dowlatshahi, M. Moallem, **H. Khani**, "A New Approach for Voltage Profile Enhancement in Distribution Power Systems Using Fixed and Thyristor Controlled Series Capacitor (TCSC)," in *Proc. 2010 18th Iranian Conf. Elec. Eng. (ICEE)*, Isfahan, Iran.

7. **H. Khani**, M. Moallem, and S. Sadri, "A Novel Algorithm for Determining the Exact Location of Switched Capacitor Banks in Distribution Systems," in *Proc. 2009 Trans. Dist. Conf. Expos.: Asia and Pacific*, Seoul, South Korea.

8. **H. Khani**, M. Moallem, and S. Sadri, "On Tracking and Finding the Location of Switched Capacitor Banks in Distribution Systems," in *Proc. 2009 Trans. Dist. Conf. Expos.: Asia and Pacific*, Seoul, South Korea.